



IN THE UNITED STATES PATENT AND TRADEMARK OFFICE

In re Application of: §
§
LEVAVA ROIZ ET AL. §
§
Serial No.: 10/069,454 §
§
Filed: February 26, 2002 § Group Art Unit: 1632
§
For: METHODS OF AND COMPOSITIONS §
FOR INHIBITING THE §
PROLIFERATION OF MAMMALIAN §
CELLS §
§
Examiner: CHEN, Shin-Lin, Ph.D. § Attorney
§ Docket: 02/23357
§

Commissioner for Patents
P. O. Box 1450 Alexandria VA 22313

DECLARATION OF PROF. ODED SHOSEYOV UNDER 37 CFR 1.132

I am presently employed as researcher at The Hebrew University of Jerusalem, Faculty of Agriculture, Institute of Plant Sciences and Genetics in Agriculture, where I am an Associate Professor. I received my Ph.D. degree from the The Hebrew University of Jerusalem in 1998, worked as a post-doctoral fellow in University of California Davis, and was a visiting Professor at University of British Colombia. A curriculum vitae is enclosed.

My research focuses on protein engineering. Since the beginning of my career, I have published 90 scientific articles in highly regarded journals and books, and have presented my achievements at many international scientific conferences.

I am a co-inventor of the subject matter claimed in the above-referenced U.S. patent application.

I have read the Official actions issued with respect to the above-identified application.

In this Official action, the Examiner has rejected claims 1-7, 15-20 and 45-52

under 35 U.S.C. § 112 first paragraph based on the contention that the specification does not enable the ordinarily skilled artisan to practice the invention commensurate in scope with the claims, namely whereby (i) the RNase is any of various RNases of the T2 family or its mutants that substantially lack ribonuclease activity; (ii) administration of the RNase is effected via any of various routes; (iii) the abnormally proliferating cells are cancer cells of any of various types; and (iv) the process associated with abnormally proliferating cells is any of various such relevant processes.

The Appendix section enclosed herewith describes experimental results obtained by the present inventors illustrating that the specification indeed provides adequate teachings enabling one of ordinary skill in the art to practice the invention over the full scope of the claims, in sharp contrast to the Examiner's contention that it does not. Namely, results set forth in the Appendix section conclusively demonstrate such teachings, specifically whereby:

(i) The T2-family RNase belongs to various members of the T2 RNase family derived from highly phylogenetically divergent sources, including the prokaryote-derived RNase I, the fungal (*A. oryzae*)-derived RNase T2 (Appendix, page 1, Figure 1), or the mammalian/human-derived RNase 6PL (Appendix, page 2, Figures 2-5), or RNase B1 (Appendix, pages 3-10, Figures 6-15);

(ii) The administration route is any of various administration routes, including the systemic/intravenous (Appendix: page 3, Figure 7; page 8, Figure 9), systemic/intraperitoneal (Appendix: page 3, Figure 6; page 4, Figures 8-9; page 8, Figures 12-14), or the local/subcutaneous route (Appendix, page 6, Figures 10-11);

(iii) The abnormally proliferating cells are any of various types of cancer cells, including melanoma cells (Appendix, page 3, Figures 6-11), mammary carcinoma cells (Appendix, page 7, Table 1) or colon carcinoma cells (Appendix: pages 8-10, Figures 9-15 and Table 1); and

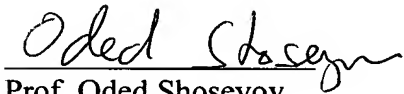
(iv) The process associated with abnormally proliferating cells is any of various such relevant processes, including proliferation/growth (Appendix: pages 3-5, Figures 6-9; page 8, Figure 12), colonization/metastasis (Appendix: pages 3-5, Figure

7; page 7, Table 1; page 10, Table 1), and/or angiogenesis/a pro-angiogenic process (Appendix: page 5, Figure 6; page 6, Figures 10-11; page 9, Figure 15).

These results conclusively prove that the methodology described and claimed in the instant application can indeed be utilized to practice the invention over the entire scope claimed, thereby proving that the rejections of claims 1-7, 15-20 and 45-52 under 35 U.S.C. § 112, first paragraph, are unfounded.

I hereby declare that all statements made herein of my own knowledge are true and that all statements made on information and belief are believed to be true; and further that these statements were made with the knowledge that willful false statements and the like so made are punishable by fine or imprisonment, or both, under Section 1001 of Title 18 of the United States Code and that such willful false statements may jeopardize the validity of the application or any patent issued thereon.

15th April , 2004



Prof. Oded Shoseyov
The Institute of Plant Sciences and Genetics in Agriculture,
The Faculty of Agriculture,
The Hebrew University of Jerusalem, Rehovot, Israel

Enc.:

CV of Oded Shoseyov and Appendix

APPENDIX:
EXPERIMENTAL DATA CONFIRMING TEACHING OF FULL SCOPE OF CLAIMED
METHOD BY SPECIFICATION

Anticancer/antiangiogenic properties of RNase T₂ family members derived from prokaryotes, mammals and fungi other than A. niger:

Ribonucleases of the T₂ family have been shown to share fundamental characteristics, e.g. complete homology of catalytic active site, optimal RNase activity at high temperature and low pH, molecular weight of at least 24 kDa (twice that of RNase A family) and the presence of glycan chains. Since RNase B1 (*Aspergillus niger* RNase B1) has been found to be anti-angiogenic, the standard human umbilical vein endothelial cell (HUVEC) tube formation assay was used to examine the anti-angiogenic effect of other members of the T₂ family. *Aspergillus oryzae* RNase T₂ (Sigma) and *E. coli* RNase I (Ambion) were used for this assay. Generally, the experiment was conducted as previously described for RNase B1. Wells of 96-well plates were coated with Matrigel, in which 14,000 HUVECs per plated/well. The growth medium employed was supplemented with 1 µg/ml angiogenin, to induce tube formation (angiogenesis). Different treatments were added to the growth media, to a final concentration of 2 µM RNase B1, RNase T₂ (29 kDa) or RNase I (27 kDa). For controls, cells were plated under the same conditions, in the absence or in the presence of any of the above RNases, but in the absence of angiogenin. The 96-well plate was incubated for 24 h at 37 degrees centigrade under a humidified atmosphere and 5% carbon dioxide. Three replications were performed for each treatment.

Fig 1. summarizes the results as observed following the overnight incubation. HUVECs incubated in medium in the absence of angiogenin and RNase (Control), formed only few delicate tubes on the Matrigel surface (Fig. 1A), whereas in the presence of angiogenin (Positive Control) massive tubes appeared (Fig. 1B). RNase B1 or RNase T₂ did not have any effect on the cells when given alone (Negative Control) (Fig. 1C, E), however they clearly inhibited angiogenin-induced tube formation (Fig. 1D, F). The RNase T₂ was found to have weaker inhibitory effect than the RNase B1. Nonetheless, a complete inhibition of tube formation was get with 10 µM of RNase B1 or 50 µM of RNase T₂ (not shown). RNase I had a significant inhibitory effect on tube formation, without (Fig. 1G) or with angiogenin (Fig. 1H).

These results demonstrate that T2-family RNases from highly divergent sources display similar antiangiogenic/anticancer properties. These results are unique to the instant invention

since, up to the present, no publication has shown or suggested the anti-angiogenic activity of RNases belonging to the T₂ family.

Anticancer/antiangiogenic properties of human RNase T₂, RNase 6PL: Deletion of a region of chromosome 6 in humans (6q27) has been considered to be associated with several human malignancies (Cooke et al. 1996. *Allele loss on chromosome arm 6q and fine mapping of the region at 6q27 in epithelial ovarian cancer*. Genes Chromosomes Cancer 15:223-233; Saito et al. 1992. *Fine-scale deletion mapping of the distal long arm of chromosome 6 in 70 human ovarian cancers*. Cancer Res 52:5815-5817). It was found that this region contains the putative tumor suppressor RNase6PL gene which shares homology with the RNase T₂ family (Trubia et al. 1997. *Mammalian Rh/T2/S-glycoprotein ribonuclease family genes: cloning of a human member located in a region of chromosome 6 (6q27) frequently deleted in human malignancies*. Genomics 42:342-344; Acquati et al. 2001. *Molecular cloning, tissue distribution, and chromosomal localization of the human homolog of the R2/Th/Stylar ribonuclease gene family*. Meth Mol Biol 160:87-101), including RNase B1. Due to the anti-cancer capacities of T2-family RNases, human RNase T2 represents a highly advantageous agent for treating cancer by virtue of its being of endogenous human origin, and thereby being optimally non-immunogenic and non-toxic when administered to humans.

The sequence of the gene for RNase 6PL was identified in the human genome project (Fig. 2). Out of 28,751 bp of the full gene, only 719 bp (arranged in 9 exons) form the open reading frame. A synthetic gene optimized for expression in *Pichia pastoris* yeast (GenArt GmbH, Germany) was designed according to the cDNA sequence. The synthetic gene was ligated into pPIC9K plasmid (Invitrogene) and cloned in *P. pastoris*. The recombinant yeasts were grown under inductive conditions, and one colony was found to contain the gene insert of about 750 bp (Fig. 3A), as well as to express the human protein at the expected size of 27 kDa (Fig. 3B). Additional tests showed that the recombinant protein had RNase activity (not shown), indicating accurate folding during protein synthesis.

The positive colony was cultured under adequate conditions to overexpress the recombinant RNase 6PL. The yeast protein extract was passed through a Q Sepharose column in a Fast Protein Liquid Chromatography (FPLC) (Amersham Pharmacia Biotech, Buckinghamshire, U.K.) and a 27 kDa purified protein (15 mg) was obtained (Fig. 4). The recombinant human T₂-RNase maintained its thermostability (Fig. 5A) and RNase activity (Fig. 5B) even at even at boiling point.

These properties are typical of a T₂-RNase family member, and strongly indicate that human the human T₂-family RNase, RNase 6PL, possesses the same anti-cancer/anti-angiogenic capacities of RNase B1.

MELANOMA MODELS

Systemic/intraperitoneal administration of RNase B1 inhibits melanoma tumor growth

Mice: CD BDF1 and Balb/c.

Tumor cells: Mouse melanoma B16 F1 (low metastatic).

Procedure: This experiment was conducted following the protocol in (Geran et al. 1972. *Protocol for screening chemical agents and natural products against animal tumors and other biological systems*. In: Cancer Chemotherapy Reports Part 3 Vol 3 No 2). Cells (2×10^6 /mouse) were injected into the intraperitoneal cavity of mice. RNase B1 (5 mg/mouse in 100 μ l PBS) or PBS alone was injected ip twice, 24 h and 5 days after cells injection.

At day 14 after cell injection, the mice were sacrificed and the melanoma tumors were taken for histopathological examinations.

Results: The effect of RNase B1 in ip/ip experiments was scored by qualitative tumor observations. At day 14 of experiment, abdomen cavity demonstrated the tumor growth-inhibitory effect of RNase B1. In both BDF1 and Balb c mice, melanoma cells induced massive tumors filling the abdominal cavity and spreading over the intestinal gut (Fig. 6A, C), whereas in RNase B1-treated mice only few small tumors were observed (Fig. 6B, D). In this experiment the total amount of RNase B1 was 10 mg/mouse. Similar results were obtained when mice were treated by a single injection of 10 mg RNase B1 or by 10 daily injections of 1 mg RNase B1 (not shown).

Systemic/intravenous administration of RNase B1 inhibits metastasis/colonization and growth of highly metastatic malignant melanoma tumors

Mice: Balb/c

Tumor cells: B16 F10 (highly metastatic) melanoma cells.

Procedure: Cells (5×10^5 or 5×10^6 cells/mouse) were injected into the lateral tail vein. RNase B1 (10 mg RNase B1 in 100 μ l PBS) or PBS was injected by the same manner, starting 24 h after cells injection and in four days intervals with a total of three injections. At the end of experiment, the lungs were removed, weighted and surface metastases were quantified.

Results: In the i.v./i.v. model, melanoma cells injected in the tail vein lead to development of lung metastases in about two weeks. The black metastases could be easily noticed (Fig.7A), thus when 5×10^5 cell were injected, the reductive effect (76%, $P < 0.001$) of RNase B1 on the number of metastases was apparent (Fig.7B). Initial bolus of 5×10^6 cells/mouse was highly intense, as in the control mice the metastases were too dense to be counted. In this case we found that in RNase B1-treated mice the lung weight (Fig 7C) and tumor size (Fig. 7D) were significantly smaller (25%, $P < 0.01$ and 25%, $P < 0.001$, respectively) than in the control. These results therefore convincingly demonstrate that RNase B1 can be used to efficiently inhibit the growth and metastasis of highly metastatic malignant melanoma tumors.

Systemic/intraperitoneal administration of RNase B1 inhibits growth and metastasis/colonization of metastatic human melanoma tumors

Mice: Male athymic BALB/c nude mice (were purchased from the Animal Production Area of the National Cancer Institute, Frederick Cancer Research Facility (Frederick, MD). The mice were housed in laminar flow cabinets under specific pathogen-free conditions and used at 7-9 weeks of age)

Tumor cells: The highly tumorigenic and metastatic human melanoma A375SM cell line was used.

Procedure: To prepare tumor cells for inoculation, cells in exponential growth phase were harvested by brief exposure to a 0.25% trypsin/0.02% ethylenediaminetetraacetic acid solution (w/v). The flask was sharply tapped to dislodge the cells and supplemented medium was added. The cell suspension was pipetted to produce a single-cell suspension. The cells were washed and resuspended in $\text{Ca}^{2+}/\text{Mg}^{2+}$ -free Hanks' balanced salt solution (HBSS) to the desired cell concentration. Cell viability was determined by trypan blue exclusion, and only single-cell suspensions of >90% viability was used. Subcutaneous tumors were produced by injecting 10^5 tumor cells/0.1 ml HBSS over the right scapular region of the mice. Growth of subcutaneous tumors was monitored by weekly examination of the mice and measurement of tumors with calipers. The mice were killed 5 weeks after injection, and tumors were frozen in OCT compound (Sakura Fineter, Torrance, CA), or formalin fixed and then processed for immunostaining and hematoxylin and eosin (H&E) staining.

For experimental lung metastasis, 10^6 tumor cells in 0.1 ml of HBSS were injected into the lateral tail vein of nude mice. The mice were killed after 60 days, and the lungs were

removed, washed in water, and fixed with Bouin's solution for 24 hours to facilitate counting of tumor nodules. The number of surface tumor nodules was counted under a dissecting microscope. Both the subcutaneous and intravenous groups were treated every other day with either 1 mg/100 μ l of RNase B1 aqueous solution or with phosphate-buffered saline (PBS) by intraperitoneal injection.

Results: In the first set of experiments, we determined the effect of RNase B1 on the tumor growth of human melanoma cells in nude mice. A375SM melanoma cells (5×10^5) were injected subcutaneously into nude mice ($n = 5$). Three days later, animals injected with tumor cells were subsequently injected with 1 mg of RNase B1 or control PBS intraperitoneally every other day for 30 days. Tumor cells in the animals treated with PBS grew progressively and produced large tumors reaching the size up to 700 mm³ mean volume (Fig. 8). In contrast, treatment with RNase B1 reduced tumor growth to maximum 100 mm³ mean volume during the same periods of time (Figure 9). A second set of mice ($n = 8$) were injected and treated exactly as described and showed exactly the same effects of RNase B1 on tumor growth (not shown).

To determine the effect of RNase B1 on metastasis of human melanoma cells, A375SM 10^6 cells were injected intravenously into nude mice to produce experimental lung metastasis. Five days later, animals injected with tumor cells were also injected with RNase B1 or control PBS intraperitoneally every other day for 60 days. It was found that both the incidence and number of lung metastasis of A375SM cells were reduced in RNase B1-treated mice, when compared with the control group. In control mice, A375SM cells produced numerous lung metastases (median, 65; range, 16 to 200), whereas treatment with RNase B1 significantly inhibited the ability of A375SM cells to form metastasis in nude mice (median, 10; range, 0 to 75; $P < 0.05$). Collectively, these data demonstrate that treatment of mice with RNase B1 leads to suppression of tumor growth and metastasis.

Systemic/intraperitoneal administration of RNase B1 inhibits production of the pro-angiogenic factor matrix metalloproteinase-2 (MMP-2) by highly metastatic human melanoma tumors

Procedure: For CD31 and MMP-2 staining, sections of frozen tissues were prepared from tumor xenografts. The slides were then rinsed twice with PBS, and endogenous peroxidase was blocked by the use of 3% hydrogen peroxide in PBS for 12 minutes. The samples were then washed three times with PBS and incubated for 10 minutes at room temperature with a protein-

blocking solution consisting of PBS (pH 7.5) containing 5% normal horse serum and 1% normal goat serum. Excess blocking solution was drained and the samples were incubated for 18 hours at 4°C with a 1:100 dilution of monoclonal rat anti-CD31 (1:800) antibody or anti-MMP-2 (1:200) (PharMingen, San Diego, CA). The samples were then rinsed four times with PBS and incubated for 60 minutes at room temperature with the appropriate dilution of peroxidase-conjugated anti-mouse IgG1, anti-rabbit IgG, or anti-rat IgG. The slides were rinsed with PBS and incubated for 5 minutes with diaminobenzidine (Research Genetics, Huntsville, AL). The sections were then washed three times with distilled water and counterstained with Gill's hematoxylin. For the quantification of MVD, ten fields of the CD31 stained samples were counted at 100x magnification.

Sections (4 µm thick) of formalin-fixed, paraffin-embedded tumors were also stained with H&E for routine histological examination.

Results: To determine whether RNase B1 suppressed the expression of MMP-2 *in vivo*, we performed immunohistochemical analysis on the melanoma derived from A375SM cells. The protein expression of MMP-2 *in vivo* was evaluated by immunohistochemistry using anti-MMP-2 antibodies. As shown in Fig. 6, MMP-2 staining was observed in control-injected A375SM tumors, but was significantly decreased in RNase B1-treated tumors. Thus, we conclude that RNase B1 in melanoma cells inhibited the expression of MMP-2 *in vivo* as well as *in vitro*.

Local/subcutaneous administration of RNase B1 inhibits angiogenesis of malignant melanoma tumors

Immunofluorescent Staining of CD31/PECAM-1: Frozen gelfoam specimens were sectioned (10-12 µm), mounted on positively charged slides, air-dried for 30 min, and fixed in cold acetone for 5 min, followed by acetone:chloroform (1:1) for 5 min, and acetone alone for an additional 5 min. The samples were washed three times with PBS, incubated for 20 min at room temperature with a protein-blocking solution containing 4% fish gelatin in PBS, and then incubated for 18 h at 4°C with a 1:800 dilution of rat monoclonal anti-mouse CD31 antibody (PharMingen, San Diego, CA). After the samples were rinsed with PBS three times for 3 min each, the slides were incubated for 1 h in the dark at room temperature with 1:200 dilution of secondary goat anti-rat antibody conjugated to Goat anti-rat Alexa 594 (Molecular Probes Inc., Eugene, OR). Samples were washed three times with PBS for 3 min each and then mounted with Vectashield mounting medium for fluorescence with Hoechst 33342, trihydrochloride, trihydrate

10 mg/mL solution in water (Molecular Probes Inc., Eugene, Oregon). Immunofluorescence microscopy was performed using a Zeiss Axioplan microscope (Carl Zeiss, New York, NY) equipped with a 100-W HBO mercury bulb and filter sets from Chroma, Inc. (Burlington, VT) to individually capture red, green, and blue fluorescent images. Images were captured using a C5810 Hamamatsu color chilled 3CCD camera (Hamamatsu, Japan) and digitized using Optimas imaging software (Silver Springs, MD). Images were further processed using Adobe PhotoShop software (Adobe Systems, Mountain View, CA). Endothelial cells were identified by red fluorescence.

Results: Since MMP-2 is an important angiogenic factor, we determined whether RNase B1 could affect melanoma tumor angiogenesis. Tumor-associated neovascularization as indicated by microvessel density (MVD) was determined by immunohistochemistry using anti-CD31 antibodies. As shown in Fig. 10, we found a significant reduction in tumor MVD per field after treatment with RNase B1 as compared with control tumors. The mean number of MVD was 12 ± 5 in RNase B1-treated A375SM tumors. In contrast, the mean number of MVD was 43 ± 7 for control A375SM tumors. Moreover, the number of TUNEL-positive tumor cells was inversely correlated with MVD in the studied tumors. The number of tumor cells undergoing apoptosis was higher in the RNase B1-treated animals than in tumors in control mice (Figure 11). The percentage of apoptotic cells was $31.2 \pm 7.3\%$ in RNase B1-treated A375SM melanoma tumors. In contrast, the percentage of apoptotic cells was $2.2 \pm 1.1\%$ for control A375SM tumors. The above data indicate that RNase B1 treatment significantly decreased melanoma tumor-associated neovascularization and subsequently increased apoptosis of tumor cells.

MAMMARY CARCINOMA

RNase B1 inhibits colonization by mammary carcinoma cells

ZR-75-1 breast cancer cells were treated (or not for control) with 1 and 10 μ M RNase B1 for 4 days. Wells and Matrigel-coated inserts of a commercially available 24-well invasion chamber (Becton Dickinson, Bedford, MA) were rehydrated in 0.5 ml of serum free medium overnight and processed according to the manufacturer's instructions. 0.5 ml of ZR-75-1 control or RNase B1-treated cell suspensions containing 2.5×10^4 cells each were added to the top of the chambers and 0.750 ml of DMEM media containing 10% FCS was added to the lower chamber. The invasion chambers were incubated for 22 hours in a 37 degrees centigrade cell culture incubator. The non-invading cells on the upper surface of the membrane of the insert were

removed by scrubbing. The cells on the lower surface of the membrane were stained with Diff-Quik™ stain. The membranes were fixed and the cells were counted at X200 magnification under a light microscope. The assay was carried out in triplicate.

Results: Since RNase B1 was shown to affect cancer cell's morphology and actin organization we examined whether cell motility is also affected. ZR-1-70 cells were able to penetrate the Matrigel-coated filters (Table 1). RNase B1 significantly and dose dependently (1 and 10 μ M) inhibited invasiveness of ZR-1-70 cells through Matrigel-coated filters.

Table 1. The Effect of RNase B1 on ZR-75-1 breast cancer and HT-29-colon cancer cell invasiveness through Matrigel-coated filters. In HT-29 and ZR-75-1 cells, RNase B1 at 1 μ M ($P < 0.05$ and $P < 0.01$, respectively) and 10 μ M ($P < 0.01$ and $P < 0.001$, respectively) inhibited cell invasiveness in a dose-responsive manner.

Cell lines	Control	RNase B1 concentration	
		1 μ M	10 μ M
HT-29	963.7 \pm 95.7	623.3 \pm 104.2	223.7 \pm 13.1
ZR-75-1	1297.7 \pm 62.5	784.0 \pm 51.5	271.7 \pm 16.6

COLON CARCINOMA MODELS

Systemic/intravenous administration of RNase B1 inhibits colon carcinoma growth

Mice: CD-1 nu/nu (nude mice), 4-5 weeks old males

Tumor cells: HT29 human colon cancer.

Procedure: Cancer cells (2×10^6 /mouse) were injected subcutaneously into the left hip of mice. RNase B1 (5 mg in 100 μ l PBS) or PBS alone was injected into the tail vein 24 h, 5 and 10 days after cells injection. After 15 days, mice were sacrificed and the tumors or the area of injection were taken for histopathological examinations.

Results: In RNase B1-treated mice, a 60% reduction in tumor weight was observed compare to control (Fig. 9A, B). These results show that the intravenous administration of RNase B1 administration is highly effective in inhibiting colon carcinoma tumor growth.

Systemic/intraperitoneal administration of RNase B1 inhibits colon carcinoma growth

Mice: CD-1 nu/nu (nude mice), 4-5 week-old males

Tumor cells: HT29 colon carcinoma.

Procedure: On Day 1, cells were injected into the left hips of mice (10^6 cells/mouse). RNase B1 was injected into peritoneal cavity, starting from day 2 and every other day. Two

experiments were performed. In the first experiment, RNase B1 at doses of 1 and 5 mg/injection in 100 μ l PBS was applied. In the second experiment, doses of RNase B1 ranged between 0.01-1 mg/injection. PBS alone was injected as control. The tumors were excised at day 30 of experiment, for size measurements and histopathological examinations. Tumor volume was calculated using the equation $(\text{length} \times \text{width}^2)/2$.

Results: In the s.c./i.p. mouse model, RNase B1 significantly inhibited the growth of HT-29 derived-carcinoma (Fig. 12). At 1 and 5 mg/injection (50 and 250 mg/kg), tumor volume was reduced by 44% and 41% respectively ($P < 0.05$, Fig. 12A). At 0.01, 0.1, 0.5 and 1 mg/injection (0.5, 5, 25 and 50 mg/kg, respectively), tumor volume was reduced by 41.5%, 34.4%, 51.1% and 62.2% respectively (Fig. 12B), as compared to control ($P < 0.05$). It should be mentioned that RNase B1 was effective even at the lowest dose. This result is consistent with our previous *in vitro* experiments with HT-29 cells, in which RNase B1 at concentrations ranged between 1-4 μ g/100 μ l (0.25-1 μ M) had similar inhibitory effect on the rate of clonogenicity. As for now, we could not gain a dose responsive manner of RNase B1, probably because the doses used were off-scale. Immunostaining showed that the RNase B1 accumulates onto the peritoneum (Fig. 13) and then finds its way towards the basal membrane of tumor blood vessels (Fig. 14). In this mode of application, RNase B1 did not show any toxic effect to nude mice, as body weight and other behavioral parameters looked normal during the experiment.

Therefore, these experiments demonstrate that RNase B1 can be applied via a systemic mode, such as via intraperitoneal injection to inhibit colon carcinoma growth.

Administration of RNase B1 inhibits tumor angiogenesis in colon carcinoma tumors

Procedure: Paraffin sections (10- μ m) from tumors from DMH treated and DMH+ RNase B1 treated were stained for CD31 immunohistology, and for the terminal deoxynucleotidyl transferase-mediated dUTP-nick end-labeling (TUNEL) procedure. CD31 was immunolocalized in paraformaldehyde-fixed tumors using the PECAM-1 (H-300), sc-8306 antibody (Santa Cruz Biotechnology, Inc. Santa Cruz, CA). Blood vessels in median tumor cross sections were counted and their diameters were measured. In each tumor, the ratio between blood vessel total area and tumor-section area was calculated. The experiments were repeated twice, and each treatment was applied to 6-to-10 rats.

Results: Tumor-associated neovascularization, as indicated by microvessel density (MVD) was determined by means of identifying blood vessels within the tumor (Fig. 15). RNase

B1 administration was found to significantly reduce the number of blood vessels (angiogenesis) per tumor.

RNase B1 inhibits invasiveness/colonization capacity of colon carcinoma cells

HT-29 colon cancer cells were treated (or not for control) with 1 and 10 μ M RNase B1 for 4 days. Wells and Matrigel-coated inserts of a commercially available 24-well invasion chamber (Becton Dickinson, Bedford, MA) were rehydrated in 0.5 ml of serum free medium overnight and processed according to the manufacturer's instructions. 0.5 ml of HT-29 control or RNase B1-treated cell suspensions containing 2.5×10^4 cells each were added to the top of the chambers and 0.750 ml of DMEM media containing 10% FCS was added to the lower chamber. The invasion chambers were incubated for 22 hours in a 37 degrees centigrade cell culture incubator. The non-invading cells on the upper surface of the membrane of the insert were removed by scrubbing. The cells on the lower surface of the membrane were stained with Diff-QuikTM stain. The membranes were fixed and the cells were counted at X200 magnification under a light microscope. The assay was carried out in triplicate.

Results: Since RNase B1 was shown to affect cancer cell's morphology and actin organization we examined whether cell motility is also affected. HT-29 cells were able to penetrate the Matrigel-coated filters (Table 1). RNase B1 was found to significantly and dose-dependently (1 and 10 μ M) inhibit the invasiveness/colonization capacity of colon carcinoma cells.

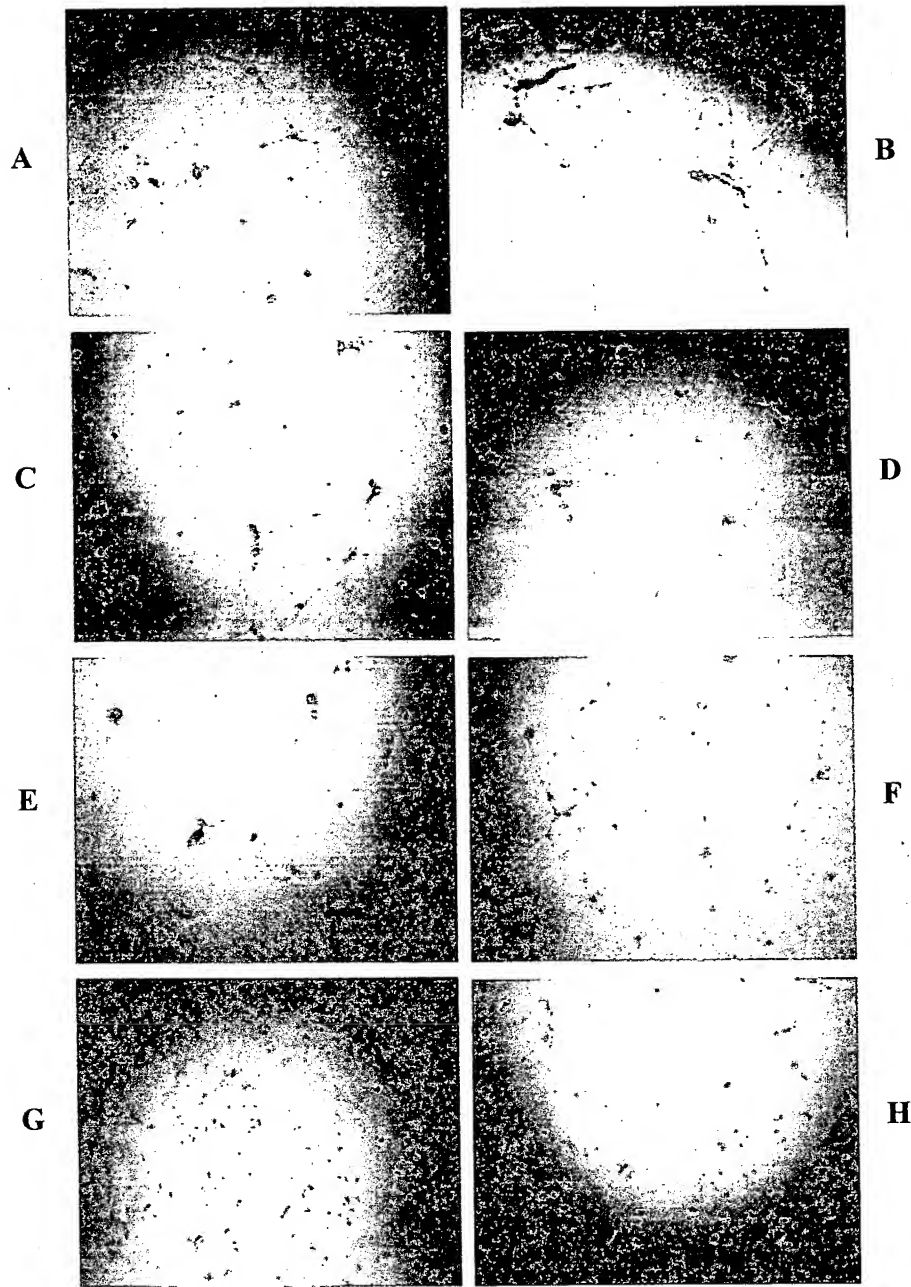
FIGURES

Fig. 1. HUVEC tube formation on Matrigel in the presence or absence of 1 μ g/ml angiogenin, and in the presence or absence of RNases (2 μ M each). **A.** Absence of angiogenin and RNase (Control). **B.** Angiogenin (Positive Control). **C.** RNase B1 (Negative Control). **D.** RNase B1 + angiogenin. **E.** RNase T₂ (Negative Control). **F.** RNase T₂ + angiogenin. **G.** RNase I (Negative Control). **H.** RNase I + angiogenin.

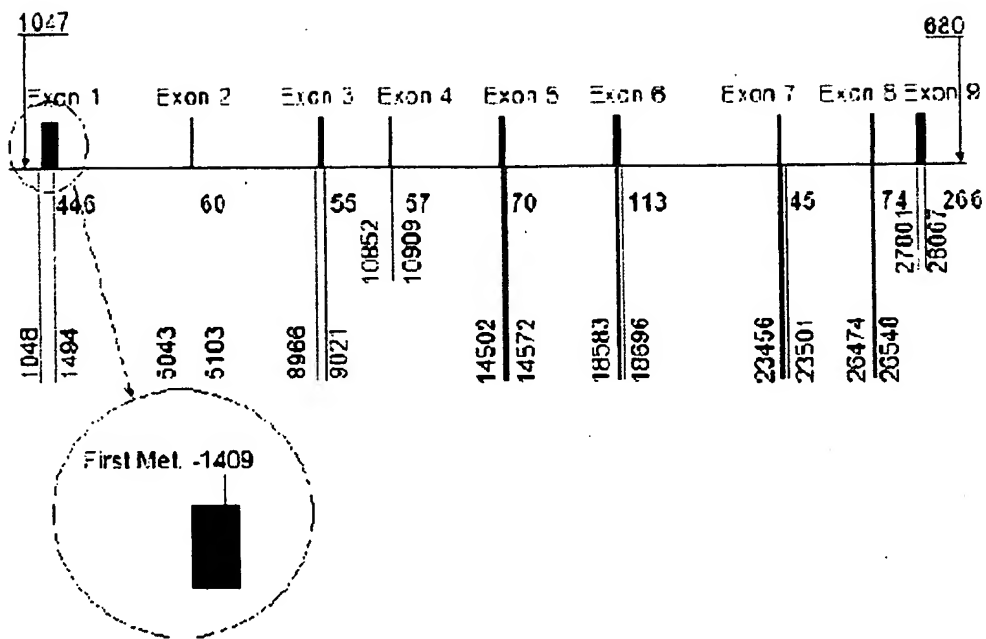


Fig. 2. DNA sequence of the human gene encoding for RNase 6PL, located in chromosome 6q27. Out of 28,751 bp of the full gene, only 719 bp (arranged in 9 exons) form the open reading frame.

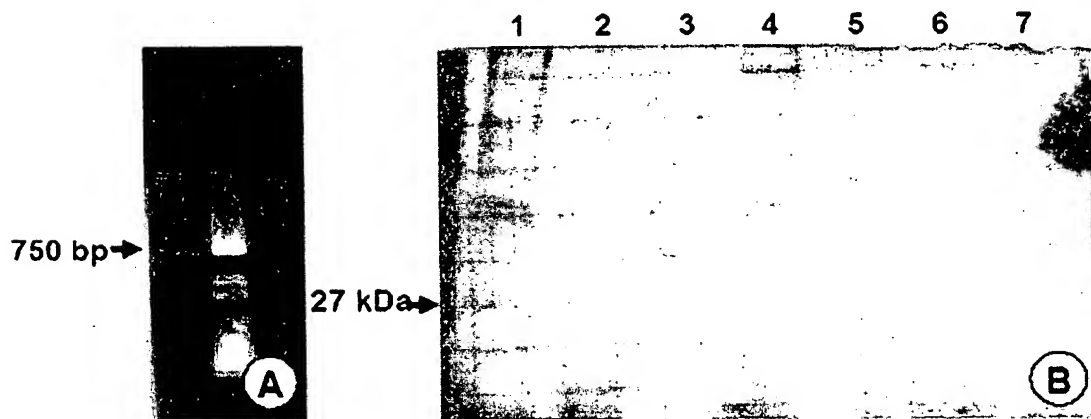


Fig. 3. Analysis of recombinant *P. pastoris*, after successful insertion of the RNase 6PL gene via pPIC9K vector. A. PCR analysis shows 750 bp DNA fragment, as expected. B. Silver stained protein SDS-PAGE shows the presence of the recombinant 27 kDa protein in one of the yeast colonies (lane 1). Other colonies do not express the recombinant protein (Lanes 2-6). Lane 7: control (colony without the vector).



Fig. 4. Recombinant RNase 6PL expressed by *P. pastoris* proliferated in a rich medium. The yeast protein extract was passed through a Q Sepharose column in a Fast FPLC and a 27 kDa purified protein was obtained (Lane 1). Lane 2: protein molecular markers.

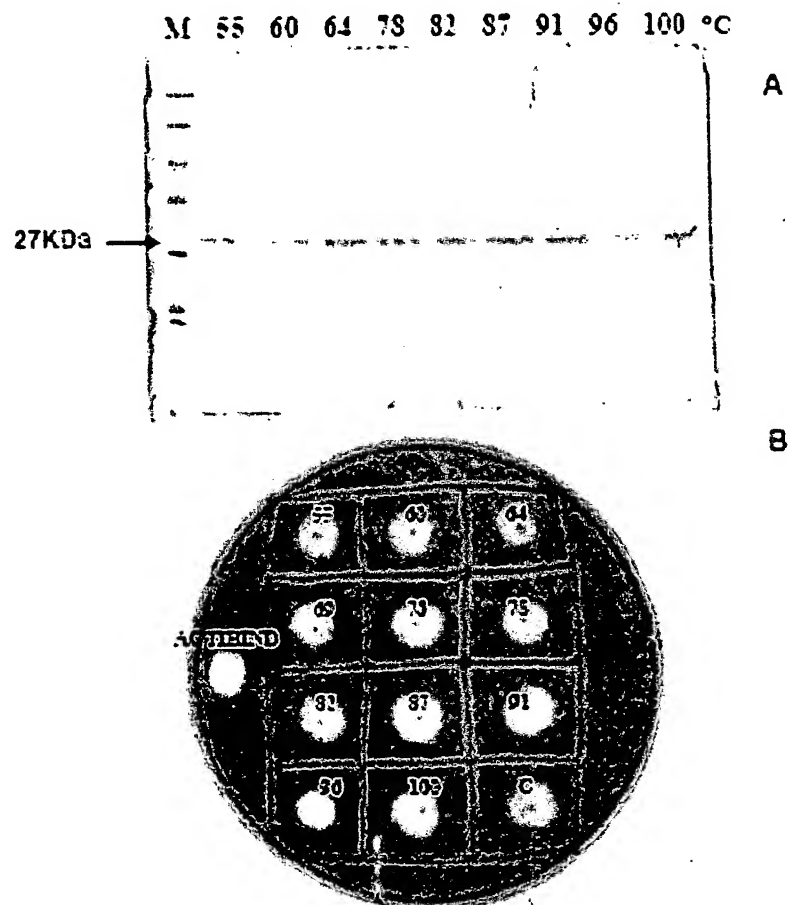


Fig. 5. Recombinant human T2-RNase, RNase 6PL, is an active and thermo-stable protein.
A. Protein SDS-PAGE. B. RNase activity assay.

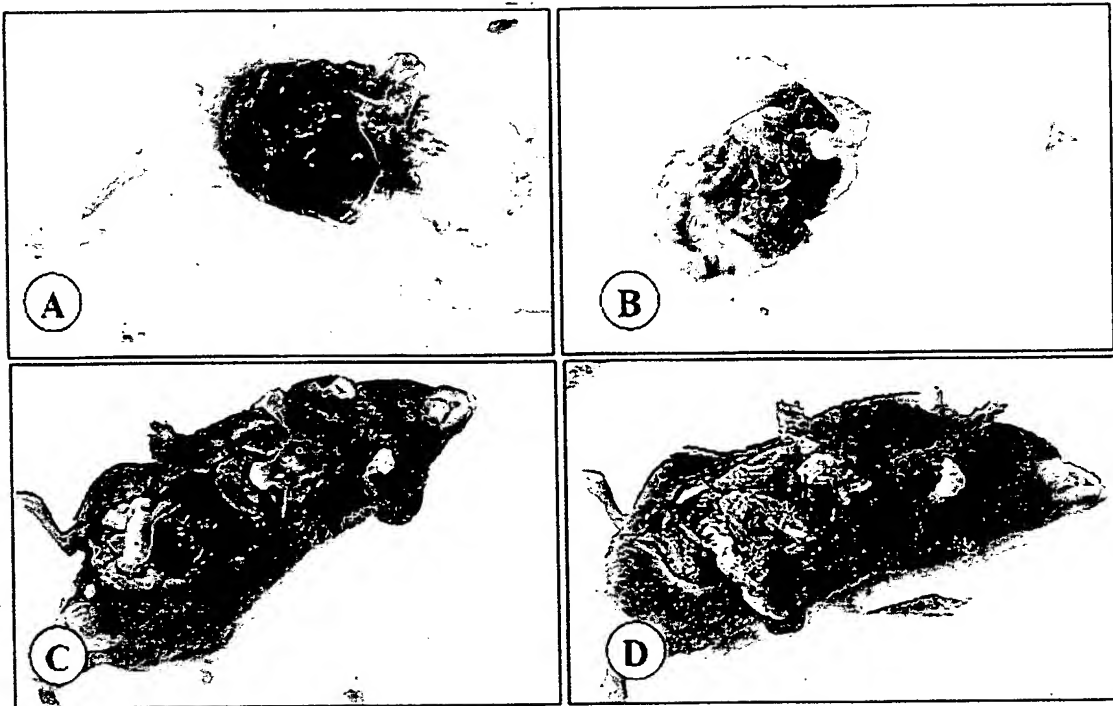


Fig. 6. The effect of RNase B1 on B16F1 melanoma in ip/ip experiment in BDF1 (black) and Balb/c (white) mice. Control mice show highly developed typical black tumors (A, C), compared with considerably smaller tumors in RNase B1- treated mice (B, D).

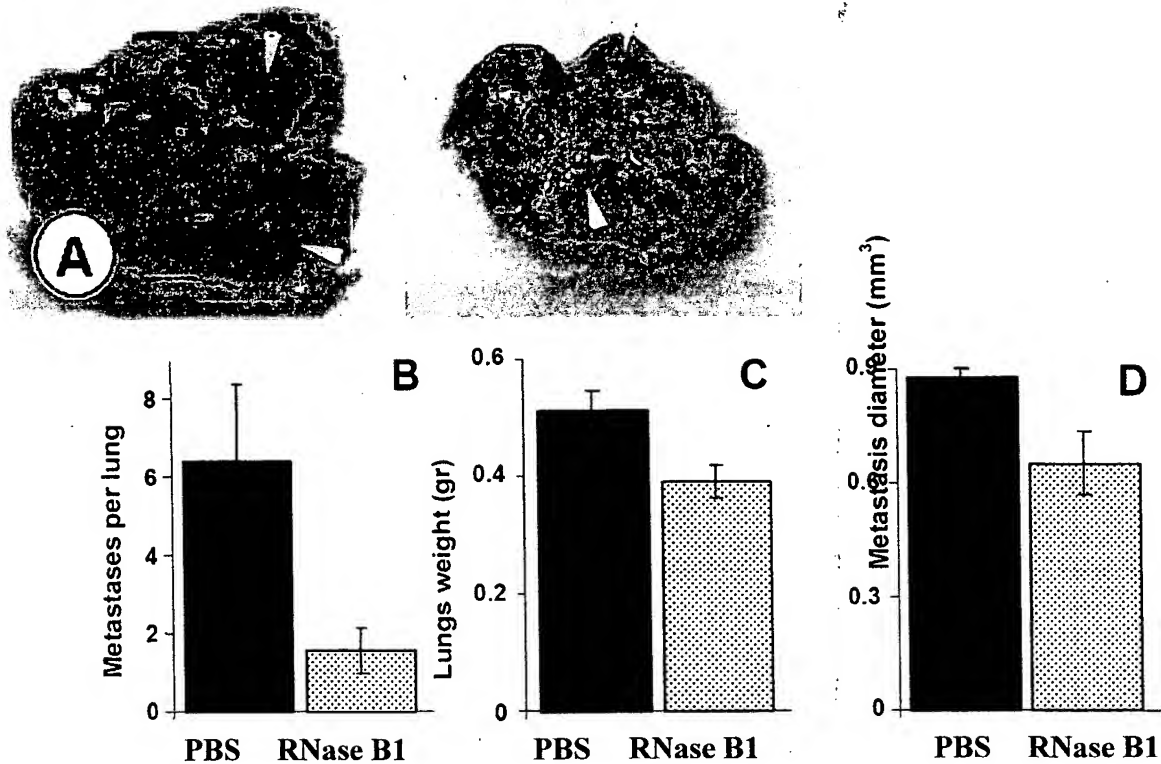


Fig. 7. RNase B1 reduces the development of B16F10 melanoma foci formed in the lungs of balb/c mice, implanted with 5×10^5 (A, B) or 5×10^6 (C, D) cells/mouse. A. View of control (left) and RNase B1-treated mice (right) lungs. B. RNase B1 reduces the number of metastases/lung (76%, $P < 0.001$). C. RNase B1 reduces lung weight (25%, $P < 0.01$). D. RNase B1 decreases mean metastasis diameter (25%, $P < 0.001$).

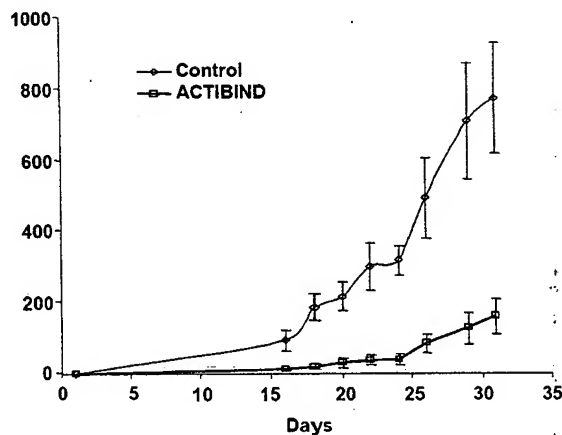


Fig. 8. The effect of RNase B1 on the tumor growth of human melanoma cells in nude mice. A375SM melanoma cells (5×10^5) were injected subcutaneously into nude mice ($n = 5$). Three days later, animals injected with tumor cells were subsequently injected with 1 mg of RNase B1/mice or control PBS intraperitoneally every other day (3 days a week) for 30 days. Tumor dimensions were recorded every other day (3 days a week) and volume calculated and expressed as a function of time.

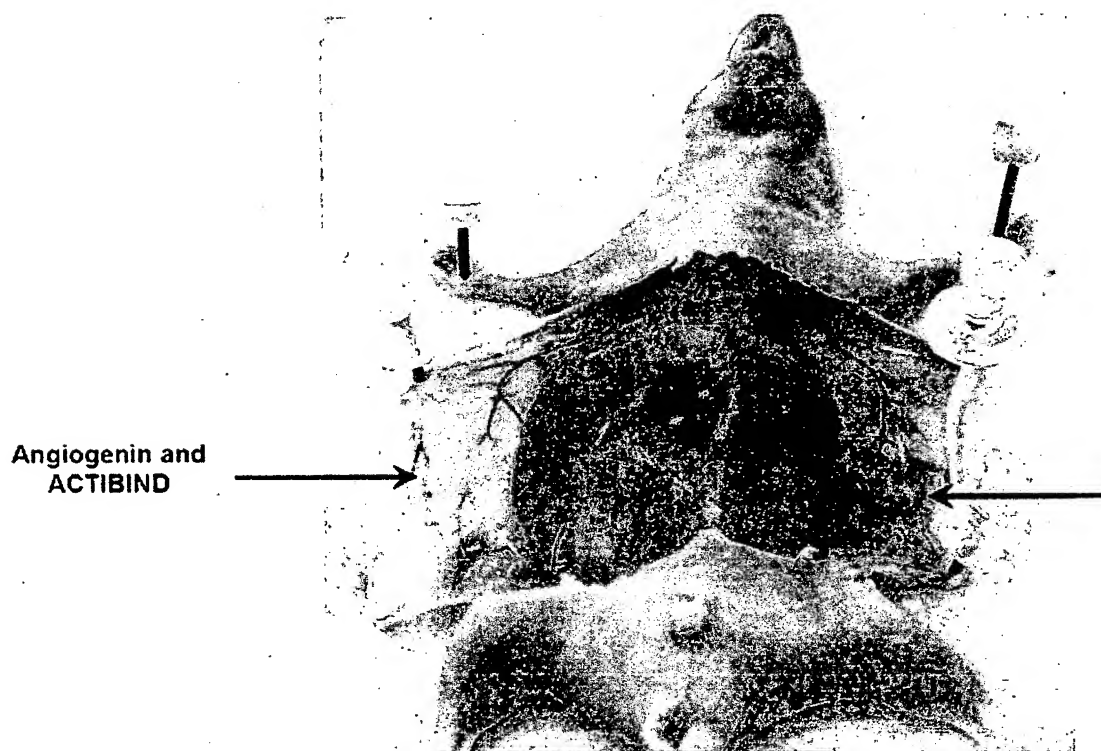
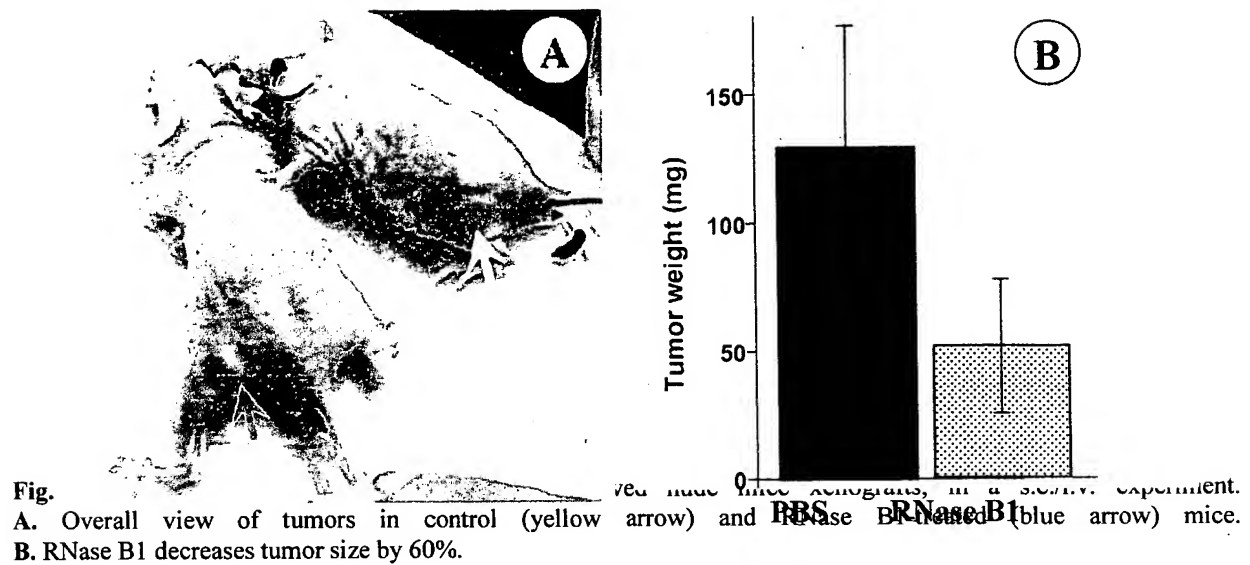


Fig. 10. In vivo angiogenesis assay: The effect of impregnation of gel foams with RNase B1 and angiogenin and implanted subcutaneously into nude mice compared to gel foams impregnated with only angiogenin. RNase B1 significantly inhibited the angiogenin-induced development of blood vessels.

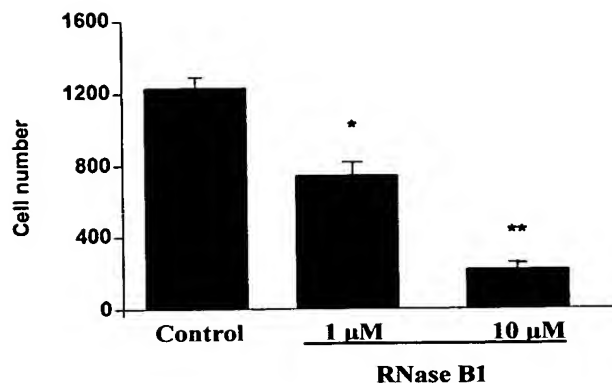


Fig. 11. RNase B1 significantly and dose dependently inhibited the ability of A375SM cells to invade through a Matrigel-coated filter, as compared to control cells: $1,216 \pm 68$ control A375SM cells penetrated Matrigel-coated filters versus 725 ± 59 A375SM cells treated with $1 \mu\text{M}$ RNase B1, $P < 0.01$; and 211 ± 14 for A375SM cells treated with $10 \mu\text{M}$ RNase B1, $P < 0.001$.

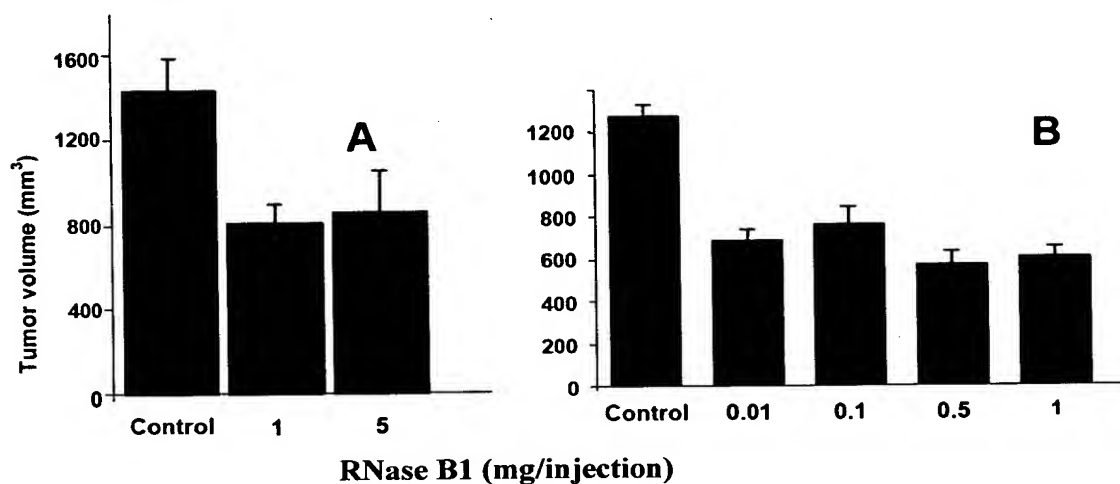


Fig. 12. HT-29-derived nude mice xenografts in sc/ip model. RNase B1 was injected starting from 24 h after cells implantation (10^6 cell/mouse) and every other day. Tumor size was measured 30 d after onset of RNase B1 treatment. RNase B1 was found to reduce tumor size in about 60% in both subsequent experiments (A and B), at a wide range of doses.

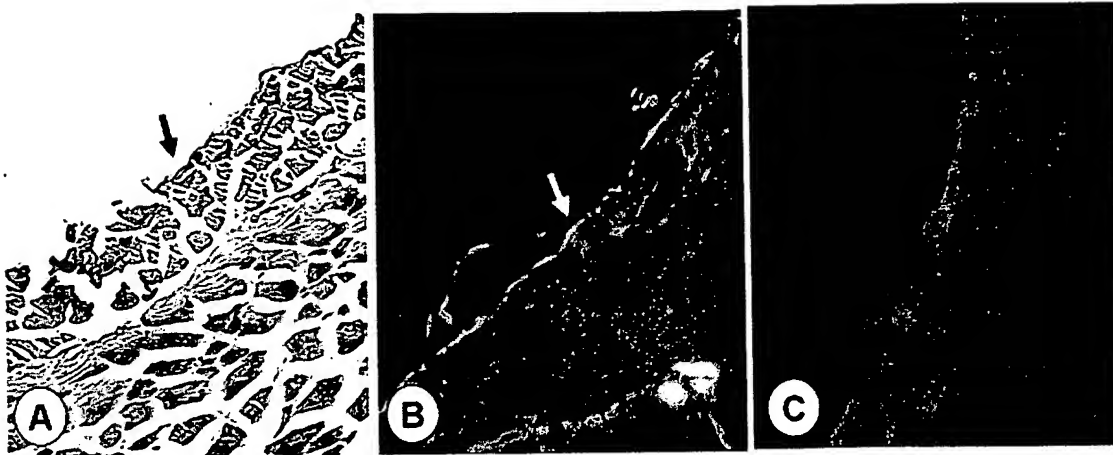


Fig. 13. Peritoneum cross sections from nude mice treated sc/ip by HT-29 cells in the presence or absence of RNase B1. **A.** Hematoxylin and eosin (H&E) staining. Note the thin peritoneum (arrow) overlaying the muscle. **B.** Immunostaining of peritoneum taken from an RNase B1-treated mouse, using rabbit anti-RNase B1 and FITC-conjugated goat anti-rabbit. Green fluorescence shows RNase B1 accumulating onto the peritoneum. **C.** The same as B, unless peritoneum was taken from a PBS-treated mouse.

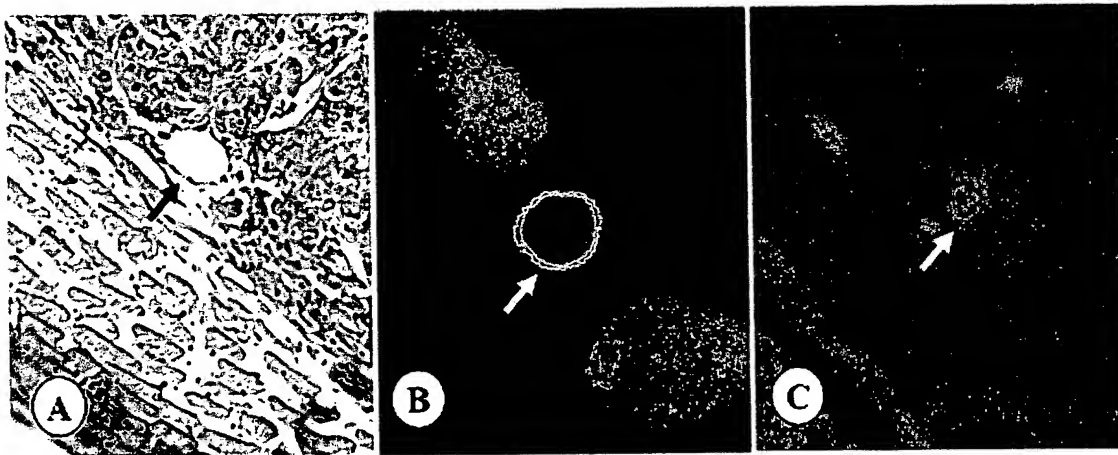


Fig. 14. Cross sections from HT-29-derived tumors from nude mice treated s.c./i.p. **A.** H&E staining. **B.** Immunostaining of a blood vessel from an RNase B1-treated tumor, using rabbit anti- RNase B1 and FITC-conjugated goat anti-rabbit. RNase B1 is accumulating onto the basal membrane. **C.** A PBS-treated tumor, labeled as described in B. Arrows indicate blood vessels.

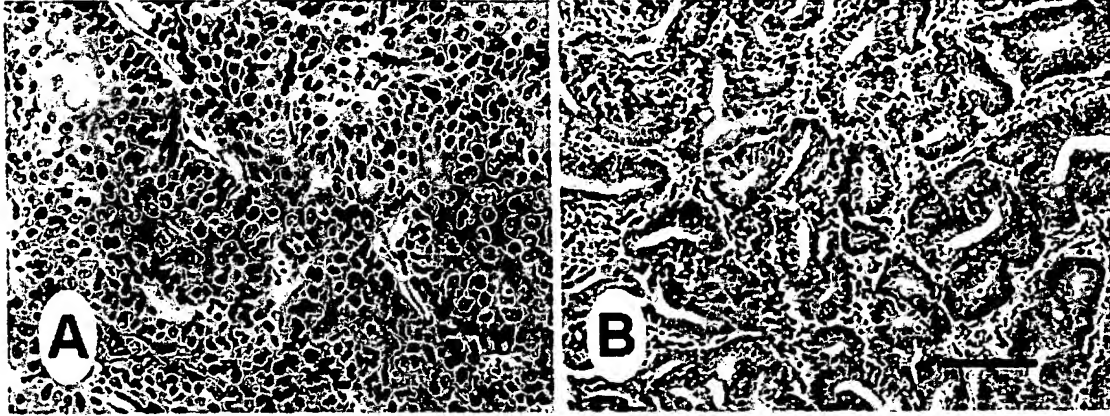


Fig. 15. The effect of RNase B1 on CD31 expression on DMH-induced colonic tumors. **A.** Section of tumors of control DMH-treated rats, CD31 staining reveals high number of large blood vessels. Magnification X200. **B.** CD31 staining of blood vessels of tumors of RNase B1-treated rats. The number and size of blood vessels is significantly lower than in control DMH-treated rats. Scale bar = 100 μ m.

CURRICULUM VITAE

4.4.04

Oded Shoseyov. The Institute of Plant Science and Genetics in Agriculture and The Otto Warburg Center for Agricultural Biotechnology, The Hebrew University of Jerusalem, The Faculty of Agriculture, Food and Environmental Quality Sciences, P.O.B. 12 Rehovot 76100, Israel.

Personal:

Birth : July 31, 1956; Rehovot, Israel.

Nationality: Israeli.

Status: Married + three children.

IDF military service: 3.5 years of active duty and currently as a Major in the reserve force.

Home address: 5 Erez, Karmeit Yosef

Education:

B.Sc. with excellence, 1981, The Hebrew University of Jerusalem.

M.Sc. with excellence, 1983, The Hebrew University of Jerusalem.
Thesis: Out of season grape production by one year old cuttings.

Ph.D. awarded *SUMMA CUM LAUDE*, 1988 The Hebrew University of Jerusalem, Thesis: The effect of the chemical composition of must on wine quality.

Postdoctoral research. Department of Biochemistry and Biophysics University of California Davis. May 1988 - August 1990.

Academic position:

Assoc. Professor since April 2002

Senior Lecturer October 1994-April 2002.

Lecturer October 1990 to September 1994.

Awards:

The Outstanding Scientist Polak Award for 2002

The 1999 Kay Award for innovative and applied research.

Elected by the students to the list of the best lecturers of the Hebrew University of Jerusalem at 1998-1999 academic year.

Other professional activities:

Scientific founder of CBD-Technologies Inc. A Biotech company established at 1995.

-Scientific co-founder of Fulcrum SP Ltd. A Biotech company established 2001.

Member of the Otto Warburg Center for Agricultural Biotechnology. 1991-present.

Sabbatical year 7.96-7.97 at the Laboratory of Biotechnology at University of British Columbia Vancouver Canada.

Member of the organizing committee for the 1996 International OIV Congress.

Member of a Agricultural Biotechnology Delegation of the Israeli Academy of Science to China. 1997.

Member of the Agricultural Biotechnology Delegation of the Israeli Ministry of Science to Korea 1998.

Member of the organizing committee for the 1996 Third International Symposium on in vitro culture and horticultural breeding. ISHS.

Member of the library committee of the Faculty of Agriculture 1995-1997.

Member of BARD competitive grant scientific peer review committee, for Horticulture 1991-1994.

Member of the scientific peer review committee for Horticulture of the Ministry of Agriculture Chief Scientist. 1991-1994.

Member of the scientific peer review steering committee for Horticulture ("MOP") of the Ministry of Agriculture Chief Scientist 1993 – 1995.

Elected representative of the Lecturers in the Council of the Faculty of Agriculture and the Senate of the Hebrew University of Jerusalem 1993-1994.

Member of the steering committee for Biotechnology of the Hebrew University (2002-present)).

Member of the infrastructure committee of the Hebrew University (2002-present)

Member of the Biotechnology committee of the Israeli National Council of High Education (2002-present).

Member in scientific societies

Member of the International Society of Plant Molecular Biology.

Member of the American Society of Microbiology.

Member of the Israeli Society of Plant Tissue Culture and Molecular Biology.

Member of the Israeli Society of Microbiology.

Member of the Israeli Society of Carbohydrates.

LIST OF PUBLICATIONS.

Theses.

1. Shoseyov O. (1988). The effect of the chemical composition of the must on the quality of the wine. Ph.D. Thesis The Hebrew University of Jerusalem. (Supervisors: Prof. B. Bravdo and Prof. R. Ikan).

Chapters in Proceedings and Books.

2. Bravdo, B., S. Shoseyov and S. Lavee (1986). The effect of ethephon on photosynthesis of grapevines. In: Dejong T.M. ed. Regulation of photosynthesis in fruit crops. International Workshop U.C. Davis, CA.
3. Shoseyov, O., B. Bravdo, R. Ikan and I. Chet. (1987). Monoterpene glycoside hydrolysis by beta-glucosidase from immobilized *Aspergillus niger*. Proc. Int. Symp. The aromatic substances in grapes and wines. eds: A. Scienza and G. Versini. pp. 63-71.
4. Bravdo, B., O. Shoseyov, R. Ikan and A. Altman (1987). Free and bound monoterpene content of leaves and berries and their biosynthesis by *in vitro* grown berries. Proc.Int.Symp. The aromatic substances in grapes and wines. eds: A. Scienza and G.Versini. pp. 55-62.
5. Cohen, S., O. Shoseyov and B. Bravdo (1987). The relationship between aroma, color and monoterpene content of non muscat varietal wines. Proc.Int.Symp. The aromatic substances in grapes and wines. eds: A. Scienza and G. Versini. pp. 279-288.
6. Shoseyov, O., and M. Dekel-Reichenbach (1992). The role of endo-1,4-beta-glucanase in plant cell elongation. In-vitro studies of peach pollen. Acta Hort.329: 225-227.
7. Droby S., M. Wisniewski, C. Wilson, A. Avraham, O. Shoseyov and E. Chalutz. (1992) Possible modes of action of yeast antagonists of postharvest diseases. IOBC-EFPP workshop Nov. 1992 Wageningen, Holand Bul. OILB/SROP 16:186-189.
8. Doi R.H., M. Takagi, M.A. Goldstien, S. Hashida, O. Shoseyov, and M. McGloughlin (1993). Biotechnology approaches to problems in agriculture; analysis of *Clostridium cellulovorans* Cellulase. In: BIOTECHNOLOGY, Theory and Applications, eds. Tien W., S.F. Chen,

L. Lo, and Y.T. Shyu. The Third Pacific Rim Biotechnology Conference. Development Center for Biotechnology.

9. Ikan R., V. Weinsten, Y. Milner, B. Bravdo, and O. Shoseyov, D. Siegel A. Altman and I. Chet. Natural glycosides as potential odorants and flavorants. In: International Symposium on Medical and Aromatic Plants, eds. Palevitch D. and E. Putievskky. Tiberias, Israel March 1993.

10. Doi R.H., M.A. Goldstien, J.S. Park, C.C. Liu, S. Hashida, Y. Matano, M. Takagi, S. Hashida, F.C. Foong, T. Hamamoto, I. Segel and O. Shoseyov. Structure and Function of the Subunits of the *Clostridium cellulovorans* cellulosome. In: Genetics, Biochemistry, and Ecology of Lignocellulose Degradation, eds. Shimada K., K. Ohmiya, Y. Kobayashi, S., Hoshino, K. Sakka and S. Karita. pp 43-52. Uni Publishers, Tokyo, Japan, 1994.

11. Altman A., A. Ya'ari, D. Pelah, A. Gal, T. Tzfira, W-X, Wang, O. Shoseyov, A. Vainstein and J. Riov.(1995) In vitro organogenesis, transformation and expression of drought-related proteins in forest tree cultures. In: Current Issues in Plant Molecular and Cellular Biology ed. M. Terzi. pp. 87-94. Kluwer Academic Publishers. Netherlands.

12. Pelah D., A. Ya'ari, A. Altman O. Shoseyov, and J. Riov. Growth, in vitro propagation and desiccation-specific proteins of *Populus* and *Pinus* tissues. Proc. IVFRO, Beijing, 1994.

13. Altman, A., D. Pelah, O. Yarnitsky, T. Tzfira, A. Ya'ari, W-X. Wang, O. Shoseyov, A. Vainstein, A. Huttermann and S. Wang (1996). Towards water stress-tolerant poplar and pine trees: Molecular biology, transformation and regeneration. In: M.R. Ahuja, W. Boerjan and D.B. Neal, eds., Somatic Cell Genetics and Molecular Genetics of Trees, pp. 47-56, Kluwer Academic Publishers, Dordrecht.

14. Pelah D, Altman A and Shoseyov O (1997) Drought tolerance a molecular perspective. Proceeding of the Third International ISHS Symposium on In Vitro Culture and Horticultural Breeding. Eds. A Altman and M. Ziv. Acta Horticulturae 447: 439-445.

15. Wang, W., D. Pelah, A. Altman, and O. Shoseyov. (1997). Clonal differences in the expression of a water stress related protein BspA in populus spp. Proceeding of the Third International ISHS Symposium on

In Vitro Culture and Horticultural Breeding. Eds. A Altman and M. Ziv. Acta Horticulturae 447: 467-468.

16. Shoseyov O., E. Shpigel, and L. Roiz (1997) Cellulose-binding domain (CBD) modulates in-vitro elongation of different plant cells. Proceeding of the Third International ISHS Symposium on In Vitro Culture and Horticultural Breeding. Eds. A Altman and M. Ziv. Acta Horticulturae 447: 583-589.

17. Shani Z., E. Shpigel, L. Roiz, R. Goren, B. Vinocur, T. Tzfira, A. Altman. Shoseyov O., Cellulose binding domain, increases cellulose synthase activity in *Acetobacter xylinum*, and biomass of transgenic plants (1999). In: A. Altman, M. Ziv, S. Izhar, eds., Plant Biotechnology and In Vitro Biology in the 21st Century, pp. 213-218 Kluwer Academic Publishers

18. Shani Z., M. Dekel, G. Tzbary, C. S. Jensen, T. Tzfira R. Goren, A. Altman and O. Shoseyov. Expression of *Arabidopsis thaliana* endo-1,4- β -glucanase (cell) in transgenic plants (1999). In: A. Altman, M. Ziv, S. Izhar, eds., Plant Biotechnology and In Vitro Biology in the 21st Century, pp. 209-212. Kluwer Academic Publishers

19. W. X. Wang, T. Tzfira, N. Levin, O. Shoseyov and A. Altman. Plant tolerance to water and salt stress: The expression pattern of a water stress responsive protein (BspA) in transgenic aspen plants (1999). In: A. Altman, M. Ziv, S. Izhar, eds., Plant Biotechnology and In Vitro Biology in the 21st Century, pp. 561-565. Kluwer Academic Publishers.

20. Doi, R.H., Goldstein, M., Takagi, M., Hashida, S., Shoseyov, O. and Segel, I. (1999). Structure and function of *Clostridium cellulovorans* cellulase subunits. In Environment, Science and Technology: The Challenge of the 21st Century, p. 479-485. Chulabhorn Research Institute, Bangkok, Thailand

21 Bravdo B. and O. Shoseyov (2000). Aroma studies of fruits and wine in Israel. Acta Hort. 526: 399-406.

22 Shoseyov O. and B. Bravdo (2001). Enhancement of wine aroma; biotechnological approach. In: Molecular Biology and Biotechnology of Grapevine. Kalliopei A. Roubelakis-Angelakis, Editor. pp. 225-237. Kluwer Publishers.

23 Oded Shoseyov, Ilan Levy, Ziv Shani, and Shawn Mansfield. Modulation of wood fibers and paper by cellulose binding domains (CBDs). Proceedings of *The 223th American Chemical Society National Meeting*. April 2002. Orlando, Florida, USA. (In press)

Review articles

24. Shoseyov O., Tsabary G. and Reuveni O. Detection of dwarf somaclones of banana cultivars (*Musa*) by RAPD markers. Pp. 595-601. In *Somaclonal Variation and Induced Mutations in Crop Improvement*. Eds. S. Mohan Jain, D. S. Brar, and B.S. Ahloowalia. (1998) ISBN 0-7923-4162-1 Kluwer Academic Publishers.

25. Shoseyov O., and R.A.J. Warren (1997) Cellulose binding domains- A novel fusion technology for efficient, low cost purification and immobilization of recombinant proteins. in *Novation* 7:1-3.

26. Shoseyov O. (2002) Cellulose binding domains: Industrial and biotechnological application. *Biotechnol. Adv.* **20**:191-213.

27 Ilan Levy, Ziv Shani and Oded Shoseyov. (2002) Modification of polysaccharides and plant cell wall by Endo-1,4- β -glucanase (EGase) and Cellulose binding domains (CBD). *Biomol. Eng.* **19**:17-30

28. Ilan Levy and Oded Shoseyov (2004). Cross Bridging Proteins In Nature and their Utilization in Bio- and Nanotechnology. (review). *Curr Protein Pept Sci.* **5**(1):33-49.

29.. Wang W.X., B. Vinocur, O. Shoseyov and A. Altman (2004) The role of plant heat-shock proteins/molecular chaperones in the abiotic stress response. *Trends in Plant Science*. (in press).

Publications in peer reviewed journals

30. Shoseyov, O., B. Bravdo, R. Ikan and I. Chet (1988). Endo-beta-glucosidase from *Aspergillus niger* grown on a monoterpene glycoside-containing medium. *Phytochemistry* **27**:1973-1976.

31. Shoseyov, O., B. Bravdo, D. Siegel, A. Goldman, S. Cohen and R. Ikan. (1990). Iso-geraniol, 3,6-octadiene-3,7-dimethyl-1-ol: A novel monoterpene in *Vitis vinifera* L. c.v. Muscat Roy. *Vitis* 29:159-153.
32. Shoseyov, O., B. Bravdo, D. Siegel, A. Goldman, S. Cohen, L. Shoseyov and R. Ikan. (1990). Immobilized endo-beta-glucosidase enriches flavor of wine and passion fruit juice. *J.Agric.Food Chem.*39:1387-1390.
33. Bravdo, B., O. Shoseyov, R. Ikan and A. Altman. (1990). Monoterpene glycoside biosynthesis in detached grape berries grown *in vitro*. *Physiol. Plant.* 78:93-99.
34. Shoseyov O., T. Hamamoto, F. Foong and R.H. Doi. (1990). Cloning of *Clostridium cellulovorans* endo-1,4-beta-glucanase genes. *Biochem. Biophys. Res. Comm.* 169:667-672.
35. Hamamoto, T., O. Shoseyov, F. Foong and R.H. Doi (1990). A *Clostridium cellulovorans* gene, engD, codes for both endo-beta-1,4-glucanase and cellobiosidase activities. *FEMS microbiol. Lett.* 72:285-288.
36. Shoseyov, O. and R.H. Doi (1990). Essential 170 kDa subunit for degradation of crystalline cellulose by *Clostridium cellulovorans* cellulase. *Proc. Nat. Acad. Sci. USA.* 87:2192-2195.
37. Bruckner, R., O. Shoseyov and R.H. Doi (1990). Multiple active forms of novel serine protease from *Bacillus subtilis*. *Mol. Gen. Genet.* 221:486-490.
38. Shoseyov, O., M. Goldstein, F. Foong, T. Hamamoto and R.H. Doi (1991). Nucleotide sequence of *Clostridium cellulovorans* gene, homologous to cyclic-AMP dependent kinase. *Nucleic Acids Research.* 19:1710.
39. Foong, F., T. Hamamoto, O. Shoseyov and R.H. Doi (1991). Nucleotide sequence and characteristics of endoglucanase gene engB from *Clostridium cellulovorans*. *J. Gen. Microbiol.* 137:1729-1736.
40. Shoseyov, O., M. Takagi, M.A. Goldstein and R.H. Doi (1992). Primary sequence of *Clostridium cellulovorans* cellulose binding protein A (cbpA). *Proc. Nat. Acad. Sci. USA.* 89:3483-3487.

41. Hamamoto, T., F. Foong, O. Shoseyov and R.H. Doi. (1992) Analysis of functional domains of endoglucanases from *Clostridium cellulovorans* by gene cloning, nucleotide sequencing and chimeric protein construction. *Mol. Gen. Genet.* 231:472-479.
42. Goldstien, M.A., M. Takagi, S. Hashida, O. Shoseyov, R.H. Doi and I. H. Segel (1993). Characterization of the Cellulose Binding Domain of the *Clostridium cellulovorans* Cellulose Binding Protein A (Cbpa). *J. Bacteriol.* 175: 5762-5768.
43. Levitov, S., O. Shoseyov and S. Wolf. (1994). Roles of different seed components in controlling tomato seed germination at low temperatures. *Scientia. Hort.* 56: 197-206.
44. Rotem Y., O. Shoseyov and A. Sztejnberg. (1995). The Roll of 'cellulase' (endo-1,4-beta-glucanase) in gummosis diseases of apricot. *J. of Phytopathology* 143:7-10.
45. Levitov S., O. Shoseyov and S. Wolf. (1995). Involvement of endomannanase in the control of tomato seed germination under low temperature conditions. *Annals of Botany.* 76: 1-6.
46. Roiz L. and O. Shoseyov (1995) Stigmatic RNase in self-compatible peach (*Prunus persica*) . *Int. J. Plant Sci.* 156(1):37-41.
47. Pelah D., O. Shoseyov and A. Altman (1995) Characterization of BspA, a major boiling-stable, water-stress-responsive protein in aspen (*Populus tremula*). *Tree Physiol.* 15:673-678.
48. Lider O., L. Cahalon, D. Gilat, R. HersHKoviz, D. Siegel, R. Margalit, O. Shoseyov and I. R. Cohen (1995). A Disaccharide that inhibits Tumor Necrosis Factor- α is formed from the extracellular matrix by the enzyme heparanase. *Proc. Nat. Acad. Sci. USA* 92:5037-5041.
49. Roiz, L., R. Goren and O. Shoseyov. (1995) Stigmatic RNase in calamondin (*Citrus reticulata* var. *austera* x *Fortunella* sp.). *Physiol. Plant.* 94:585-590.
50. Izhaki, A., O. Shoseyov and D. Weiss (1995). A petunia cDNA encoding S-adenosylmethionine synthetase. *Plant Physiol.* 108(2):841-2.

51. Birk, R., B., Bravdo and O. Shoseyov (1996). Detoxification of cassava by *Aspergillus niger* B-1. App. Microbiol. Biotechnol.45(3): 411-414.
52. Izhaki, A., O. Shoseyov and D. Weiss (1996). Temporal, spatial and hormonal regulation of the S-adenosylmethionine synthase gene in petunia. Physiol. Plant. 97:90-94.
53. Pelah D, Wang W-X, Altman A, Shoseyov O and Bartels D (1997) Differential Accumulation of water-stress related proteins in populus species which differ in their water-stress response. Physiol Plant 99:153-159.
54. Birk, R., Ikan, A., Bravdo, B, Braun, S., and O. Shoseyov (1997). Synthesis of isopropyl-1-thio- β -D-glucopyranoside (IPTGlc), an inducer of *Aspergillus niger* B1 β -glucosidase production. App. Biochem. and Biotechnol. 66: 25-30.
55. Shani, Z., Dekel M., Tsabary G., and O Shoseyov (1997). Cloning and characterization of elongation specific endo-1,4- β -glucanase (*cell*) from *Arabidopsis thaliana*. Plant Mol.Biol. 34: 837-842.
56. Pelah D., O.Shoseyov, A. Altman and D. Bartels (1997). Water-stress response in aspen (*Populus tremula*): Differential accumulation of dehydrin, sucrose synthase, GAPDA homologues, and soluble sugars. J. Plant Physiol. 151: 96-100.
57. Shpigel E., L. Roiz R. Goren and O. Shoseyov (1998) Bacterial Cellulose-Binding Domain Modulates in Vitro Elongation of Different Plant Cells. Plant Physiol. 117: 1185-1194.
58. Shpigel E., D. Elias, I.R. Cohen and O. Shoseyov (1998) Production and purification of a recombinant human hsp60 epitope using the cellulose-binding domain in *Escherichia coli*. Protein Expression & Purification 14: 185-191.
59. Rechter M., O. Lider, L. Cahalon, E. Baharav, M. Dekel, D. Seigel, I. Vlodavsky, H. Aingorn, I. Cohen and O. Shoseyov. (1999). A Cellulose-Binding Domain-Fused to Recombinant Human T Cell

Connective Tissue Activating Peptide-III Manifests Heparanase Activity. *Biochem. Biophys. Res. Com.* 225: 657-662.

60. Shpigel, E., A. Goldlust, G. Efroni, A. Avraham, A. Eshel, M. Dekel, and O. Shoseyov (1999). Immobilization of recombinant heparinase I fused to cellulose-binding domain. *Biotechnology and Bioengineering* 65(1): 17-23.

61. Maurice, S., H. Dietland, M. Dekel, R. Friedman, A. Gertler and O. Shoseyov. (1999). A-Protein from achromogenic atypical *Aeromonas salmonicida*: molecular cloning, expression, purification, and characterization. *Protein Expression and Purification*. 16:396-404.

62. Roiz L., Ozeri U., Goren R. and O. Shoseyov. (2000). Characterization of *Aspergillus niger* B-1 RNase and its inhibitory effect on pollen tube growth in some fruit trees. *J. Am. Soc. Hort. Sci.* 121(1):9-14.

63. Shani Z., Dekel M., Jensen C. S., Tzfira T., Goren R. (R), Altman A. (R) and Shoseyov O. (2000) *Arabidopsis thaliana* endo-1,4- β -glucanase (*cell1*) promoter mediates *uidA* expression in elongating tissues of aspen (*Populus tremula*). *J. Plant Physiol.* 156: 118-120.

64. Siegel D., I. Marton, M., Dekel, B. Bravdo, S. He, S.G. Withers, and O. Shoseyov (2000). Cloning, expression, characterization and nucleophile identification of family 3, *A. niger* β -glucosidase. *J. Biol. Chem.* 275(7): 4973-4980.

65. Kauffmann C., E. Shpigel, E. A. Bayer, R. Lamed, Y. Shoham, R. Mandelbaum, and O. Shoseyov (2,000) A novel methodology for enzymatic removal of atrazine from water by CBD-fusion protein immobilized on cellulose. *Environ. Sci. Technol.* 34(7):1292-1296.

66. Shpigel E., A. Goldlust, A. Eshel, I. Kaplan Ber, G. Efroni, Y. Singer, I. Levi, M. Dekel, and O. Shoseyov (2000). Expression, purification and applications of staphylococcal protein A fused to cellulose-binding domain. *Biotechnology and Applied Biochemistry* 31(3)-197.

67. Neta-Sharir I., O., Shoseyov and D. Weiss (2000). Sugar enhance the expression of gibberlin-induced genes in developing petunia flowers *Physiol. Plant.* 109:196-202.
68. Levy I., and O. Shoseyov (2001). Expression refolding and indirect immobilization of horseradish peroxidase (HRP) to cellulose via a phage selected peptide and cellulose binding domain (CBD). *J. Peptide Science.* 7: 50-57.
69. Regev G., M. Dekel O. Shoseyov and Z. Kerem (2001) Resveratrol and a novel tyrosinase in Carignan grape juice. *J. Agric. Food Chem.* 49(3): 1479-1485.
70. Ilan Levy, Amos Nussinovitch, Etai Shpigel and Oded Shoseyov. (2002) Recombinant cellulose crosslinking protein: a novel paper-modification biomaterial. *Cellulose* 9:91-98.
71. Galit Tsabary, Ziv Shani, Levava Roiz, Ilan Levy, Joseph Riov and Oded Shoseyov. (2003) Abnormal "wrinkled" cell walls and retarded development of transgenic *Arabidopsis thaliana* plants expressing endo-1,4- β -glucanase (cell) antisense. *Plant Mol. Biol.* 15:213-224
72. Ayelet Fishman, Ilan Levy, Uri Cogan and Oded Shoseyov. (2002) Stabilization of horseradish peroxidase in aqueous-organic media by immobilization onto cellulose using a cellulose-binding domain. *J. Mol. Catal. B-Enzym.* 18:115-125.
73. Wang WX, Pelah D., Alegrant T., Shoseyov O., and A. Aaltman (2002). Characterization of SP1, a stress-responsive, boiling-soluble, homo-oligomeric protein from aspen. *Plant Physiology* 130(2): 865-75.
74. Ilan Levy, Gary Ward, Yitzhak Hadar, Oded Shoseyov and Carlos G. Dosoretz. (2003). Oxidation of 4-bromophenol by recombinant cellulose binding domain horseradish peroxidase fused protein immobilized to cellulose. *Biotech. Bioeng.* (In press).
75. Maurice S, Dekel M, Shoseyov O, Gertler A. (2003). Cellulose beads bound to cellulose binding domain-fused recombinant proteins; an adjuvant system for parenteral vaccination of fish. *Vaccine.* 21:3200-7.
76. Ilan Levy, Tzur Paldi, Dan Siegel and Oded Shoseyov (2003)

Cellulose binding domain from *Clostridium cellulovorans* as a paper modification reagent. *Nordic Pulp and Paper Research Journal*. 18:421-7.

77. Regev-Shoshani G, Shoseyov O, Bilkis I, Kerem Z. (2003) Glycosylation of resveratrol protects it from enzymic oxidation. *Biochem J*. 374:157-63.

78. Tsabary Galit, Ziv Shani, Levava Roiz, Ilan Levy, Joseph Riov and Oded Shoseyov. (2003) Abnormal "wrinkled" cell walls and retarded development of transgenic *Arabidopsis thaliana* plants expressing endo-1,4- β -glucanase (*cell*) antisense. *Plant Mol. Biol.* 15:213-224.

79. Tzur Paldi, Ilan Levy and Oded Shoseyov.(2003) Starch binding domain from *Aspergillus niger* B1: molecular cloning, and functional characterization. *Biochem. J*. 372:905-10.

80. Ilan Levy, Gary Ward, Yitzhak Hadar, Oded Shoseyov and Carlos G. Dosoretz.(2003) Oxidation of 4-bromophenol by recombinant cellulose binding domain horseradish peroxidase fused protein immobilized to cellulose. *Biotech. Bioeng.* 82:223-31.).

81. Wang W.X., O. Dgany, O. Dym A. Altman O. Shoseyov and O. Almog(2003) Crystallization and preliminary X-ray crystallographic analysis of SP1, a novel chaperone-like protein. *Acta Crystallogr D Biol Crystallogr*. 59:512-4.

82. Ilan Levy, Tzur Paldi and Oded Shoseyov (2004) Engineering a bifunctional starch-cellulose cross-bridge protein. *Biomaterials*. 25:1841-9.

83. Shu Wei, Ira Marton, Mara Dekel, Dror Shalitin , Efraim Lewinsohn, Ben-Ami Bravdo, and Oded Shoseyov (2004) Manipulating volatile emission in tobacco leaves by expressing *Aspergillus niger* β -glucosidase in different subcellular compartments. *Plant Biotechnol. J* (in press)

Patents

84. Shoseyov, O., B. Bravdo and R. Ikan . High volume "on column" injector for head space analysis in fused silica capillary column. Israel patent No. 84616, 1987
85. Shoseyov, O. B. Bravdo , R. Ikan and I. Chet. Production and utilization of specific endo-beta-glucosidase for food, wine and perfume industries. Israel patent No. 8290-2 1987.
86. Cohen I. R., O. Lider, L. Cahalon, O. Shoseyov and R. Margalit. (1999). Methods for regulation of active TNF-alfa. U.S. patent 5,861,382.
87. Shoseyov O., L. Roiz, U. Ozeri, B. Bravdo and R. Goren. (1996). Methods for the biological control of pollen in plants. U.S. Patent 5,552,139.
88. Shoseyov O., I. Shpigel, Goldstien, M.A., and R.H. Doi. (1996). Nucleic acids encoding a cellulose binding domain. U.S. Patent 5,496,934
89. Shoseyov, O., Shpigel, I., Goldstein, M.A., and Doi, R.H. (1995). Methods of use of cellulose binding domain. US Patent 5,670,623
90. Shoseyov, O. (1998). Kits and methods of detection using cellulose binding domain fusion proteins. US Patent 5,738,984
91. Shoseyov, O., Shpigel, I., Goldstein, M.A., and Doi, R.H. (1999). Methods of detection using of cellulose binding domain fusion product. US Patent 5,856,201
92. Shoseyov, O. Shpigel, E. Goldstein, M. A. Doi, R. H. (1998) Cellulose Binding Domains Fusion Proteins. US Patent 5,719,044
93. Shoseyov, O., Shpigel, I., Goldstein, M.A., and Doi, R.H. (1998). Cellulose Binding Domain Proteins. US Patent 5,837,814
94. Shoseyov, O. Shani, Z. Shpigel, E. (2001). Transgenic plants of altered morphology. US patent 6,184,440.

95. Shoseyov, O. Shani, Z. (1999). *Arabidopsis Thaliana* Endo-1,4- β -glucanase gene, promoter and protein. US patent allowed
96. Kilburn, D., Warren, R.A.J., Stoll, D., Gilkes, N.R., Shoseyov, O., Shani, Z.. (1998). Use of mannan binding domain to alter plant morphology. US patent pending
97. Siegel, D., Shoseyov, O (1999). Method of releasing solid matrix affinity adsorbed particulates. US patent pending.
98. Siegel, D., Shoseyov, O (1999). Method of concentrating microorganisms using affinity separation US patent pending.
99. Shani, Z. , Shoseyov, O (1999). Process of expressing and isolating recombinant protein products from plants, plant derived tissues or cultured plant cells. US patent pending.
100. Cohen I. R., O. Lider, L. Cahalon, O. Shoseyov and R. Margalit. (2001). Compositions for regulation of cytokines. European Patent 0669827.
101. Ilan levy, Amos Nussinovitch and Oded Shoseyov. Modification of polysaccharide containing materials. PCT, WO 01/34091 A2.

Papers in non-reviewed journals.

102. Shoseyov, O., B. Bravdo, R. Ikan and I. Chet and D. Siegel (1988). The improvement of wine quality. Ladaat 18:3-4 (Hebrew).
103. Shoseyov O. (1999). Cellulose binding proteins and their applications. Chemistry 46: 20-23 (Hebrew).
104. Shoseyov O. (2000). Cellulose binding proteins, a platform technology. Tazpit (in press Hebrew).

Lectures in scientific meetings.

105. Shoseyov, O., B. Bravdo and R. Ikan. Free and bound monoterpenoides in non muscat varieties. Int. Symp. Vitic. Enol. 1986 Kecskemet, Hungary.

106. Shoseyov, O. B. Bravdo, R. Ikan and I. Chet. Improvement of wine quality by immobilized endo-beta-glucosidase. ASEV Ann. Meet. 1988 Reno Nevada, USA
107. Shoseyov, O., and M. Dekel-Reichenbach. The role of endo-1,4-beta-glucanase in plant cell elongation. In-vitro and in-vivo studies of peach pollen tubes and transgenic *Arabidopsis thaliana* plants. 7th International Symposium on Plant Growth Regulators in Fruit Production. June 1992 Jerusalem, Israel.
108. Shoseyov O. I. Shpigel, L. Roiz, G. Shoham and O. Almog. Cellulose binding protein: structure and function. The joint meeting of the Israeli Societies for Botany and Plant Molecular Biology. February 1993. Jerusalem, Israel.
109. Shoseyov O., L. Roiz , and E. Shpigel. Cellulose binding protein modulates plant cell elongation. 4th International Congress of Plant Molecular Biology. June 1994 Amsterdam, The Netherlands.
110. Shoseyov O., L. Roiz, and E. Shpigel. Cellulose binding protein modulates plant cell elongation: mode of action. The Cell Wall Meeting. 1995 Spain.
111. Shoseyov O. Cellulose-binding domain (CBD) modulates in-vitro elongation of different plant cells. The Third International ISHS Symposium on In Vitro Culture and Horticultural Breeding. June 1996. Jerusalem, Israel.
112. Shoseyov O. Cellulose binding domain, increases cellulose synthase activity in *Acetobacter xylinum* and biomass of transgenic plants. Plant Biotechnology and Invitro Biology in the 21st Century. IX International Congress of Plant Tissue and Cell Culture. June 1998 Jerusalem, Israel (Invited speaker).
113. Shoseyov O. Modification of polysaccharide biosynthesis by cellulose binding domain. Biotechnology of polysaccharides Meeting. 1998 Beer Sheva, Israel. (Invited speaker)
114. Shoseyov O. Transgenic plants expressing new genes for polysaccharide modifications. The Israel Biotechnology Committee, November 1998 Rehovot Israel (Invited speaker)

115. Shoseyov O. Biotechnological applications of cellulose binding domain. The 2nd FISEB meeting. December 1998 Eilat Israel.
116. Shoseyov O. Cellulose binding domains: a new platform for protein engineering. The annual meeting of the Israel society of Microbiology 1999 Rehovot Israel (Invited speaker)
117. Shoseyov O. Modification of polysaccharide biosynthesis by cellulose binding domain. May 1999 The Wolf Prize Symposium Haifa, Israel. (Invited speaker).
118. Shoseyov O. Cellulose binding domain: A novel enhancer of agricultural productivity of transgenic plants. Cambridge Helthtech Institute's meeting on Molecular Biology's Role in Enhancing Agricultural Productivity. March 1999 Amsterdam, The Netherlands. (Invited speaker)
119. Shoseyov O. Why plant cellulases lack CBDs. Gordon Research Conference on "Cellulases and Cellulosomes". July 1999 Proctor Academy, New Hampshire USA. (Invited speaker).
120. Shoseyov O. "Advanced Course of Forest Biotechnology and Enzymology" 1999. The Royal Institute of Technology, Sweden. (Invited lecturer)
121. Shoseyov O. Transgenic poplar trees expressing cellulose binding domain. Forestry Biotechnology meeting. November 1999 Pune, India. (Invited speaker).
122. Shoseyov O. Modifications of polysaccharide biosynthesis and plant growth by cellulose binding domain and endo-1,4-beta-glucanase in transgenic plants. The 219th American Chemical Society National Meeting. Biotechnology Applications in Food and Agriculture. March 2000 San Francisco, USA. (Invited speaker).
123. Shoseyov O. Biotechnological applications of CBDs. Gordon Research Conference on "Cellulases and Cellulosomes". July 2001 Proctor Academy, New Hampshire USA. (Invited speaker).
124. Shoseyov O. Modulation of wood fibers and studies on the mode of action of cellulose-binding domains (CBDs). Tree Biotechnology in

the new millennium. IUFRO/Molecular biology of forest trees. July 2001
Colombia River Gorge, USA. (Invited speaker).

125. Shoseyov O. Modulation of wood fibers and studies on the mode of action of cellulose-binding domains (CBDs). 9th International Cell Wall Meeting. September 2001 Tolosan, France.

126. Oded Shoseyov, Ziv Shani, Ilan Levy, Zur Paldi. CBD fusion proteins; novel components of composite materials in-vivo and in-vitro. Gordon Research Conferences "cellulases and cellulosomes". Proctor Academy Andover, USA. August 2001.

127. Oded Shoseyov, Ziv Shani, Ilan Levy, and Shawn Mansfield. Modulation of wood fibers and paper by cellulose binding domains (CBDs). The 223th American Chemical Society National Meeting. April 2002. Orlando, Florida, USA (Invited speaker).

128. Oded Shoseyov, Ziv Shani, Ilan Levy, Shawn Mansfield, and Mara Dekel. Modification of wood fibers by carbohydrate-binding modules. XXIst International Carbohydrate Symposium. July 2002. Cairns, Australia. (Invited speaker)

129. Ilan Levy, Tzur Paldi and Oded Shoseyov. Engineering carbohydrate-binding modules for polysaccharide crosslinking. XXIst International Carbohydrate Symposium. July 2002. Cairns, Australia.

130. Oded Shoseyov, Ziv Shani, Etai Shpigel, Galit Tsabary, Levava Roiz, Mara Dekel, Ilan Levy. Modification of polysaccharide biosynthesis and plant growth by cellulose-binding domain and endo-1 4-beta-glucanase in transgenic plants. 28th Meeting of the Federation of European Biochemical Societies. October 2002 Istanbul, Turkey. (Invited speaker).

131. Shoseyov O. Industrial applications of Polysaccharide Binding Moduels. Gordon Research Conference on "Cellulases and Cellulosomes". July 2003 Proctor Academy, New Hampshire USA. (Invited speaker).

J Drug Target. 1999;6(6):439-48.

Related Articles, Links

Technology to obtain sustained release characteristics of drugs after delivered to the colon.**Hu Z, Kimura G, Ito Y, Mawatari S, Shimokawa T, Yoshikawa H, Yoshikawa Y, Takada K.**

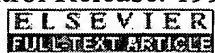
Department of Pharmacokinetics, Kyoto Pharmaceutical University, Japan.

To determine the necessary technology by which sustained drug release is obtained after drug is delivered to the colon, two kinds of microcapsules were prepared and were filled in a pressure-controlled colon delivery capsule (PCDC). As a model drug 5-aminosalicylic acid (5-ASA) was used, because the target site of 5-ASA is the entire large intestine. 5-ASA was microencapsulated using a water-insoluble polymer, ethylcellulose (EC) or with pH-sensitive polymers, Eudragit L-100 or S-100 and encased in PCDC. The particle size of these microcapsules was around 800 microns and the loading efficiencies of 5-ASA were approximately 90%. In vitro dissolution tests were performed with the prepared microcapsules. The release rate of 5-ASA from the microcapsules was significantly prolonged as compared to 5-ASA powder, although there were no significant differences in the release rates between these microcapsules. By incorporating the 5-ASA microcapsules into PCDC, sustained release PCDCs for colon delivery were prepared and in vivo evaluation was performed using beagle dogs. As a fast release colon delivery system, PCDCs were prepared with 5-ASA powder suspended in suppository base. After oral administration of the test preparations to beagle dogs, plasma 5-ASA concentrations were measured and sustained release characteristics of 5-ASA from the test preparations were evaluated from the plasma 5-ASA concentration-time profiles. The first appearance time of 5-ASA into the systemic circulation after oral administration were 3 h for all the colon delivery preparations and it was thought that these test preparations were delivered to the colon. Both EC microcapsules and Eudragit S-100/RS-100 microcapsules in PCDC showed longer the mean residence time MRT, 8.2 ± 0.6 h and 8.7 ± 0.9 h, than Eudragit L-100/RS-100 microcapsules in PCDC where the MRT was 6.6 ± 0.2 h. Since PCDCs containing 5-ASA powder exhibited a MRT of 7.0 ± 1.0 h, these two types of preparations have suggested sustained release characteristics.

PMID: 10937289 [PubMed - indexed for MEDLINE]

J Control Release. 1999 Jun 2;59(3):361-76.

Related Articles, Links

**Evaluation of colonic absorbability of drugs in dogs using a novel colon-targeted delivery capsule (CTDC).****Ishibashi T, Ikegami K, Kubo H, Kobayashi M, Mizobe M, Yoshino H.**

Pharmaceutics Research Laboratory, Tanabe Seiyaku Co., Ltd., 16-89, Kashima 3-chome, Yodogawa-ku, Osaka 532, Japan. ryu-i@tanebe.co.jp

A series of dog studies were performed to examine the in vitro/in vivo relationship of drug release behavior of the newly developed colon-targeted delivery capsule (CTDC). The four kinds of CTDCs containing theophylline, each of which has a different in vitro dissolution lag time, were orally administered to four beagle dogs under fasted condition, and the onset times of drug absorption were compared. The CTDC with longer in vitro lag time had a later onset of drug absorption. It was also found that the time difference between the gastric emptying and the onset of drug absorption was almost equal to the in vitro dissolution lag time of the capsule, suggesting a similar performance of CTDC in the gastrointestinal tract. From the comparison to the absorption behavior of the colon arrival marker, i.e. sulfasalazine, it was proved that the CTDC with the lag time of 3 h can deliver the drug directly to the colon. This result implied that the CTDC can be used as a non-invasive means for assessing the regional absorbability of drugs in the gastrointestinal tract. To evaluate the absorbability of drugs in the colon, three model drugs, theophylline (THEO), acetaminophen (ACET), and phenylpropanolamine hydrochloride (PPA) were directly delivered to the colons of beagle dogs using the CTDC with the lag time of about 3 h. The obtained relative bioavailabilities to the solution form were as high as 94.2%, 71.0%, and 91.5% for THEO, ACET and PPA, respectively, suggesting that the colonic absorbability of those drugs is essentially good.

PMID: 10332066 [PubMed - indexed for MEDLINE]

J Drug Target. 1996;4(2):59-67.

Related Articles, Links

Effect of food intake on the delivery of fluorescein as a model drug in colon delivery capsule after oral administration to beagle dogs.**Matsuda K, Takaya T, Shimoji F, Muraoka M, Yoshikawa Y, Takada K.**

Department of Pharmaceutics and Pharmacokinetics, Kyoto Pharmaceutical University, Japan.

The effect of food on the release time of a model drug, fluorescein (FL), has been studied after oral administration to beagle dogs in colon delivery capsule in comparison to conventional gelatin capsule and enteric capsules. The dose of FL was 30 mg for each animal. After oral administration of each test preparation in fasted or postprandial condition (100 grams of commercial solid food was given at 30 min before drug administration), blood samples were collected and plasma FL concentrations were measured spectrofluorometrically. Pharmacokinetic analysis was performed with plasma FL concentration vs. time data and the following parameters were determined; T_{max} (the time when plasma FL concentration reaches to its maximum concentration), C_{max} (peak plasma FL concentration), T_{lag} (the time when FL appeared at first into the systemic circulation), AUC (area under the plasma FL concentration vs. Time curve) and MRT (mean residence time). For gelatin capsule, mean T_{max} appeared at 0.83 ± 0.33 (S.E.) h after administration and MRT was 2.67 ± 0.21 h in fasted condition. By feeding, T_{max} and MRT increased to 1.50 ± 0.76 h and 3.09 ± 0.49 h. For two enteric HPMCP and Eudragit S capsules, MRT were 2.90 ± 0.48 h and 5.24 ± 0.32 h in fasted condition, and 11.30 ± 1.10 h and 12.83 ± 0.34 h in postprandial condition, respectively. T_{lag} also increased by postprandial administration. As colon delivery capsule, time-controlled release capsule (TCC) and two types of intestinal inner pressure-controlled release capsules (PCC) (#1 is a separate type and #2 is a seamless one) were tested. MRT of TCC was 4.76 ± 0.29 h and 6.43 ± 0.66 h in fasted and postprandial conditions, respectively. This capsule did not receive the effect of food intake. For #1 PCC, MRTs were 5.32 ± 0.22 h and 12.28 ± 0.26 h in fasted and postprandial conditions, respectively. For #2 PCC, MRTs were 5.51 ± 0.26 h and 13.36 ± 0.84 h in fasted and postprandial conditions, respectively. In addition, the effect of two times feedings was studied with two PCCs and longer MRTs, 28.44 ± 1.39 h and 26.32 ± 1.64 h, were obtained. The release time of FL from PCCs increased by postprandial administration. As compared to the results on two enteric capsules, these PCCs are thought to disintegrate in the colon. However, TCC is thought to disintegrate in the stomach after postprandial administration.

PMID: 8894965 [PubMed - indexed for MEDLINE]

J Pharm Pharmacol. 1995 Jun;47(6):474-8.

Related Articles, Links

Development of a colon delivery capsule and the pharmacological activity of recombinant human granulocyte colony-stimulating factor (rhG-CSF) in beagle dogs.

Takaya T, Ikeda C, Imagawa N, Niwa K, Takada K.

Department of Pharmaceutics and Pharmacokinetics, Kyoto Pharmaceutical University, Japan.

A peroral dosage form was examined to deliver recombinant human granulocyte colony-stimulating factor (rhG-CSF) to the colon in beagle dogs. A new gelatin capsule with its inside surface coated with ethylcellulose was prepared for this purpose. RhG-CSF was dissolved with propylene glycol and was filled in the capsule. Several kinds of ethylcellulose-gelatin capsules with an ethylcellulose layer of thickness 46 to 221 μ m were used. The capsule was filled with propylene glycol solution containing fluorescein as an absorption marker, castor oil derivative and citric acid. The hardness of the capsule was tested after the gelatin layer was dissolved using a hardness tester and was dependent on the thickness of the ethylcellulose layer of the capsule. The time, T_{max} , at which plasma fluorescein level reaches its maximum following oral administration of ethylcellulose capsules was used as a parameter for the in-vivo disintegration time of the ethylcellulose capsule into the colon. Capsules of thickness 84 μ m with a T_{max} of 4-6 h were filled with rhG-CSF solution containing fluorescein and were administered to dogs. After administration, blood samples were collected for 96 h and the blood total leucocyte (BTL) counts were measured as a pharmacological index of rhG-CSF. The maximum BTL count appeared at 10 h then gradually decreased and returned to its normal level at 48 h. These results suggest the usefulness of ethylcellulose capsules for the delivery of rhG-CSF to the colon and the possibility of a new oral rhG-CSF dosage form has been elucidated.

PMID: 7545751 [PubMed - indexed for MEDLINE]

J Pharm Sci. 1997 Sep;86(9):1016-21.

Related Articles, Links



Chitosan capsules for colon-specific drug delivery: improvement of insulin absorption from the rat colon.

Tozaki H, Komoike J, Tada C, Maruyama T, Terabe A, Suzuki T, Yamamoto A, Muranishi S.

Department of Biopharmaceutics, Kyoto Pharmaceutical University, Japan.

The objective of this study was to estimate colon-specific insulin delivery with chitosan capsules. In vitro drug release experiments from chitosan capsules containing 5(6)-carboxyfluorescein (CF) were carried out by the Japan Pharmacopoeia (J. P.) rotating basket method with some slight modifications. The intestinal absorption of insulin was evaluated by measuring the plasma insulin levels and its hypoglycemic effects after oral administration of the chitosan capsules containing insulin and additives. Little release of CF from the capsules was observed in liquid 1, an artificial gastric juice (pH 1), or in liquid 2, an artificial intestinal juice (pH 7). However, the release of CF was markedly increased in the presence of rat cecal contents. A marked absorption of insulin and a corresponding decrease in plasma glucose levels was observed following the oral administration of these capsules that contain 20 IU of insulin and sodium glycocholate (PA% = 3.49%), as compared with the capsules containing only lactose or only 20 IU of insulin (PA% = 1.62%). The hypoglycemic effect started from 8 h after the administration of chitosan capsules when the capsules entered the colon, as evaluated by the transit time experiments with chitosan capsules. These findings suggest that chitosan capsules may be useful carriers for the colon-specific delivery of peptides including insulin.

PMID: 9294815 [PubMed - indexed for MEDLINE]

Life Sci. 1999;64(13):1155-62.

[Related Articles](#), [Links](#)

ELSEVIER
FULL-TEXT ARTICLE

Colon-specific delivery of R68070, a new thromboxane synthase inhibitor, using chitosan capsules: therapeutic effects against 2,4,6-trinitrobenzene sulfonic acid-induced ulcerative colitis in rats.

Tozaki H, Fujita T, Odoriba T, Terabe A, Suzuki T, Tanaka C, Okabe S, Muranishi S, Yamamoto A.

Department of Biopharmaceutics, Kyoto Pharmaceutical University, Japan.

The objective of this study was to estimate the therapeutic effects of R68070, a new thromboxane synthase inhibitor, on 2,4,6-trinitrobenzenesulfonic acid sodium salt (TNBS)-induced ulcerative colitis in rats. We also examined the acceleration of the healing effect of R68070 with chitosan capsules to achieve its colon-specific delivery. The colonic injury and inflammation were assessed by measuring the myeloperoxidase (MPO) activities, colon wet weight/body weight (C/B) ratio and the damage score, respectively. These markers were decreased by the oral administration of R68070 with chitosan capsules and carboxymethyl-cellulose (CMC) suspension. The therapeutic effects of R68070 against ulcerative colitis were observed in both dosage forms in a dose dependent manner. In addition, its therapeutic effects were increased by the use of chitosan capsules, compared with CMC suspension. These results suggest that chitosan capsule might be a very useful dosage form for the colon-specific delivery of R68070 as an anti-inflammatory drug and for the therapy of ulcerative colitis.

PMID: 10210278 [PubMed - indexed for MEDLINE]

An angiogenin-binding protein from endothelial cells

(angiogenesis/receptors/heparan sulfate)

GUO-FU HU, SOO-IK CHANG, JAMES F. RIORDAN, AND BERT L. VALLEE*

Center for Biochemical and Biophysical Sciences and Medicine, Harvard Medical School, 250 Longwood Avenue, Boston, MA 02115

Contributed by Bert L. Vallee, December 26, 1990

ABSTRACT A 42-kDa bovine protein that binds bovine angiogenin [angiogenin binding protein (AngBP)] has been identified as a dissociable cell-surface component of calf pulmonary artery endothelial cells and a transformed bovine endothelial cell line, GM7373. Binding of ^{125}I -labeled bovine angiogenin (^{125}I -Ang) to AngBP occurs with an apparent $K_d \approx 5 \times 10^{-10}$ M and is specific, saturable, and inhibited by excess unlabeled angiogenin. ^{125}I -Ang can be crosslinked efficiently to AngBP by a water-soluble carbodiimide, 1-ethyl-3-(3-dimethylaminopropyl)carbodiimide. Bovine ribonuclease A competes with the binding of ^{125}I -Ang to AngBP, but lysozyme does not. Direct binding to AngBP of ^{125}I -labeled bovine ribonuclease A is, however, much weaker than that of ^{125}I -Ang. Two enzymatically active derivatives of angiogenin cleaved at residues 60-61 and 67-68, respectively, fail to induce angiogenesis and also bind to AngBP only weakly. AngBP has been isolated by treatment of cells with heparan sulfate, affinity chromatography on angiogenin-Sepharose of the material dissociated from the cell surface, and gel filtration HPLC. The results suggest that AngBP has the characteristics of a receptor that may likely function in angiogenesis.

Angiogenin, a 14-kDa protein first isolated from HT-29 human colon adenocarcinoma cells (1), is a potent blood vessel inducer present in mammalian plasma and milk (2-4). It has a unique ribonucleolytic activity (5, 6) that is essential for neovascularization. It also stimulates endothelial cells to form diacylglycerol (7) and to secrete prostacyclin (8) by activating phospholipase C and phospholipase A_2 , respectively. It binds to calf pulmonary artery endothelial (CPAE) cells (9) and has been found to modulate a mitogenic effect in certain other cells (10). When angiogenin is modified by mutagenesis (11) or by limited proteolysis (12) in the region of residues 61-67, it loses angiogenin activity and will not compete with the native protein in the chicken embryo chorioallantoic membrane (CAM) assay. In contrast, angiogenin modified at either of the active-site histidine residues involved in ribonucleolytic activity, although inactive itself on the CAM, will compete with the native protein in this angiogenesis assay (13). These second-messenger binding and modulatory effects have led to the postulation of a dual-site model for the organogenic activity of angiogenin (12), which assumes that angiogenin interacts directly with cells, presumably through a membrane receptor, to exert this biological function.

We report here the identification, isolation, and initial characterization of a bovine endothelial cell angiogenin-binding protein (AngBP) whose properties are consistent with its being a component of a cellular receptor of angiogenin.

The publication costs of this article were defrayed in part by page charge payment. This article must therefore be hereby marked "advertisement" in accordance with 18 U.S.C. §1734 solely to indicate this fact.

MATERIALS AND METHODS

Materials. Bovine angiogenin, isolated from bovine milk as described (4), migrated as a single band in SDS/PAGE, induced vascularization in the chicken embryo CAM assay, and stimulated a second-messenger response in endothelial cells. Single-site mutants H13A and H114A in which the ribonucleolytic active-site histidine residues are changed to alanine,[†] the regional mutant ARH-I,[‡] native human angiogenin, placental ribonuclease inhibitor (PRI), and bovine angiogenin were provided by R. Shapiro. The two proteolytic derivatives of human angiogenin, angiogenin K (cleaved at residues 60-61) and angiogenin E (cleaved at residues 67-68) were from T. Hallahan (12). ^{125}I -Ang, prepared with Enzymobeads (Bio-Rad; immobilized glucose oxidase-lactoperoxidase system), had a specific activity of 1.08 μCi (40 kBq)/ μg . Heparan sulfate was purchased from Sigma; RNase A, from Boehringer Mannheim; Na^{125}I , from Du Pont/New England Nuclear; and 1-ethyl-3-(3-dimethylaminopropyl)carbodiimide (EDC), disuccinimidyl suberate, and disuccinimidyl tartrate, from Pierce.

Cell Culture. GM7373 cells, obtained from the National Institute of General Medical Sciences, Human Genetic Mutant Cell Repository (Institute for Medical Research, Camden, NJ), were derived from fetal bovine aortic endothelial cells by transformation with benzo(a)pyrene (14). The cells were propagated at 37°C in humidified 5% CO_2 /95% air as monolayer cultures in Dulbecco's modified Eagle's medium supplemented with 10% (vol/vol) heat-inactivated fetal bovine serum, 2 mM glutamine, 1 μg of Fungizone per ml, and 5 μg of gentamicin sulfate per ml. CPAE and COS-7 (African green monkey kidney) cells from American Type Culture Collection were cultured in the same way, except that the medium for CPAE cells contained 20% (vol/vol) fetal calf serum. Subconfluent cells were kept in serum-free Dulbecco's modified Eagle's medium for 24 hr before experimentation. Human lymphocyte (HL-60) cells, from American Type Culture Collection, were cultured in RPMI 1640 medium supplemented with fetal calf serum, L-glutamine, Fungizone, and gentamicin sulfate as above. Subconfluent cells were kept in serum-free RPMI 1640 medium for 24 hr before experimentation.

Solubilization of Cells. Cell monolayers previously exposed to ^{125}I -Ang and treated with EDC were solubilized with radioimmunoprecipitation assay buffer (RIPA buffer; 150 mM NaCl/1% Nonidet P-40/0.5% desoxycholate/0.1%

Abbreviations: AngBP, angiogenin-binding protein; CPAE, calf pulmonary artery endothelial; CAM, chorioallantoic membrane; EDC, 1-ethyl-3-(3-dimethylaminopropyl)carbodiimide; PRI, human placental ribonuclease inhibitor.

*To whom reprint requests should be addressed.

[†]Mutant proteins are designated by the single-letter code for the original amino acid followed by its position in the sequence and the single-letter code for the new amino acid.

[‡]ARH-I is the extension derivative Met-angiogenin (methionyl residue at position -1) in which residues 58-70 have been replaced by residues 59-73 of RNase A.

SDS/10 mM Tris, pH 7.5). When cell monolayers were solubilized prior to addition of ^{125}I -Ang and carbodiimide crosslinking, Tris in the RIPA buffer was replaced with 10 mM phosphate (pH 7.5).

Release of Cell-Surface Proteins by Heparan Sulfate. Subconfluent starved-cell monolayers in 10-cm² dishes (Falcon) were washed three times with phosphate-buffered saline (PBS), and 0.4 ml of PBS containing 1 mg of heparan sulfate per ml was added. The cells were incubated at room temperature for 30 min with occasional shaking, and the released material was removed and clarified by centrifugation at 1500 rpm ($700 \times g$) for 5 min.

Purification of AngBP. Saturated ammonium sulfate, adjusted to pH 7.4 with NaOH, was added at 0°C to crude AngBP from supernatant solutions of heparan-treated subconfluent starved and washed GM7373 cells to give 50% saturation. The precipitate was dissolved in PBS, dialyzed against PBS overnight at 4°C, and applied to an angiogenin-Sepharose affinity column. The column was washed sequentially with 5–10 column volumes each of PBS, 3 M NaCl, and H₂O. AngBP was eluted with 3% SDS that was 0.5% in 2-mercaptoethanol. Fractions were pooled, and protein was precipitated with equal volumes of 30% trichloroacetic acid. SDS was removed by washing the precipitate with 80% ice-cold acetone three times. The precipitate was dissolved in 0.5 M NH₄OH, diluted 1:1 with solvent A, and applied to a protein PAK-125 (Waters) HPLC column. Elution was achieved with 50:50 (vol/vol) solvent A/solvent B; solvent A was 0.1% trifluoroacetic acid, and solvent B was 3:2:2 (vol/vol) isopropanol/acetonitrile/water containing trifluoroacetic acid at a final concentration of 0.08%.

Densitometry. Autoradiogram intensities were recorded with a densitometer (E-C Apparatus), and areas were measured by weighing the excised peaks. The densitometric results were uncorrected for nonlinear response.

RESULTS

Identification of AngBP. The water-soluble carbodiimide EDC crosslinked ^{125}I -Ang to an AngBP present on the surface of CPAE or GM7373 cells. Crosslinking of either monolayers of CPAE cells (Fig. 1, lane A) or a crude cell lysate (Fig. 1, lane B) generated a single major product of 58 kDa detected by SDS/PAGE. A similar result was obtained with monolayers of GM7373 cells, a transformed endothelial cell line (Fig. 1, lane D), and its corresponding cell lysate (Fig. 1, lane E). The latter cell line is better suited to isolation of cell-surface proteins in quantity by virtue of its stability and rapid growth characteristics; it was therefore used for further experiments.

The intensity of the band for cell monolayer-derived AngBP (Fig. 1, lanes A and D) was much weaker than that for cell lysate-derived AngBP, and this suggested that some of the AngBP or its complex with angiogenin was lost, perhaps during one of the washing steps. Therefore, the dissociability of AngBP from GM7373 cells was examined by treating the cells with heparan sulfate, a procedure sometimes used for release of cell-surface proteins (15). AngBP was indeed present in the heparan sulfate-released material (Fig. 1, lane F) and was crosslinked to ^{125}I -Ang by EDC with the formation of a single, characteristic 58-kDa band. The same result was obtained with heparan sulfate-released material from CPAE cells (Fig. 1, lane C). Neither disuccinimidyl tartrate (Fig. 1, lane F) nor its longer-chain homolog, disuccinimidyl suberate (Fig. 1, lane G), was able to crosslink ^{125}I -Ang with AngBP as efficiently as EDC under conditions typically used with di(*N*-hydroxy)succinimidyl ester reagents. AngBP preparations obtained from GM7373 cells by this heparan sulfate method were used for subsequent experiments.

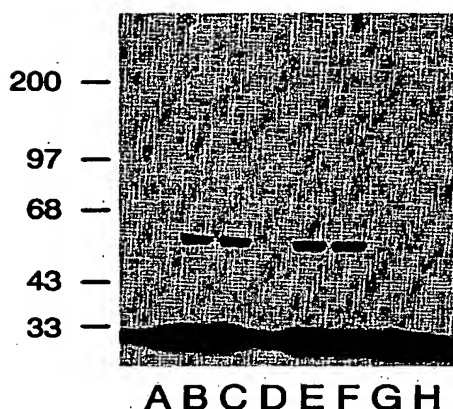


Fig. 1. SDS/PAGE of products of crosslinking ^{125}I -Ang to AngBP. Initial amounts of starved subconfluent CPAE (lanes A–C) or GM7373 (lanes D–H) cells from 10-cm² dishes and of ^{125}I -Ang are identical for all lanes. EDC crosslinking reactions (lanes A–G) were quenched with Tris at a final concentration of 100 mM (pH 8.0). For lane A, ^{125}I -Ang was crosslinked to AngBP in CPAE cell monolayers (passage 17). After a 30-min exposure of monolayers to 40 ng of ^{125}I -Ang, unbound ^{125}I -Ang was removed by washing three times with PBS. Bound ^{125}I -Ang was fixed with 10 mM EDC at room temperature for 30 min. After the reaction was quenched, the cells were washed three times with PBS and solubilized with 0.4 ml of RIPA buffer. For lane B, ^{125}I -Ang was crosslinked to AngBP in a crude CPAE cell lysate. Cell monolayers were solubilized with the phosphate modification of RIPA buffer, and a 50- μl sample of the released material was incubated with 5 ng of ^{125}I -Ang for 30 min at room temperature. EDC was added to a final concentration of 10 mM, and the mixture was incubated at room temperature for 30 min and then quenched. For lane C, ^{125}I -Ang was crosslinked to AngBP in heparan sulfate-released material from CPAE cells as for lane B. Other lanes: D–F, as in lanes A–C except with GM7373 cells; G, as in lane F except the crosslinking agent was 0.2 mM disuccinimidyl suberate; H, as in lane G, except the crosslinking agent was 0.2 mM disuccinimidyl tartrate.

Specificity of Angiogenin Binding to AngBP. An excess (2 μg) of either unlabeled bovine or human angiogenin competed with ^{125}I -Ang for binding to AngBP under the conditions given for Fig. 1, and the intensities of the 58-kDa bands were reduced by factors of 50 and 7, respectively, as determined by densitometric analysis. RNase A, a close natural homolog of angiogenin with 35% sequence identity, competed with ^{125}I -Ang in a binding and crosslinking experiment with AngBP, though not as effectively as angiogenin. In the presence of 2 μg of RNase A the intensity of the ^{125}I -Ang-AngBP band was reduced by a factor of 3.4. However, only a very faint band was seen after attempting to bind and crosslink ^{125}I -labeled RNase A to AngBP (data not shown). Under the same conditions, lysozyme, a strongly basic protein, did not compete at all. No AngBP was detected in heparan sulfate-released preparations from COS-7 and HL-60 cells under the same conditions as were used with CPAE and GM7373 cells.

PRI Prevents the Binding of ^{125}I -Ang to AngBP. Preincubation of ^{125}I -Ang with PRI before addition to the heparan sulfate-released material prevented subsequent formation of a cross-linkable complex with AngBP (data not shown). Angiogenin binds with extraordinary avidity to PRI (16). The K_d for this interaction, 7×10^{-16} M, is 60-fold stronger than that for the interaction of PRI with RNase A. Remarkably, when an excess of AngBP and PRI in equal proportions is added to ^{125}I -Ang, only the ^{125}I -Ang-AngBP product is observed. This suggests that under these conditions angiogenin

binds to AngBP preferentially, although the stability of PRI in the released material has not been established.

Saturability of Binding of ^{125}I -Ang to AngBP. Formation of the ^{125}I -Ang-AngBP complex depends on the concentration of added angiogenin (Fig. 2). A plot of bound vs. free ^{125}I -Ang clearly shows that binding to AngBP is saturable. A Scatchard plot (not shown) indicates an apparent K_d of 5×10^{-10} M, computed on the assumptions that the yield of crosslinking of bound ^{125}I -Ang to AngBP is constant and occurs much faster than dissociation of ^{125}I -Ang-AngBP and that disappearance of free ^{125}I -Ang and free AngBP also occurs much faster than dissociation of ^{125}I -Ang-AngBP.

Specificity of Binding of Mutant and Clipped Angiogenins. Two mutant forms of angiogenin, H13A and H114A, in which active-site histidine residues are replaced by alanine with resultant loss of ribonucleolytic and angiogenic activity, also competed for ^{125}I -Ang binding to AngBP: in the presence of 2 μg of either H13A or H114A, a reduction in the 58-kDa band intensity by a factor of 3 or 5, respectively, was observed. These mutants also competed efficiently with angiogenin both in the chicken embryo CAM assay and in a second-messenger response assay, indicating that they both retain an intact receptor binding site. Two proteolytically clipped forms of angiogenin, on the other hand, angiogenins K and E, which do not compete with the native protein in the chicken embryo CAM assay when at 20-fold excess (12), competed only weakly (17–33% reduction in band intensity) in ^{125}I -Ang binding to AngBP. These two derivatives have single peptide bond cleavages at residues 60–61 and 67–68, respectively, which are thought to lie in the receptor binding region of angiogenin (12). Mutagenic and chemical changes in this region are accompanied by loss of angiogenic activity but retention of ribonucleolytic activity (12).

Purification of AngBP. Many proteins were released from bovine endothelial cells by treatment with heparan sulfate (Fig. 3, lane A). AngBP was purified from this mixture by starting with ammonium sulfate fractionation, in which all of the ^{125}I -Ang binding activity was recovered in the 50% saturation precipitate. This was taken up in PBS and applied to an angiogenin-Sepharose column to which AngBP bound tightly. Most impurities were removed by washing with PBS, and no ^{125}I -Ang binding was found in subsequent 3 M NaCl and H_2O washes. AngBP was eluted by washing with 3% SDS/0.5% 2-mercaptoethanol and was freed from SDS by precipitation with trichloroacetic acid. Subsequent washing with aqueous acetone afforded material that migrated as a single major 42-kDa band in SDS/PAGE (Fig. 3, lane B).

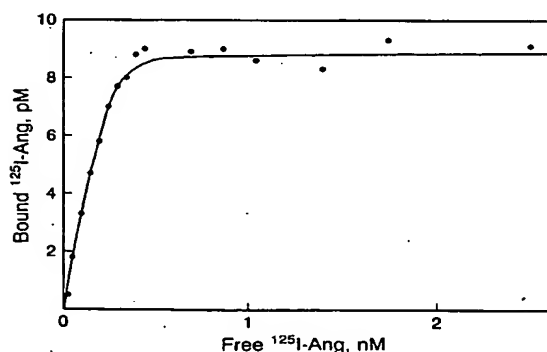


FIG. 2. Saturability of binding of ^{125}I -Ang to AngBP. ^{125}I -Ang samples at various concentrations were incubated with crude native AngBP and crosslinked with EDC as in Fig. 1. The gel slices containing the ^{125}I -Ang-AngBP product were located by autoradiography, cut, and assayed for radioactivity. The resulting cpm were defined as bound ^{125}I -Ang.

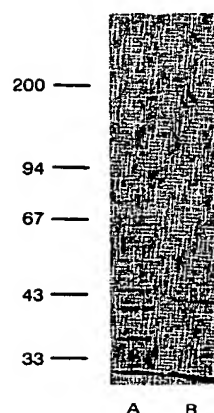


FIG. 3. SDS/PAGE analysis of AngBP samples. Lane A shows cell-surface species released by heparan sulfate treatment. The cell-free supernatant solution, which contained crude AngBP, was analyzed with SDS/7% PAGE and Coomassie brilliant blue stain. Lane B shows purified AngBP prepared as described in *Materials and Methods*. A sample taken after the acetone wash was dissolved in 0.5 M NH_4OH and analyzed by SDS/PAGE as in Fig. 1.

AngBP was isolated from a gel slice containing this band by electroelution in 0.1 M NH_4HCO_3 buffer. After lyophilization, AngBP was renatured by incubation in PBS at 4°C overnight. This highly purified product binds ^{125}I -Ang as measured by crosslinking with EDC and autoradiography (see Fig. 1).

An aliquot of the trichloroacetic acid precipitate dissolved in 0.5 M NH_4OH and applied to a HPLC gel filtration column, PAK-125, was eluted as a single peak of AngBP (Fig. 4). An amino acid analysis of the pooled fractions from this single peak showed that AngBP differs markedly from PRI (data not shown). The latter is characterized by seven leucine-rich repeats and a cysteine content much higher than observed for AngBP. Anti-PRI polyclonal antibodies did not recognize AngBP (data not shown).

DISCUSSION

Characterization of an angiogenin receptor is essential to an understanding of not only the mechanism of action of angiogenin and its signal-transduction pathway but also the control of angiogenesis. The preceding paper in this issue (12) showed that two distinct regions of angiogenin are crucial for the expression of its biological activity. One region encompasses the residues involved in ribonucleolytic activity, and the other is a cellular recognition site that spans residues 60–68. A functional catalytic site and an intact cell-binding site are both required for angiogenin's organogenic activity. This dual-site mechanism also implicates a complementary recognition site on the outer membrane of the target cell. Evidence that the angiogenic process is receptor-mediated includes the activation by angiogenin of phospholipases C

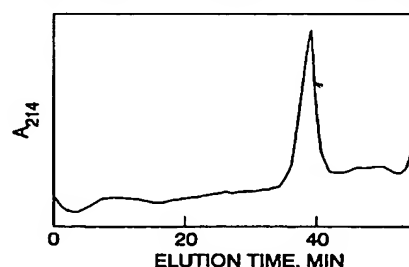


FIG. 4. Gel filtration HPLC of purified AngBP. A sample from the active fraction from affinity chromatography, prepared as in Fig. 1, lane B, was subjected to HPLC gel filtration on a PAK-125 column. The resultant single peak at 39 min was subjected to amino acid analysis.

and A₂ in vascular endothelial and smooth muscle cells (7, 8) as well as the inhibition of angiogenesis by certain inactive angiogenin mutants (13).

This study identifies a 42-kDa endothelial cell membrane protein that specifically binds angiogenin. Previous studies had indicated that angiogenic factors such as acidic and basic fibroblast growth factors (17, 18), transforming growth factors α and β (17, 18), and vascular endothelial growth factor (19) most likely induce angiogenesis by interacting with endothelial cells. In addition Badet *et al.* (9) demonstrated that ¹²⁵I-labeled recombinant human angiogenin binds to CPAE cells in a manner that is concentration dependent, reversible, and saturable in the presence of increasing amounts of unlabeled angiogenin. They also found that it binds to endothelial cells from bovine aorta, cornea, and adrenal cortex capillaries but not to Chinese hamster lung fibroblasts. The binding sites on CPAE cells had an apparent K_d of 5×10^{-9} M and were considered to satisfy the criteria for an angiogenin receptor.

Preliminary investigations in this laboratory (S.-I.C., unpublished observations) revealed a marked degree of species dependency for angiogenin binding to endothelial cells. Consequently, subsequent work was carried out with bovine angiogenin isolated from bovine milk and bovine endothelial cells, primarily GM7373 cells. Initial efforts to identify an angiogenin receptor used conventional crosslinking techniques with both cell monolayers and membrane preparations. Although a wide variety of conditions and reagents were tested, the results were largely inconclusive. Both high (>200,000) and low (\approx 60,000) molecular weight bands could be detected by autoradiography after crosslinking with labeled angiogenin but not consistently nor of appreciable intensity. It is now apparent that at least two technical reasons contributed to this problem. For one, the di(*N*-hydroxy)succinimidyl esters that were used are not very effective in cross linking ¹²⁵I-Ang and AngBP. More importantly, perhaps, is the tendency of AngBP to dissociate from the endothelial cell surface. Although the circumstances under which this occurs have not been investigated completely as yet, dissociation is clearly enhanced by heparan sulfate (Fig. 1). It is therefore possible that loss of AngBP or ¹²⁵I-Ang-AngBP from the cell surface during washing steps could have contributed to the low yields of product seen in these early experiments.

Materials released from cell surfaces with heparan sulfate (15) are largely proteoglycans, which are known to participate in cell-cell adhesion, intercellular communication, and ligand-receptor binding. Among the last are the receptors for transferrin (20), lymphocyte homing (21), lipoprotein lipase (22), and transforming growth factor β [TGF- β (type III)] (23). These peripheral membrane proteoglycans are thought to be an integral membrane receptor component noncovalently linked either through a glycosaminoglycan side chain or the core protein. Non-proteoglycan cell-surface proteins may also be released (24–28) [e.g., by proteolysis (26)]. Secreted forms of such proteins may arise as a result of alternative splicing of mRNA (27, 28) or from multiple genes (25).

Whatever the nature of AngBP, its release from the cell surface by heparan sulfate and crosslinking to ¹²⁵I-Ang with EDC provides a sensitive and specific assay for its purification. AngBP is the single angiogenin-specific binding species detected by this means. It is readily purified from the material dissociated from the cell surface to yield a single band in SDS/PAGE analysis. Whether AngBP is the entire receptor, the extracellular component, or a fragment will likely be apparent after sequence analysis and correlation with biological function.

The evidence obtained thus far indicates that the binding of angiogenin to AngBP is specific, saturable, and inhibited by

PRI. These studies have been largely carried out with crude preparations of AngBP (heparan sulfate releasates) and obviously must be repeated with pure material before explicit interpretations are possible. The competition for binding by RNase A, for example, is not entirely consistent with the results of direct binding of ¹²⁵I-labeled RNase A to AngBP. The failure of PRI to compete with AngBP is unexpected since the K_i for PRI inhibition, 7×10^{-16} M, is vastly different from the apparent K_d for AngBP binding, 5×10^{-10} M. It may well be that this reflects an instability of PRI in the crude AngBP mixture. It should be noted, incidentally, that these results suggest that AngBP is probably not PRI or some modified form of PRI. The amino acid composition of AngBP is also consistent with this view.

Unlabeled bovine angiogenin competes with ¹²⁵I-Ang for binding to AngBP, but lysozyme, which is a similarly basic protein, does not. Thus, the binding is not due solely to a charge interaction. Competition is also seen with two catalytic-active-site mutants of angiogenin, H13A and H114A. These proteins are known to compete with angiogenin in the chicken embryo CAM assay and hence must have an intact receptor binding site (12). However, they lack ribonucleolytic activity and, therefore, are unable to induce blood vessel formation. Conversely, the two proteolytically cleaved derivatives of angiogenin examined (angiogenins K and E) do not compete with the native protein in the chicken embryo CAM assay presumably because of disruption of their receptor binding site (12). That they also fail to compete effectively in the AngBP binding assay is consistent with this view. Indeed, the results overall are further confirmation of the dual-site model for the mechanism of action of angiogenin.

The availability of purified AngBP will allow a more detailed investigation of its interaction with angiogenin as well as complete characterization of its structure. The latter, in conjunction with cDNA sequence information, should provide greater insight to its mode of association with the endothelial cell membrane and to its function as an angiogenin receptor. It is premature to define the specific biological role of AngBP. It could participate directly in transmembrane signalling. Alternatively, it could be involved in receptor presentation or delivery, potentiate angiogenin-RNA binding, or serve as an indirect mediator of angiogenin action. Further studies will clarify its function and perhaps provide a basis for the design of agents to modulate receptor binding and to control angiogenin-induced angiogenesis.

We thank Drs. Sigita Verselis and Anatole Klyosov for early investigations on angiogenin receptors, Daniel J. Strydom for amino acid analysis, and Robert Shapiro and Thayer C. French for valuable discussions and help in preparation of the manuscript. This work was supported by funds from Hoechst, A. G. under agreements with Harvard University.

1. Fett, J. W., Strydom, D. J., Lobb, R. R., Alderman, E. M., Bethune, J. L., Riordan, J. F. & Vallee, B. L. (1985) *Biochemistry* 24, 5480–5486.
2. Shapiro, R., Strydom, D. J., Olson, K. A. & Vallee, B. L. (1987) *Biochemistry* 26, 5141–5146.
3. Bond, M. D. & Vallee, B. L. (1988) *Biochemistry* 27, 6282–6287.
4. Maes, P., Damart, D., Rommeus, C., Montreuil, J., Spik, G. & Tostar, A. (1988) *FEBS Lett.* 241, 41–45.
5. Shapiro, R., Riordan, J. F. & Vallee, B. L. (1986) *Biochemistry* 25, 3527–3532.
6. St. Clair, D. K., Rybak, S. M., Riordan, J. F. & Vallee, B. L. (1987) *Proc. Natl. Acad. Sci. USA* 84, 8330–8334.
7. Bicknell, R. & Vallee, B. L. (1988) *Proc. Natl. Acad. Sci. USA* 85, 5961–5965.
8. Bicknell, R. & Vallee, B. L. (1989) *Proc. Natl. Acad. Sci. USA* 86, 1573–1577.
9. Badet, J., Soncin, F., Guitton, J.-D., Lamare, O., Cartwright,

- T. & Barritault, D. (1989) *Proc. Natl. Acad. Sci. USA* 86, 8427–8431.
10. Heath, W. F., Moore, F., Bicknell, R. & Vallee, B. L. (1989) *Proc. Natl. Acad. Sci. USA* 86, 2718–2722.
11. Harper, J. W. & Vallee, B. L. (1989) *Biochemistry* 28, 1875–1884.
12. Hallahan, T. W., Shapiro, R. & Vallee, B. L. (1991) *Proc. Nat. Acad. Sci. USA* 88, 2222–2226.
13. Shapiro, R. & Vallee, B. L. (1989) *Biochemistry* 28, 7401–7408.
14. Grinspan, J., Mueller, S. N. & Levine, E. M. (1983) *J. Cell. Physiol.* 114, 328–338.
15. Höök, M., Kjellén, L., Johansson, S. & Robinson, J. (1984) *Annu. Rev. Biochem.* 53, 847–869.
16. Lee, F. S., Shapiro, R. & Vallee, B. L. (1989) *Biochemistry* 28, 225–230.
17. Blood, C. H. & Zetter, B. P. (1990) *Biochim. Biophys. Acta* 1032, 89–118.
18. Folkman, J. & Klagsbrun, M. (1987) *Science* 235, 442–447.
19. Vaisman, N., Gospodarowicz, D. & Neufeld, G. (1990) *J. Biol. Chem.* 265, 19461–19466.
20. Fransson, L.-A. (1987) *Trends Biochem. Sci.* 12, 406–411.
21. Jalkanen, S., Jalkanen, M., Bargatze, R., Tammi, M. & Butcher, E. C. (1988) *J. Immunol.* 141, 1615–1623.
22. Saxena, U., Klein, M. G. & Goldberg, I. J. (1990) *J. Biol. Chem.* 265, 12880–12886.
23. Andres, J. L., Stanley, K., Cheifetz, S. & Massagué, J. (1989) *J. Cell Biol.* 109, 3137–3145.
24. Gavin, J. R., Buell, D. N. & Roth, J. (1972) *Science* 178, 168–169.
25. Kress, M., Cosman, D., Khoury, G. & Jay, G. (1983) *Cell* 34, 189–196.
26. Fujimoto, J., Stewart, S. J. & Levy, R. (1984) *J. Exp. Med.* 160, 116–124.
27. Weber, W., Grill, G. N. & Spiess, J. (1984) *Science* 224, 294–297.
28. Krangel, M. S. (1986) *J. Exp. Med.* 163, 1174–1190.

Actin is a binding protein for angiogenin

(angiogenesis)

GUO-FU HU, DANIEL J. STRYDOM, JAMES W. FETT, JAMES F. RIORDAN, AND BERT L. VALLEE

Center for Biochemical and Biophysical Science and Medicine, Harvard Medical School, 250 Longwood Avenue, Boston, MA 02115

Contributed by Bert L. Vallee, November 9, 1992

ABSTRACT The 42-kDa angiogenin binding protein isolated previously has been purified to electrophoretic homogeneity. It has been identified as a member of the actin family by peptide mapping and partial amino acid sequencing. The interaction of bovine muscle actin with angiogenin is similar to that of the angiogenin binding protein. Angiogenin induces the polymerization of actin below the critical concentration for spontaneous polymerization. The interaction occurs both in solution and on a poly(vinylidene difluoride) membrane. It is inhibited by excess unlabeled angiogenin and also by platelet factor 4 and protamine, which are known inhibitors of angiogenesis. Two other angiogenic molecules, basic fibroblast growth factor and tumor necrosis factor α , bind to ^{125}I -labeled actin and can be crosslinked by a water-soluble carbodiimide. Both actin and an anti-actin antibody inhibit the angiogenic activity of angiogenin in the chicken embryo chorioallantoic membrane assay. The results indicate that the angiogenin binding protein is a cell surface actin and suggest that the reaction between angiogenin and this actin is an essential step in the angiogenesis process induced by angiogenin.

Angiogenin is a 14-kDa protein purified initially from serum-free supernatants of an established human adenocarcinoma cell line, HT-29 (1). It was the first human tumor-derived angiogenic protein to be isolated based on its *in vivo* activity. It stimulates endothelial cells to produce diacylglycerol (2) and secrete prostacyclin (3) by phospholipase activation. It supports endothelial and fibroblast cell adhesion (4) and modulates a mitogenic effect in certain cells (5). An angiogenin binding protein (AngBP), which has properties consistent with its being a component of a cellular receptor for angiogenin, has been identified and isolated from a transformed endothelial cell line, GM7373 (6). It is a cell-surface protein with an apparent molecular mass of 42 kDa and is released from endothelial cells by exposure to heparin, heparan sulfate, or angiogenin itself.

We report here the further purification and characterization of AngBP. Tryptic peptide mapping and amino acid sequence analysis indicate that AngBP is a member of the actin family. The binding of angiogenin to bovine muscle actin and the inhibitory effect of actin and anti-actin antibodies on angiogenin-induced neovascularization on the chicken embryo chorioallantoic membrane (CAM) are also reported. The mechanism by which AngBP is released from the cell surface and the physiological significance of its presence and displacement remain to be elucidated.

MATERIALS AND METHODS

Materials. Bovine angiogenin, purified by the method of Bond and Vallee (7), was provided by R. Shapiro. ^{125}I -labeled angiogenin and ^{125}I -labeled actin of specific activities 25 $\mu\text{Ci}/\mu\text{g}$ and 10 $\mu\text{Ci}/\mu\text{g}$, respectively (1 Ci = 37 GBq), were

prepared with Enzymobeads (Bio-Rad). CNBr-activated Sepharose 6MB was from Pharmacia; bovine (A3653) and porcine (A0541) muscle actin, platelet factor 4 (PF-4), and protamine were from Sigma; basic fibroblast growth factor (bFGF), tumor necrosis factor α (TNF- α), and transforming growth factor β (TGF- β) were from Genzyme; Na ^{125}I was from DuPont/New England Nuclear; and 1-ethyl-3-(3-dimethylaminopropyl)-carbodiimide was from Pierce. A polyclonal rabbit anti-actin antiserum (A2668) was purchased from Sigma. Its IgG fraction was prepared by protein A-Sepharose chromatography. Normal rabbit IgG was prepared similarly.

Isolation of AngBP. GM7373 cells (8) were cultured and used to prepare AngBP as described (6).

Binding of Angiogenin to Actin. *In solution.* Actin either in depolymerization buffer (2 mM Tris, pH 8.0/0.2 mM CaCl $_2$ /0.2 mM ATP/0.2 mM dithiothreitol) or in phosphate-buffered saline (PBS), was mixed with angiogenin or ^{125}I -labeled angiogenin. The mixture was incubated at room temperature for 30 min and then 1-ethyl-3-(3-dimethylaminopropyl)-carbodiimide was added at a final concentration of 10 mM. After another 30-min incubation, the reaction was quenched by the addition of 0.1 vol of 1.0 M Tris-HCl (pH 8.0). The crosslinked complex was separated from free actin and angiogenin by SDS/PAGE and visualized by silver staining or autoradiography.

Affinity chromatography. An 8 \times 20 mm column of angiogenin-Sepharose on which angiogenin (0.5–1 mg) was immobilized (6) was equilibrated with PBS, and 1 ml of actin (0.2 mg/ml) in the same buffer was applied at a flow rate of 20 ml/hr. Bound actin was subjected to the same procedure of washing and elution as described above for the purification of AngBP.

Membrane blotting. Actin was separated either by SDS/PAGE or by two-dimensional electrophoresis and electrotransferred onto a poly(vinylidene difluoride) microporous membrane. The membrane was blocked by overnight agitation at 4°C in rinse buffer (10 mM Tris-HCl, pH 7.5/150 mM NaCl/1 mM EDTA/0.02% Triton X-100) containing 5% (wt/vol) bovine serum albumin. The membrane was then incubated with ^{125}I -labeled angiogenin (10 6 cpm/ml) in rinse buffer containing 0.3% bovine serum albumin at 4°C overnight with shaking. After three washes in the rinse buffer, the membrane was air-dried and subjected to autoradiography.

Biological Assay. Angiogenesis was measured on the CAM by the method of Knighton *et al.* (9) as described (1). Potential inhibitors were mixed with angiogenin 15 min prior to application onto the discs.

RESULTS

Purification of AngBP. AngBP was purified to electrophoretic homogeneity by the procedures described above. HPLC

Abbreviations: AngBP, angiogenin binding protein; CAM, chorioallantoic membrane; bFGF, basic fibroblast growth factor; TNF- α , tumor necrosis factor α ; PF-4, platelet factor 4; TGF- β , transforming growth factor β .

The publication costs of this article were defrayed in part by page charge payment. This article must therefore be hereby marked "advertisement" in accordance with 18 U.S.C. §1734 solely to indicate this fact.

(C₄ column) of the eluate from the angiogenin-Sepharose column gave four major peaks with retention times of 27, 31, 35 and 40 min (Fig. 1). The 27-, 31-, and 35-min peaks contained proteins of 15 kDa, 67 kDa, and 42 kDa, respectively, by SDS/PAGE. No protein was detectable in the 40-min peak fraction by either SDS/PAGE or amino acid analysis. Binding and crosslinking assays with ¹²⁵I-labeled angiogenin indicated that the 42-kDa protein was AngBP (data not shown). The nature of the 15-kDa and 67-kDa proteins is unknown as yet, but amino acid analysis and immunodiffusion experiments with an anti-albumin antibody indicated they are not angiogenin or serum albumin.

Tryptic Peptide Mapping and Amino Acid and Sequence Analyses. Affinity-purified AngBP (40 µg) was reduced with dithiothreitol, carboxymethylated, desalted, and digested overnight with 5% (wt/wt) trypsin. The tryptic peptides were separated by HPLC (C₁₈ column) and a single seemingly well-resolved peak was selected for sequence analysis. Specific assignments could not be made for the first few residues but thereafter the sequence became clear as Xaa-Xaa-Xaa-Xaa-Pro-Asp-Gly-Gln-Val-Ile-Thr-Ile-Gly-Asn. A search for identities via the Protein Identification Resource at the National Biomedical Research Foundation revealed complete identity with residues 243–252 of bovine smooth muscle actin.

Tryptic peptide mapping was performed in parallel with 20 µg of C₄-purified AngBP or bovine skeletal muscle actin. Similar peptide patterns were obtained with no obvious extraneous peptide peaks (Fig. 2). Most fractions from the peptide map of AngBP were sequenced: many of them could be sequenced completely. Amino acids covering ~40% of the entire protein were sequenced and corresponded exactly to seven regions of bovine actin, residues 21–61, 92–105, 119–128, 148–169, 178–188, 239–254, and 329–335. The presence of Thr-103, Leu-153, and Asn-162 identifies this protein as a muscle-type actin (10). No difference in sequence from known actins was apparent.

Table 1 lists a typical amino acid analysis of C₄-purified AngBP. It is close to that obtained for a sample of bovine skeletal muscle actin except for the high leucine/isoleucine ratio and the low tyrosine and methionine content. The actual composition of bovine skeletal muscle actin, based on its primary structure, is also shown. The composition of AngBP is even closer to that for bovine brain capillary actin (Table 1), which differs substantially in tyrosine and leucine content (11). Bovine smooth muscle actin composition is also listed for comparison.

Binding of Angiogenin to Actin. The binding of ¹²⁵I-labeled angiogenin to either bovine or porcine muscle actin was investigated by crosslinking followed by gel electrophoresis.

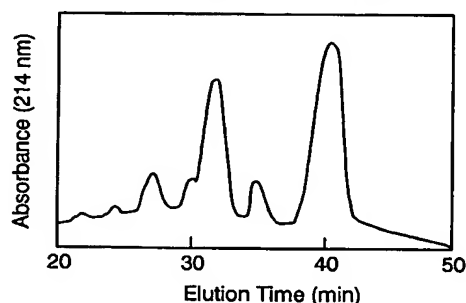


FIG. 1. Reversed-phase HPLC of AngBP. SDS eluate from the angiogenin-Sepharose column was acidified with trifluoroacetic acid to a final concentration of 0.1% and subjected to HPLC reversed-phase separation on a Supelco C₄ cartridge column. The peak at 35 min contained AngBP and was used for amino acid and sequence analyses.

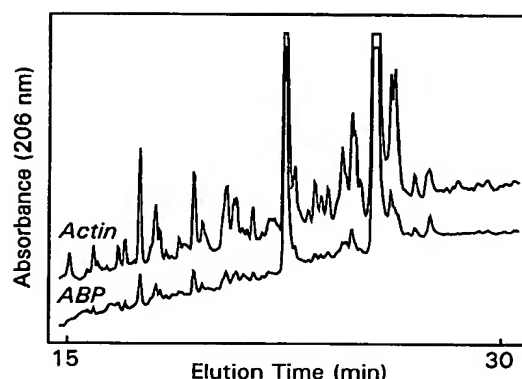


FIG. 2. Tryptic peptide map of actin and AngBP. Aliquots of bovine muscle actin (25 µg) and of AngBP (20 µg) were dissolved in 100 µl of 1% hydrogenated Triton X-100/10% (vol/vol) acetonitrile/0.3 M ammonium bicarbonate and digested with 1 µg of trypsin for 24 hr at room temperature. The peptide mixtures were dried under a stream of nitrogen, redissolved in 50 µl of 0.1% trifluoroacetic acid, and applied to a C₁₈ reversed-phase HPLC column. Elution was achieved with a 1-hr linear gradient from 100% solvent A to 100% solvent B; solvent A was 0.1% trifluoroacetic acid, and solvent B was 80% acetonitrile/0.08% trifluoroacetic acid.

Autoradiography reveals a 58-kDa band in both cases (Fig. 3a), indicating formation of a 1:1 complex between ¹²⁵I-labeled angiogenin and actin. Crosslinking of nonlabeled angiogenin to actin was also examined by mixing equal amounts of the two proteins in PBS and adding the crosslinking reagent (Fig. 3b). After SDS/PAGE and silver staining, a 58-kDa species was detected (lane C) in addition to non-crosslinked angiogenin (16 kDa) and actin (42 kDa). The 58-kDa species was not observed in control lanes B or D where only angiogenin or actin was present.

Table 1. Amino acid compositions of bovine AngBP and bovine skeletal muscle, brain capillary, and smooth muscle actins

Amino acid	Residues, no.			
	AngBP	Bovine actin		
		Skeletal muscle	Brain capillary	Smooth muscle
Asp	34.5	33.2 (34)	35	33
Glu	43.7	37.4 (39)	47	40
Ser	27.8	22.5 (23)	28	26
Gly	38.1	30.6 (28)	36	28
His	6.6	8.0 (9)	7	9
Arg	22.2	19.3 (18)	23	18
Thr	20.1	27.1 (28)	22	24
Ala	28.0	28.8 (29)	29	29
Pro	19.3	19.7 (19)	19	19
Tyr	8.2	15.5 (16)	17	16
Val	18.8	18.3 (21)	18	20
Met	6.9	16.0 (16)	5	15
Ile	16.2	24.8 (29)	17	30
Leu	38.8	26.1 (26)	30	27
Phe	11.9	12.0 (12)	13	12
Lys	22.6	19.7 (19)	20	19
Cys	ND	ND (5)	ND	6
Trp	ND	ND (4)	ND	4

Residue numbers calculated for a molecular weight of 42,000. Numbers in parentheses are residues per molecule based on the sequence of skeletal muscle actin (10). The numbers for capillary actin are recalculated from ref. 11 and those for smooth muscle actin are from ref. 10. ND, not determined.

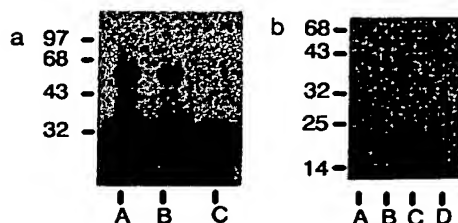


FIG. 3. SDS/PAGE analysis of binding and crosslinking between angiogenin and actin. Binding was carried out by incubating 50 ng of actin in 50 μ l of PBS with 10^6 cpm of 125 I-labeled angiogenin (lane A) or 1 μ g of actin with 1 μ g of angiogenin (lane B) at room temperature for 30 min. Crosslinking was performed by incubating the mixtures of actin and angiogenin with 10 mM carbodiimide at room temperature for 30 min. The reactions were quenched with 100 mM Tris (pH 8.0; final concentration). (a) Autoradiography. Lanes: A, bovine muscle actin; B, porcine muscle actin; C, no actin is present. (b) Silver staining. Lanes: A, blank; B, angiogenin only; C, angiogenin plus bovine muscle actin; D, bovine muscle actin only.

Increasingly higher amounts of 125 I-labeled angiogenin were mixed with a fixed amount of actin and crosslinked as with AngBP (6). Actin was also incubated with a fixed amount of 125 I-labeled angiogenin plus increasingly higher concentrations of unlabeled angiogenin and was then crosslinked. In both experiments, the 125 I-labeled angiogenin-actin complexes were separated from free ligands by SDS/PAGE. The gel slices that contained 125 I-labeled angiogenin-actin complexes were located by autoradiography, cut out, and assayed for radioactivity. A plot of bound vs. free 125 I-labeled angiogenin demonstrated that binding to actin reaches a maximum and is inhibited by excess unlabeled angiogenin. Scatchard analysis (not shown) based on the calculations and assumptions previously described (6) yields an apparent K_d value of 0.5 nM for the binding of actin and angiogenin, identical to that obtained for the binding of AngBP and angiogenin (6).

The binding of actin to angiogenin-Sepharose was carried out under the same conditions used for purification of AngBP by affinity chromatography. As judged by SDS/PAGE and protein staining, >90% of the applied actin binds to the column (data not shown). Actin also bound to the affinity column when equilibrated with actin depolymerization buffer. Bound actin could only be eluted by 3% SDS containing 0.5% 2-mercaptoethanol. The angiogenin-actin complex could not be dissociated by 3 M NaCl or H_2O .

Binding of 125 I-labeled angiogenin to actin was also analyzed by ligand blotting. 125 I-labeled angiogenin was found to bind to membrane-immobilized actin (data not shown).

Polymerization of Actin by Angiogenin. Many actin-binding proteins either promote or inhibit actin polymerization (12). Hence the effect of angiogenin on actin polymerization was examined. When angiogenin is mixed with globular actin at 0.2 mg/ml in depolymerization buffer, which is below the critical concentration of actin for spontaneous polymerization (0.5 mg/ml), visible turbidity develops within seconds due to the formation of aggregates. The aggregates sediment readily on microcentrifugation, stain strongly with BODIPY FL phalloidin (Molecular Probes), exhibit a needle-like structure under light microscopy (data not shown), and resolve into two bands corresponding to actin and angiogenin on SDS/PAGE (Fig. 4).

The catalytically inactive angiogenin mutants H13A and H114A (13) induced the polymerization of actin as effectively as native angiogenin. However, the putative receptor-binding-site-modified derivatives of angiogenin Ang-K and Ang-E (14) were qualitatively less capable of inducing polymerization as shown by band staining on SDS/PAGE. These

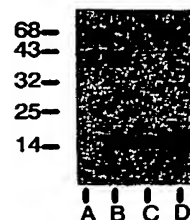


FIG. 4. Polymerization of actin by angiogenin. Angiogenin (5 μ l of a 2.78 mg/ml solution) in water was added to 10 μ g of bovine muscle actin in 100 μ l of depolymerization buffer and mixed several times by pipetting. Polymerized actin was collected by centrifugation at $15,600 \times g$ for 15 min. The supernatant and precipitate were subjected to SDS/PAGE and silver staining. Lanes: A, actin only; B, the precipitate of the actin/angiogenin mixture; C, the supernatant of the actin/angiogenin mixture; D, angiogenin only.

observations are consistent with previous evidence that Ang-K and Ang-E fail to compete efficiently for the binding of angiogenin to AngBP (6).

PF-4 and Protamine Inhibit Angiogenin Binding to Actin. Two known angiogenesis inhibitors, PF-4 and protamine, were examined for their effect on angiogenin binding to actin (Fig. 5). The crosslinking of 125 I-labeled angiogenin and actin was completely inhibited by the presence of PF-4 (0.4 μ g/ml) or protamine (10 μ g/ml), respectively.

125 I-Labeled Actin Binds Other Angiogenic Factors. The observations that angiogenin binds to actin and that PF-4 and protamine inhibit the binding raise the question of whether binding to actin is characteristic of angiogenic molecules. To examine this possibility, direct binding and crosslinking experiments of 125 I-labeled actin to bFGF, TNF- α , and TGF- β were performed. Fig. 6 shows that 125 I-labeled actin is able to bind to and form complexes with bFGF and TNF- α , as established by crosslinking. 125 I-labeled actin does not crosslink with TGF- β under the conditions described.

Actin Inhibits the Biological Activity of Angiogenin. The ability of actin to inhibit angiogenin's biological activity was assessed by the chicken CAM assay (Table 2). In five sets of assays, 10 ng of angiogenin alone induced a positive response in 48% of the eggs ($P = 0.00003$), consistent with its dose-response results in previous studies (1). In the presence of 300 ng of actin, the activity of this much angiogenin was reduced to 36%, which is a statistically significant ($P = 0.012$) positive response. With a 100-fold molar excess of actin (3 μ g), however, the effect of angiogenin in this assay was completely abolished ($P = 0.196$). Actin alone at either concentration did not induce significant angiogenesis.

Anti-Actin Antibody Inhibits the Biological Activity of Angiogenin. The involvement of actin in the induction of angiogenesis by angiogenin was tested by determining whether anti-actin antibodies interfere with this process. Indeed, a 10-fold molar excess of an anti-actin antibody inhibits ($P = 0.29$) the angiogenesis induced by 10 ng of angiogenin (Table 3). Anti-actin alone does not stimulate angiogenesis ($P = 0.58$) and nonimmune control IgG is not inhibitory at this level (data not shown).

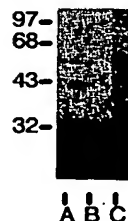


FIG. 5. Inhibition by PF-4 and protamine of the crosslinking of 125 I-labeled angiogenin to actin. Bovine muscle actin (50 ng in 50 μ l of PBS) was incubated with 10^6 cpm of 125 I-labeled angiogenin in the presence of PF-4 (0.4 μ g/ml; lane A) or protamine (10 μ g/ml; lane B). Lane C was a control without inhibitors. Crosslinking was performed as described in Fig. 3.

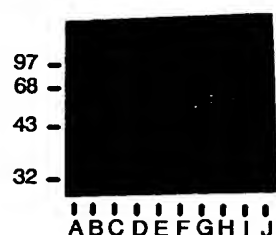


FIG. 6. Affinity crosslinking of ^{125}I -labeled actin to various angiogenic molecules. ^{125}I -labeled actin (10^6 cpm) was incubated with $0.25\ \mu\text{g}$ of an angiogenic molecule in $50\ \mu\text{l}$ of PBS at room temperature for 30 min and crosslinked with carbodiimide at a final concentration of 10 mM. The reactions were quenched by Tris (pH 8.0) at a final concentration of 100 mM. The mixtures were separated by SDS/PAGE and subjected to autoradiography. Lanes: A, molecular weight standards; B, ^{125}I -labeled actin only; C and D, angiogenin; E and F, bFGF; G and H, TGF- β ; I and J, TNF- α . The predicted molecular masses for actin-angiogenin, actin-bFGF, actin-TGF- β , and actin-THF- α are 56, 58, 59, and 54 kDa, respectively.

DISCUSSION

Actin is a ubiquitous molecule that plays an important role in cell structure, cell motility, and generation of contractile force in both muscle and nonmuscle cells. It is found in the cytosol of all cells from amoebae to humans. It accounts for 5–10% of the total protein content of eukaryotic cells and up to 20% of the protein in muscle. Multiple forms of actin or isoactins are found in many organisms. Mammals and birds synthesize six isoforms in a tissue-specific fashion (15), suggesting that there may be a functional basis for the actin isoform multiplicity although the sequences are remarkably conserved (10, 15).

Amino acid composition, tryptic peptide mapping, and sequence analysis indicate that AngBP is a member of the actin family. Indeed, its composition is closely similar to that of the most abundant protein in bovine brain microvessels, which was also identified as a form of actin by the same techniques. This latter protein was localized to the plasma membrane of the capillary endothelial cells by immunohistochemical staining (11). The differences in amino acid composition between AngBP and any of the bovine actins (Table 1) are minor and most that have been noted may be associated with the conditions for acid hydrolysis. The close similarity of the actin and AngBP peptide maps (Fig. 2) suggests a correspondingly close similarity in sequence. Thus, it remains to be established whether or not AngBP represents another form of actin or is identical to one already characterized.

Table 2. Effect of actin on the activity of angiogenin in the CAM assay

Sample	No. positive eggs/ no. total eggs	% positive	P
Angiogenin (10 ng)	46/95	48	0.00003
Actin (300 ng)	16/75	21	0.598
Actin (3 μg)	13/69	19	0.824
Angiogenin (10 ng) + actin (300 ng)	27/75	36	0.012
Angiogenin (10 ng) + actin (3 μg)	19/71	27	0.196

Combined data from five sets of assays each employing between 17 and 20 eggs. The significance was calculated from χ^2 values, based on comparison with water control samples tested simultaneously, which produced 18% positive responses (14/78). $P < 0.05$ indicates a positive sample. The amount applied per egg is shown in parentheses.

Table 3. Effect of anti-actin antibody on the activity of angiogenin in the CAM assay

Sample	No. positive eggs/ no. total eggs	% positive	P
Angiogenin (10 ng)	35/65	54	0.00013
Anti-actin (1 μg)	18/77	23	0.58
Angiogenin (10 ng) + anti-actin (1 μg)	18/65	28	0.29

Combined data from five sets of experiments employing between 9 and 27 eggs. The significance was calculated from χ^2 values, based on comparison with water control samples tested simultaneously, which produced a 19% positive response (10/52). The amount applied per egg is shown in parentheses.

We had reported (6) that AngBP is a cell surface protein that can be detached from the cell by heparan sulfate and, probably, by angiogenin. Immunofluorescent staining of cultured endothelial cells with anti-actin antibodies reveals the presence of a smooth muscle type of α -actin on the cell surface (J. Moroianu, J.W.F., J.F.R., and B.L.V., unpublished data). Exposure of the cells to angiogenin diminishes the cell surface staining with anti-actin antibodies, supporting the conclusion that AngBP is a dissociable cell surface actin. We cannot exclude the possibility, of course, that angiogenin also reacts with actin intracellularly.

Actin has been reported to be present on the surface of normal B lymphocytes (16, 17) and to be a constituent of the intercellular matrix of smooth muscle (18), fibroblasts (19), and endothelial cells (20). Furthermore, it is distributed along the vascular internal elastic membrane in small arterioles and capillaries as shown by immunohistological staining (21). The present data provide further clues for understanding the physiological significance of cell surface actins.

Angiogenin induces the polymerization of actin. This has precluded direct measurements of binding by standard spectral or fluorescent means. Nevertheless, it may relate to the physiological mode of action of angiogenin. We have reported (6) that AngBP (actin) appears to be released from the cell surface of cultured endothelial cells by addition of angiogenin to the medium. Indeed, it might be that induction of polymerization on binding of angiogenin to cell surface AngBP causes it to detach from the cell surface. Cell surface actin of cultured endothelial cells likely corresponds to extracellular matrix (ECM)-actin *in vivo*. Hence, binding of angiogenin to ECM-actin molecules could lead to cell detachment from the ECM followed by migration, proliferation, and differentiation into microvessels, all of which are components of the angiogenic process. Importantly, reorganization of extracellular actin has been observed during the growth and formation of the corneal endothelium (22).

Angiogenin is a member of the ribonuclease superfamily with 33% sequence identity to bovine pancreatic RNase A and an overall sequence similarity of $\approx 53\%$. All of the major components of the active site of RNase A are conserved and angiogenin exhibits ribonucleolytic activity, which although greatly diminished compared to that of RNase A, is nevertheless essential to its angiogenic activity. In addition the nonactive site region of angiogenin that encompasses residues 60–68 has been implicated as part of a cell surface receptor binding site that is also crucial for angiogenic activity (14). This region is relatively well conserved among the angiogenins from various species but differs markedly from the pancreatic RNases. It is notable that none of these RNases is angiogenic and only bovine seminal RNase, a dimeric protein with a number of unusual biological properties, has been reported to be an actin-binding protein, a property that is lost on monomerization (23).

The modified angiogenins Ang-K and Ang-E, whose putative cell-surface binding sites have been disrupted by

limited proteolysis (14), are much weaker inducers of the polymerization of actin than native angiogenin or the catalytic active site mutant angiogenins H13A and H114A. This suggests that the binding of angiogenin to actin involves its cell surface binding region and is consistent with the proposed dual site model for angiogenin (14).

A large number of proteins can bind to actin and function in the nucleating, capping, stabilizing, severing, bundling, and mechanical movement of actin filaments (12). Through the interactions with these proteins, actin filaments participate in several essential cellular functions, including cell motility, cytokinesis, maintenance of cell structure, and organelle movement (12). Angiogenin can be added to the growing list of actin binding proteins. One of the earliest changes in the cytoskeleton after certain ligands bind to their receptors is the polymerization of globular actin to form filamentous actin (24). An indirect association between receptor binding and rapid polymerization of actin has been demonstrated in several receptor systems on various cell types (25). A direct reaction between angiogenin and actin could be more effective. Castellani and O'Brien (26) reported that the biologically active form of nerve growth factor interacts with actin, which becomes organized into well-ordered paracrystalline arrays. They suggested that the *in vitro* formation of nerve growth factor-actin complexes may be related to the *in vivo* mechanism of action of nerve growth factor.

The crosslinking of angiogenin to actin is inhibited by protamine, a 4.3-kDa arginine-rich basic protein known for its capacity to inhibit *in vivo* angiogenesis induced by various angiogenic stimuli (embryologic, neoplastic, inflammatory, and immunogenic) (27). Another angiogenesis inhibitor, PF-4 (28), also inhibits the crosslinking of angiogenin to actin. The finding that *in vivo* angiogenesis inhibitors can antagonize ligand-receptor (or ligand-binding protein) interactions is important and implies that the binding of angiogenin to actin may have physiological significance.

It is not clear as yet whether actin is the functional receptor that is responsible for the cellular responses to angiogenin observed in cultured endothelial and smooth muscle cells (2-5) and for the *in vivo* neovascularization induced by angiogenin. However, the data suggest that the binding of angiogenin to actin may be an essential step. In particular the inhibitory effect of actin and anti-actin antibodies on angiogenin-induced angiogenesis in the CAM assay support this hypothesis. It cannot be ruled out that this inhibition has a more complex basis including but not solely related to the polymerizing effect of angiogenin on actin.

Two widely distributed multifunctional growth factors, bFGF and TNF- α , are angiogenic molecules with distinct cellular receptors for different cellular responses. Stimulation of angiogenesis induced by these molecules *in vivo* is thought to occur via binding to these receptors, which have been identified from cells in culture. The fact that both bFGF and TNF- α can bind to actin suggests that this may reflect a more general mechanism induced by different angiogenic molecules and perhaps provide a common pathway of angiogenesis. Indeed the ubiquitous distribution of actin may provide a convenient and effective way to regulate angiogenesis. Moreover, the inhibitory activity of actin on angio-

genesis induced by angiogenin in the CAM suggests a class of angiogenesis inhibitors that may have therapeutic benefit in pathological conditions characterized by excessive blood vessel growth.

We thank Wynford V. Brome and Rebecca Ettinger for technical assistance and Dr. Michael D. Bond for providing the sequence of the initial tryptic peptide from AngBP. This work was supported by funds from Hoechst, A. G., under agreements with Harvard University.

1. Felt, J. W., Strydom, D. J., Lobb, R. R., Alderman, E. M., Bethune, J. L., Riordan, J. F. & Vallee, B. L. (1985) *Biochemistry* **24**, 5480-5486.
2. Bicknell, R. & Vallee, B. L. (1988) *Proc. Natl. Acad. Sci. USA* **85**, 5961-5965.
3. Bicknell, R. & Vallee, B. L. (1989) *Proc. Natl. Acad. Sci. USA* **86**, 1573-1577.
4. Soncin, F. (1992) *Proc. Natl. Acad. Sci. USA* **89**, 2232-2236.
5. Heath, W. F., Moore, F., Bicknell, R. & Vallee, B. L. (1989) *Proc. Natl. Acad. Sci. USA* **86**, 2718-2722.
6. Hu, G.-F., Chang, S.-I., Riordan, J. F. & Vallee, B. L. (1991) *Proc. Natl. Acad. Sci. USA* **88**, 2227-2231.
7. Bond, M. D. & Vallee, B. L. (1988) *Biochemistry* **27**, 6282-6287.
8. Grinspan, J., Mueller, S. N. & Levine, E. M. (1983) *J. Cell. Physiol.* **114**, 328-338.
9. Knighton, D., Ausprunk, D., Tapper, D. & Folkman, J. (1977) *Br. J. Cancer* **35**, 347-356.
10. Korn, E. D. (1982) *Physiol. Rev.* **62**, 672-737.
11. Pardridge, W. M., Nowlin, D. M., Choi, T. B., Yang, J., Calaycay, J. & Shively, J. E. (1989) *J. Cereb. Blood Flow Metab.* **9**, 675-680.
12. Pollard, T. D. & Cooper, J. A. (1986) *Annu. Rev. Biochem.* **55**, 987-1036.
13. Shapiro, R. & Vallee, B. L. (1989) *Biochemistry* **28**, 7401-7408.
14. Hallahan, T. W., Shapiro, R. & Vallee, B. L. (1991) *Proc. Natl. Acad. Sci. USA* **88**, 2222-2226.
15. Rubenstein, P. A. (1990) *Bioessays* **12**, 309-315.
16. Owen, M. J., Auger, J., Barber, B. H., Edwards, A. J., Walsh, F. S. & Crumpton, M. J. (1978) *Proc. Natl. Acad. Sci. USA* **75**, 4484-4488.
17. Sanders, S. K. & Craig, S. W. (1983) *J. Immunol.* **131**, 370-377.
18. Jones, P., Scott-Burden, T. & Gevers, W. (1979) *Proc. Natl. Acad. Sci. USA* **76**, 353-357.
19. Chen, L. B., Murray, A., Segal, R. A., Bushnell, A. & Welsh, M. L. (1978) *Cell* **14**, 377-391.
20. Bach, P. R. & Bentley, J. P. (1980) *Connect. Tissue Res.* **7**, 185-196.
21. Accinni, L., Natall, P. G., Silvestrini, M. & De Martino, C. (1983) *Connect. Tissue Res.* **11**, 69-78.
22. Klagsbrun, M. & D'Amore, P. A. (1991) *Annu. Rev. Physiol.* **53**, 217-239.
23. Simm, F. C., Krietsch, W. K. & Isenberg, G. (1987) *Eur. J. Biochem.* **166**, 49-54.
24. Omann, G. M., Allen, R. A., Bokoch, G. M., Painter, R. G., Traynor, A. E. & Sklar, L. A. (1987) *Physiol. Rev.* **67**, 285-322.
25. Downey, G. P., Chan, C. K. & Grinstein, S. (1989) *Biochem. Biophys. Res. Commun.* **164**, 700-705.
26. Castellani, L. & O'Brien, E. J. (1981) *J. Mol. Biol.* **147**, 205-213.
27. Taylor, S. & Folkman, J. (1982) *Nature (London)* **297**, 307-312.
28. Maione, T. E., Gray, G. S., Petro, J., Hunt, A. J., Donyer, A. L., Bauer, S. I., Carson, H. F. & Sharpe, R. J. (1990) *Science* **247**, 77-79.



Associate Editor: D. Shugar

Structure-Function Relationships of Acid Ribonucleases: Lysosomal, Vacuolar, and Periplasmic Enzymes

Masachika Irie*

DEPARTMENT OF MICROBIOLOGY, HOSHI COLLEGE OF PHARMACY, EBARA 2-4-41, SHINAGAWA-KU, TOKYO 142, JAPAN

ABSTRACT. It is surprising that only relatively recently has attention been directed to the characterization of the properties of acid ribonucleases (RNases), leading to some understanding of their biochemistry and their functional roles. The present review summarizes current progress in this field under the following general topics: (1) the wide distribution of acid RNases in organisms from viruses to animals; (2) recent findings concerning their primary and three-dimensional structure; (3) the structure-function relationship of acid RNases, with a fungal RNase from *Rhizopus niveus* as a model enzyme; (4) the unique localization of acid RNases in the periplasm of bacteria, vacuoles in plants, and lysosomes of animals and protozoa; and (5) the diversity of physiological roles, depending on the organism, such as self-incompatibility factors and defense proteins in some plants, the surface protein of an animal virus related to pathogenicity, and possible relationship to human cancer. PHARMACOL. THER. 81(2):77–89, 1999. © 1999 Elsevier Science Inc. All rights reserved.

KEY WORDS. Acid RNase, distribution, localization, structure-function relationship, physiological role.

CONTENTS

1. INTRODUCTION	77	5. MECHANISM OF ACTION OF ACID RIBONUCLEASES	82
2. ACID RIBONUCLEASES	78	5.1. CHEMICAL MODIFICATION AND KINETIC STUDIES	82
2.1. ACID RIBONUCLEASES FROM FUNGI	78	5.2. PROTEIN ENGINEERING STUDIES	82
2.2. PLANT ACID RIBONUCLEASES	78	6. PHYSIOLOGICAL FUNCTIONS OF ACID RIBONUCLEASES	83
2.3. ANIMAL ACID RIBONUCLEASES	80	6.1. VIRAL SURFACE PROTEIN	83
2.4. PROTOZOAN ACID RIBONUCLEASES	80	6.2. SELF-INCOMPATIBILITY	84
2.5. BACTERIAL AND VIRAL ACID RIBONUCLEASES	80	6.3. PHOSPHATE REMOBILIZATION	85
3. PRIMARY AND THREE-DIMENSIONAL STRUCTURES OF ACID RIBONUCLEASES	81	6.4. DEFENSE AGAINST PATHOGENS	85
3.1. DISULFIDE BRIDGES	81	6.5. SENESCENCE	85
3.2. THREE-DIMENSIONAL STRUCTURES	81	6.6. LOCALIZATION OF ACID RIBONUCLEASES IN EUKARYOTIC AND PROKARYOTIC CELLS	85
4. INHIBITORS	81	7. CONCLUSIONS AND PERSPECTIVES	86
		ACKNOWLEDGEMENT	86
		REFERENCES	86

ABBREVIATIONS. CAS, conserved active-site segment; CMC, 1-cyclohexyl-3-(2-morpholinyl-4-ethyl)-carbodiimide; CSFV, classic swine fever virus; ER, endoplasmic reticulum; E-ms, envelope glycoprotein of classic swine fever virus; mutant enzyme, an enzyme whose amino acid at the *i*th residue (X) is substituted by Y by site-directed mutagenesis, is denoted as XiY—thus, H109F is a mutant enzyme in which the His residue at the 109th position has been replaced by a Phe residue; RNase, ribonuclease; S-like RNase, plant RNase without self-incompatibility activity; S-RNase, self-incompatibility factors with RNase activity.

1. INTRODUCTION

Ribonucleases (RNases) are very important enzymes for RNA metabolism in almost all organisms; they include those that hydrolyze only single-stranded RNA, double-stranded RNA, and RNA hybridized with DNA. The present review embraces RNases that hydrolyze single-stranded RNA *via* a 2',3'-cyclic phosphate intermediate at the 3'-terminus of oligonucleotides, ultimately forming oligo-

or mononucleotides with a terminal 3'-phosphate (transferase type RNase).

Transferase-type RNases are classified in several ways, e.g., by base specificity, structure, function, optimal pH, and origin. However, progress in the biochemistry of RNases has established correlations among such classifications and simplified the classification system.

Among RNases, there are two types of alkaline RNases that have optimal pHs ~7–8. One of these is guanylic acid-specific, with a molecular mass ~12 kDa, which is widely distributed in fungi and bacteria. They are classified as members of the RNase T1 family. The other alkaline

*Corresponding author's address: Akazutsumi 2-50-3, Setagaya-ku, Tokyo 156-0044, Japan.

RNase type embraces pyrimidine base-specific RNases with a molecular mass of 13–14 kDa and is found largely in vertebrates. They are referred to as the RNase A family, taking this name from the most well-known member, bovine RNase A. The RNase A family of RNases has been extensively studied, but, as regards its physiological roles, we know only that these RNases function as digestive enzymes inside and outside of cells, such as mammalian pancreatic and salivary gland RNases. However, very recently, bovine and human angiogenins, members of the RNase A family (RNase 5), have been reported to accelerate angiogenesis related to metastasis of tumor cells (Riordan, 1997). On the other hand, antitumor activities of bovine seminal RNase, and some frog egg RNases, have been reported (Youle and D'Alessio, 1997), and one of the latter, onconase from leopard frog eggs, is now under Phase 3 clinical trial as an antitumor agent.

The name "acid RNase" is used for two types of RNases in the literature. One type includes the pyrimidine base-specific RNases, which are distributed in the vertebrate liver, spleen, urine, monocytes, and other tissues (Morita *et al.*, 1986; Egesten *et al.*, 1997; Snyder and Gleich, 1997). The primary structures of these enzymes have revealed an RNase A family (Beintema *et al.*, 1988), with an optimal pH of ~6.5–7.0 (weakly acidic RNase). Since they are mainly distributed in nonsecretory organs, such as the liver and spleen, they have been termed *nonsecretory RNases* (Sierakowska and Shugar, 1977). Recently, the terms *neurotoxin-type RNase* and *RNase 2* have been coined by other investigators (Beintema *et al.*, 1997). More recent studies on these enzymes have revealed that they are cytotoxic (Snyder and Gleich, 1997) and bactericidal (Lehrer *et al.*, 1989), inhibit retrovirus transduction of many target cells (Domachowski and Rosenberg, 1997), and apparently are active against Kaposi's sarcoma (Griffiths *et al.*, 1997).

The other family comprises enzymes with an optimal pH of ~4–5, and thus, are real acid RNases. There have been many reports on this type of RNase since the early period of RNase biochemistry. They are distributed from viral surface proteins to bacteria, fungi, plants, and even to higher animals. The primary structures of these RNases have been studied extensively over the past 10 years. Some are believed to protect cells from external pathogens (Rojo *et al.*, 1994a,b). A clear correlation between enzymatic activity of acid RNases and disease, and some physiological changes in humans and other animals, has been achieved in only a few cases because of the slow development of the biochemical characterization of this class of enzymes in the past. Increases in acid RNase activity in the rat CNS (Alberghina and Griffida Stella, 1988) and rat brain (Nakamura *et al.*, 1989) with aging have been reported. Very recently, a partial sequence of the gene for human acid RNase was described. The gene coding for this RNase was cloned from the 6q27 region of chromosome 6. The 6q27 region is known to be frequently rearranged in several human malignancies and is suggested to harbor a tumor-suppressor gene (Trubia *et al.*, 1997). In this context, it would be useful to

gain a basic understanding for further development or application of these enzymes for potential clinical use. Since biochemical knowledge of acid RNases recently has expanded remarkably, we will review briefly the structure-function relationship of typical acid RNases.

2. ACID RIBONUCLEASES

2.1. Acid Ribonucleases from Fungi

Acid RNase was first purified from *Aspergillus oryzae* (Sato and Egami, 1957), as an adenylic acid-specific enzyme, but further study revealed it to be an adenylic acid-preferential, and base-nonspecific, RNase. The molecular mass estimated by gel filtration was ~35 kDa (Uchida and Egami, 1971). The primary structures of such RNases from *Rhizopus niveus* and *Aspergillus oryzae* were determined by Horiuchi *et al.* (1988) and Kawata *et al.* (1988). Subsequently, the primary structures of many fungal acid RNases, as shown in Fig. 1, were determined during the past decade. The majority of these structures are similar to that of RNase T2. They consist of ~200 amino acid residues, and contain 10 half-cystines, hence, 5 disulfide bridges. Many of these RNases are glycoproteins, exceptions being RNase Rh from *Rhizopus niveus* (Horiuchi *et al.*, 1988) and RNase Le2 from *Lentinus edodes* (Kobayashi *et al.*, 1992). A well-defined feature of these enzymes is the presence of two characteristic segments, shown as CAS (conserved active-site segment) I and II in Fig. 1. The base specificity of the many enzymes in this group is purine-nucleotide preferential, especially adenylic acid, followed by guanylic acid, but there are also some guanylic acid preferential enzymes. Three-dimensional structures of these enzymes are discussed in Section 3. In yeast, an acid RNase, which is base nonspecific, as well as single-stranded RNA preferential, has been characterized. It has a sharp pH optimum at pH 6.2, and it cleaves GpY bonds preferentially (Cannistraro and Kennell, 1997).

2.2. Plant Acid Ribonucleases

Many of the plant RNases that have been reported are acidic enzymes (Wilson, 1982; Green, 1994). In contrast to fungal RNases, the majority of plant RNases cleave RNA to 2',3'-cyclic nucleotides. Further incubation leads to slow formation of purine 3'-nucleotides, i.e., the rates of cleavage of the cyclic nucleotides are very low compared with the fungal RNases.

The primary structures of plant RNases have been studied using three approaches. (1) Anderson *et al.* (1986, 1989) cloned the S-gene and found that S-gene products, self-incompatibility factors (Section 6.2) with sequences very similar to those of fungal RNases, also contain the two CAS motifs of fungal RNases. It was further confirmed that S-gene products have RNase activity (McClure *et al.*, 1989). The acid RNases encoded by the S-gene were called S-RNases (self-incompatibility factors with RNase activity). The presence of such S-RNases has been reported in many other plants, as described by Green (1994) and Parry *et al.* (1997a). These findings make it clear that plant acid

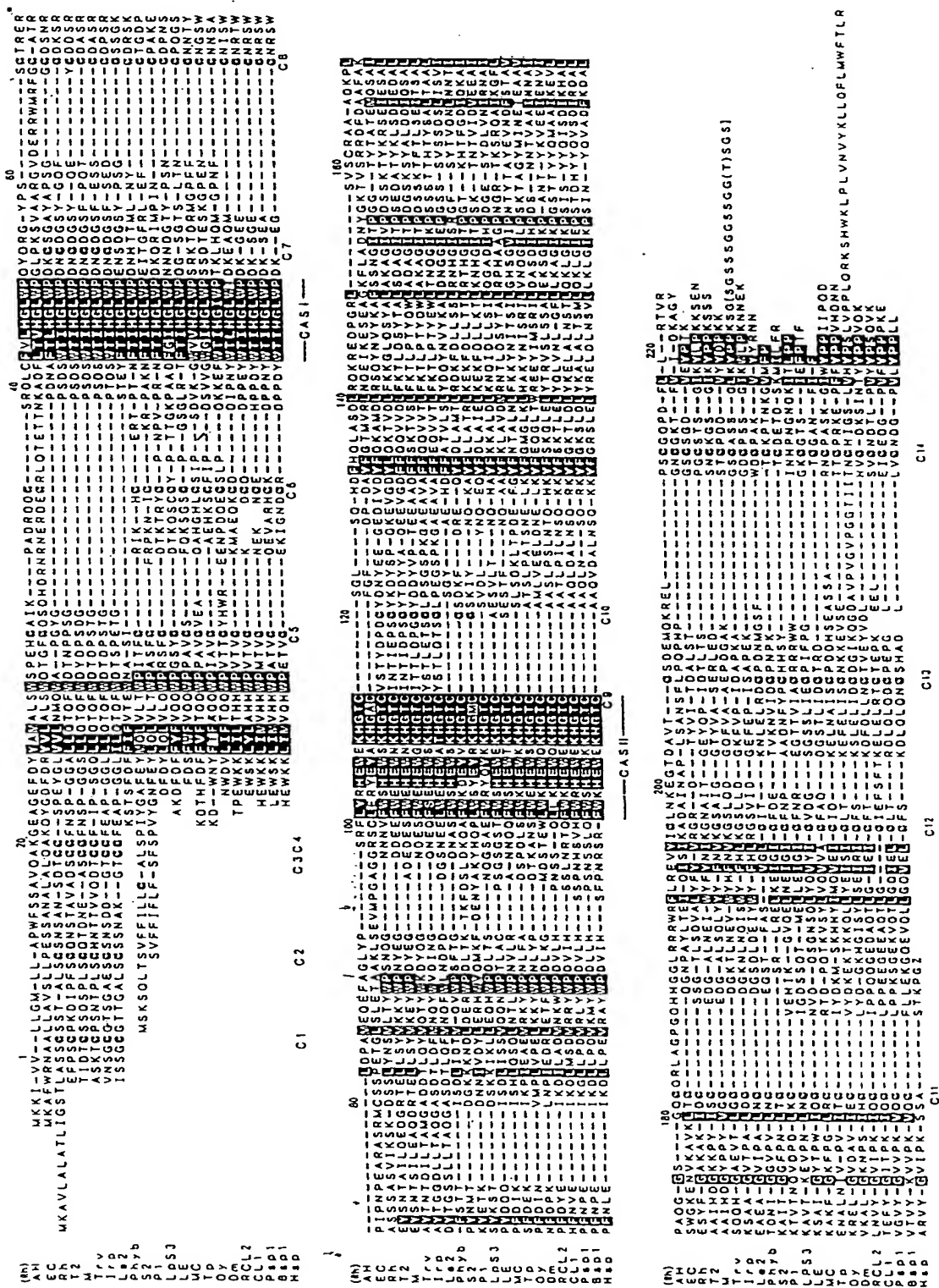


FIGURE 1. Amino acid sequences of acid RNases belonging to the RNase T2 family. AH, RNase from *Aspergillus hydrophila* (Favre et al., 1993); EC, RNase I from *Escherichia coli* (Meador and Kennell, 1990); Rh, RNase Rh from *Rhizopus niveus* (Horiuchi et al., 1991); Lp, RNase Lp from *Lycopersicon* (Kobayashi et al., 1992); Phb, RNase from *Physarum polycephalum* (Inokuchi et al., 1993); S2, S-RNase from *Nicotiana glauca* (McClure et al., 1989); P1, S-RNase from *Petunia inflata* (Ai et al., 1990); Trv, RNase Trv from *Trichoderma viride* (Inada et al., 1991); LpS3, RNase from *Lycopersicon peruvianum* (Tsai et al., 1992); LE, tomato RNase from *Lycopersicon esculentum* (Jost et al., 1991); MC, RNase LC1 from bitter melon (*Momordica charantia*) (Ide et al., 1991); Tp, squid RNase (*Todarodes pacificus*) (Kusano et al., 1998); Oy, oyster RNase (*Crassostrea gigas*) (Watanabe et al., 1993); Dm, RNase from *Drosophila melanogaster* (Hime et al., 1995); RCL2, acid RNase from bullfrog (*Rana catesbeiana*) (Inokuchi et al., 1997); CL1, chicken liver RNase (Uchida et al., 1996); Psp1, porcine spleen RNase (Kusano et al., 1997); Bsp1, bovine spleen RNase (Narumi et al., 1997); Hsp, human spleen RNase (Trubia et al., 1997). C1-C14 denote all half-cysteine residues from the N-terminus to the C-terminus. The numbers at the top of the matrix represent RNase Rh numbering. CAS, segment typically conserved in the RNase T2 family RNases, which includes catalytically important amino acid residues.

RNases are in the same family as fungal RNases. (2) Glund and associates found that excretion of acid RNase from cultured tomato cells was induced by phosphate deprivation. Simultaneously, the intracellular RNase level was raised. The structures of the excreted enzyme and two other intracellular RNases, one a vacuolar enzyme, were determined by these investigators (Jost *et al.*, 1991; Löffler *et al.*, 1993; Köck *et al.*, 1995). (3) The presence of acid RNase in mature seeds of bitter melon (Ide *et al.*, 1991), as well as *Luffa cylindrica* (K. Nakamura, K. Sasaki, M. Kino and G. Funatsu, unpublished data), was also reported. Their primary structures are very similar to those of S-gene products. These plant RNases without self-incompatibility are called *S-like RNases* because of the similarity of their primary structures (Green, 1994). Hence, the similarity between plant and fungal RNases is considered as established. The plant acid RNases basically have 8 half-cystine residues, the locations of 4 of which are superimposable on those of fungal RNases.

2.3. Animal Acid Ribonucleases

Bernardi and Bernardi (1966) reported the purification of an acid RNase from porcine spleen. Maver and Greco (1962) purified a similar RNase from bovine spleen and liver. Despite such early reports on the purification of acid RNases, the chemical nature of these enzymes and their mutual relationships were not clarified until 1992. Levy and Karpetsky (1980) reported that chicken liver contained an RNase that could hydrolyze only poly(C). Later, Miura *et al.* (1984) purified two RNases from chicken liver that hydrolyze poly(C) and poly(U), respectively. The latter enzyme was an acid RNase.

Hayano *et al.* (1993) subsequently found that the poly(C)-specific RNase and the poly(U)-specific RNase reported by Miura *et al.* (1984) were pyrimidine base-specific and base-nonspecific acid RNases, respectively. The primary structure of chicken liver acid RNase was finally elucidated by Uchida *et al.* (1996). It is homologous to fungal and plant RNases. Ohgi *et al.* (1988) have purified a bovine spleen acid RNase having characteristics very similar to those of the enzyme reported by Bernardi and Bernardi (1966). The primary structures of bovine and porcine spleen RNases were then elucidated by Narumi *et al.* (1997) and Kusano *et al.* (1997), and were found to be members of the RNase T2 family. Their structures are very similar to that of chicken acid RNase. The numbers and locations of disulfide bridges are the same as in plant RNases (Parry *et al.*, 1998).

There have been several reports on the purification of acid RNases from lower animals, including squid (Edmonds and Roth, 1960) and sea urchin (Fernlund and Josefsson, 1968). Recently, Watanabe *et al.* (1993) and Kusano *et al.* (1998) elucidated the primary structure of oyster and squid RNases, respectively, and found that these also belong to the RNase T2 family of enzymes. Although the presence of another type of acid RNase in living organisms is conceivable, all the acid RNases purified to date belong to the RNase T2 family.

The presence of another type of acid RNase was reported by Pantazaki and Georgatos (1990) in mouse liver cytosol. They partially purified two acid RNases and tested their base specificity by hydrolysis of 5S RNA. This showed an RNase fraction with an optimal pH of 5.5 and a base specificity corresponding to that of RNase A. The other enzyme, a major RNase with an optimal pH of ~6–6.5, preferentially hydrolyzes 5S RNA at GpN. The specificity of the latter enzyme appears to be very similar to that of some members of the RNase T2 family. Pantopoulos and Georgatos (1992) reported that rabbit brain nuclei contain three RNases, and that one of them is an acid RNase with an optimal pH of 6.0–6.5. Base specificity, determined with several trinucleotides and dinucleotides, showed a preference for purine-pU bonds, and the enzyme hydrolyzed homopolynucleotides in the order poly(U) > poly(I) > poly(C) > poly(A). Similarly, Ittel *et al.* (1975) earlier reported the presence of an acid RNase in beef brain nuclei that hydrolyzes the four homopolynucleotides, poly(U), poly(I), poly(C), and poly(A). Heinonen and Tuohimaa (1979) described the presence of acid RNase activity in nuclei and cytosol fractions of chick oviduct that increased with ligation of the oviduct or administration of progesterone. Although, in these cases, information on the purity, molecular weight, and sequence of these enzymes is not available, the base specificities of mouse liver and rabbit brain nuclear enzymes appear to correspond to those of members of the RNase T2 family. These examples suggest that acid RNases are located in the nuclei and cytosol, although their characterization is not sufficient to further discuss their identification, probably due to their lower content, as compared with the lysosomal fraction.

2.4. Protozoan Acid Ribonucleases

Acid RNases have been characterized in many protozoa, such as *Tetrahymena pyriformis* (Müller *et al.*, 1966; McKee and Prescott, 1991; Maouri and Georgatos, 1987), *Physarum polycephalum* (Hiramatsu *et al.*, 1969), and the cellular slime mold *Dictyostelium* (Wiener and Ashworth, 1970; Uchiyama *et al.*, 1992). The base specificity of acid RNases from *Tetrahymena* was reported by Maouri and Georgatos (1987). Because of its probable impurity, characterization remains tentative, but these enzymes appear to be base-nonspecific RNases. However, information on their molecular masses is available in only a few cases. Among protozoan RNases, the primary structures and base preferences of the last two have been elucidated (Inokuchi *et al.*, 1993; N. Inokuchi, S. Saito, H. Kobayashi, T. Koyama, S. Uchiyama, and M. Irie, unpublished data), and they also turn out to be members of the RNase T2 family.

2.5. Bacterial and Viral Acid Ribonucleases

RNase I of *Escherichia coli* was recognized long ago as an acid RNase (Neu and Heppel, 1964) located in the periplasmic space, and it is encoded by the *ma* gene. However,

the organism from which the *ma* gene has been deleted is still viable. Earlier findings were summarized by Shen and Schlessinger (1982). The overexpression of RNase I from a recombinant plasmid is not harmful to *E. coli* (Zhu *et al.*, 1990). Recently, Meador and Kennell (1990) cloned the gene encoding this enzyme and elucidated its nucleotide and amino acid sequences. From the sequence, it was evident that RNase I is a member of the RNase T2 family, as it contains the two CAS segments characteristic of these enzymes (see Fig. 1). The physiological role of RNase I is not clear, but it was thought to hydrolyze environmental RNA and facilitate the uptake of P_i . There is another type of RNase I, RNase I*, considered to be a modified form of RNase I. It was purified from the cytosol of spheroplasts. RNase I* lacks the signal sequence of RNase I, and is removed by deletion of the *ma* gene. Although the molecular weight of RNase I* is very similar to that of RNase I, there are some differences in its physicochemical properties and its behavior in response to SH-reagents (Cannistraro and Kennell, 1991). Subsequently, Favre *et al.* (1993) found that *Aeromonas hydrophila*, a gram-negative organism, contains an acid RNase similar to that of *E. coli*. The amino acid sequence of bacterial RNase has active-site amino acid residues nearly identical to those of RNase Rh, a typical fungal RNase of the RNase T2 family.

The presence of viral surface proteins with RNase activity was reported by Schneider *et al.* (1993). The primary structures of these proteins, deduced from DNA sequences, confirmed their similarity with the T2 family of RNases, especially bacterial RNases. Thus, RNase T2 family RNases are a group of enzymes distributed from viruses to mammals.

3. PRIMARY AND THREE-DIMENSIONAL STRUCTURES OF ACID RIBONUCLEASES

As described in Section 2, all acid RNases isolated to date belong to the RNase T2 family of RNases. The primary structures of typical RNases are shown in Fig. 1. One of the characteristic features of these RNases is the existence of two common sequences (CAS I and CAS II), as shown in Fig. 1. These sequences are conserved from viral to animal RNases. Amino acid residues important for the catalytic function, such as His46, His104, His109, and Glu105 (RNase Rh numbering), are located in these segments.

3.1. Disulfide Bridges

Acid RNases are classified by the location and number of half-cystine residues. Fungal RNases have 10 half-cystine residues, while animal and plant RNases have 8, 4 of which are common to all RNases, including those of microorganisms. Therefore, these 4 half-cystine residues are of fundamental importance, and the other 4 can be substituted with other amino acids. Bacterial RNases have 6 half-cystine residues, 4 of which are located at the same sites as those of the other RNases of different origins, while 2 are in positions different from those of plants and animals. In animal and plant RNases, we have observed a few common se-

quences, such as -WP- and -Y(F)P-. In addition, in all RNases, several sequences with hydrophobic amino acids, such as Leu, Ile, Phe, and Tyr, are conserved. These positions probably are necessary to maintain the active conformation via their mutual interaction in the interior of the enzyme molecules.

The locations of some of the disulfide bridges of RNase T2 (Kawata *et al.*, 1988) and S6-RNase of *Nicotiana glauca* (Ishimizu *et al.*, 1995) were determined by chemical methods, and all disulfide bridges of *Nicotiana glauca* and RNase Rh were determined by mass spectroscopy and X-ray crystallographic analysis, respectively (Oxley and Bacic, 1996; Kurihara *et al.*, 1992). In Fig. 1, all half-cystine residues in the T2 family RNases, except for those of bacteria, are numbered from the N-terminus to the C-terminus, 1C-14C. Thus, a fungal RNase, RNase Rh, contains 1C, 2C, 3C, 4C, 7C, 8C, 9C, 10C, 11C, and 14C, and its disulfide bridges are 1C-4C, 2C-7C, 3C-10C, 8C-9C, and 11C-14C (the underlined disulfide bridges are those common to plant and animal RNases). Plant RNases and animal RNases contain 5C, 6C, 8C, 9C, 11C, 12C, 13C, 14C, and some free cysteine residues (Ishimizu *et al.*, 1995) and the disulfide bridges are 5C-6C, 8C-9C, 11C-14C, and 12C-13C.

3.2. Three-Dimensional Structures

X-ray crystallographic analysis of RNase Rh was performed by Kurihara *et al.* (1992). A stereo view of the three-dimensional structure of RNase Rh is shown in Fig. 2. It is an ($\alpha + \beta$)-type structure consisting of six α -helices and seven β -strands. This is the only enzyme whose three-dimensional structure has been elucidated among the many RNase T2 family enzymes. Because of the similarity of the active sites of plant and animal RNases with those of fungal RNase, it is considered that these enzymes have very closely related three-dimensional structures. There are two preliminary reports, one on the crystallization of bitter melon RNase LC (De and Funatsu, 1992) and another on *E. coli* RNase I (Lim *et al.*, 1993). Since the numbers and locations of disulfide groups in plant and animal RNases are different from those of fungal RNases, the resolution of these crystal structures should prove of considerable interest.

4. INHIBITORS

Fungal acid RNases, such as RNase T2 from *Aspergillus oryzae*, RNase M from *Aspergillus saitoi*, and RNase Rh from *Rhizopus niveus*, are markedly inhibited by Cu^{2+} , Zn^{2+} , and Hg^{2+} to a similar extent as RNase A and the RNase T1 family RNases. Various mononucleotides, products and their analogs, inhibited competitively RNase T2, RNase Rh, and RNase M (Uchida and Egami, 1971; Komiyama and Irie, 1972; Irie, 1967). Inhibitory effects of nucleotides are in the order of 2'-AMP > 2'-GMP, 3'-AMP > 2'(3')-UMP for RNase T2 and RNase Rh, and 2'-AMP > 3'-AMP > 5'-AMP > 2'-CMP > 2'-GMP > 2'(3')-UMP for RNase M. A potent inhibitor of RNase A, human placental RNase inhibitor did not inhibit animal acid RNases such as bovine

-spleen RNase Bsp1 and squid RNase Tp. Heparin inhibited fairly well some acid RNases, such as RNase Bsp1 and RNase Tp (M. Iwama and M. Irie, unpublished data). However, for acid RNases, we are unable to find the presence of intracellular RNase inhibitors such as the human placental RNase A inhibitor. This is probably due to its localization in physiological conditions, i.e., acid RNase localized in lysosomes, vacuoles, and periplasm.

5. MECHANISM OF ACTION OF ACID RIBONUCLEASES

The reaction mechanisms of acid RNases have been studied mostly with fungal enzymes, especially RNase Rh from *Rhizopus niveus*, RNase M from *Aspergillus saitoi*, and RNase T2 from *Aspergillus oryzae*. The active site components of fungal acid RNase were first identified by means of chemical modifications and enzyme kinetics, and were subsequently established by protein engineering studies.

5.1. Chemical Modification and Kinetic Studies

Chemical modification of fungal acid RNases with iodoacetate at pH 5.0 inactivated RNase M (Irie *et al.*, 1986) and RNase T2 (Kawata *et al.*, 1991) with incorporation of car-

boxymethyl groups into His46 and His109 (RNase Rh numbering). The ratio of carboxymethyl group incorporation into His46 and His109 was about 45:55 for RNase M (Irie *et al.*, 1986) and RNase T2 (Kawata *et al.*, 1991). Incorporation of a carboxymethyl group into either one of these His residues inactivates the enzyme.

Carboxymethylation of self-incompatibility RNase (see Section 6.2) from wild-type tomato exhibited similar modifications of two histidine residues, with resultant inactivation, but in this protein, one free cysteine residue at the 150th position was modified simultaneously (Parry *et al.*, 1997b).

The participation of His residues in enzymatic activities of fungal RNases is also supported by analysis of the pH profiles of the kinetic parameters for RNase Rh (Komiyama and Irie, 1972) and for RNase M (Irie, 1969), which also suggested the presence of a functional group with a $pK_a \sim 4.0$ (probably a carboxyl group) in the active sites of these enzymes (Komiyama and Irie, 1972; Irie, 1969). The chemical modification of the carboxyl group with a water-soluble carbodiimide, 1-cyclohexyl-3-(2-morpholinyl-4-ethyl)-carbodiimide (CMC), inactivated RNase Rh, with the incorporation of 2 mol of CMC. In the presence of a competitive inhibitor, cytidine, CMC abolished up to 80% of the activity of the native RNase Rh. However, with further addition of CMC, after removal of cytidine by dialysis, RNase Rh was completely inactivated with the incorporation of one additional mole of CMC. This indicated the presence of a carboxyl group in the active site, although identification of the actual modified amino acid was unsuccessful (Sanda *et al.*, 1985).

The majority of RNases in the RNase T2 family contain 5–7 tryptophan residues. The tryptophan residues of RNase M were resistant to *N*-bromosuccinimide oxidation at neutral pH. However, at pH 2.0, at which the enzyme molecule is partly, although reversibly, denatured, 1 mol of tryptophan residue was oxidized with concomitant loss of enzymatic activity (Ohgi and Irie, 1977). Therefore, at least one tryptophan residue is essential for enzyme activity. Excitation of an RNase M-2'(3'),5'-thioinosine diphosphate complex with a UV light at 300 nm, which was absorbed by tryptophan residues, but not nucleotides, emitted fluorescence at 360 nm (Irie *et al.*, 1972). This pointed to energy transfer from a tryptophan to the bound nucleotide, indicating that some tryptophan residues are located near the active site of the enzyme (Irie *et al.*, 1972).

5.2. Protein Engineering Studies

Ohgi *et al.* (1991) cloned the cDNA of RNase Rh and expressed it in yeast cells. The expression vector was constructed by inserting the cDNA of RNase Rh with the pre-pro-sequence of aspartic protease of *Rhizopus niveus* at the N-terminus of RNase Rh, at the promoter of D-glyceraldehyde-3-phosphate dehydrogenase, via the *Bam*HI and *Sall* sites. The yeast cells transformed with this vector expressed the enzyme in a yield of ~ 40 mg/L.

With this expression system, Ohgi *et al.* (1992, 1993, 1995, 1996) prepared several site-directed mutants of the

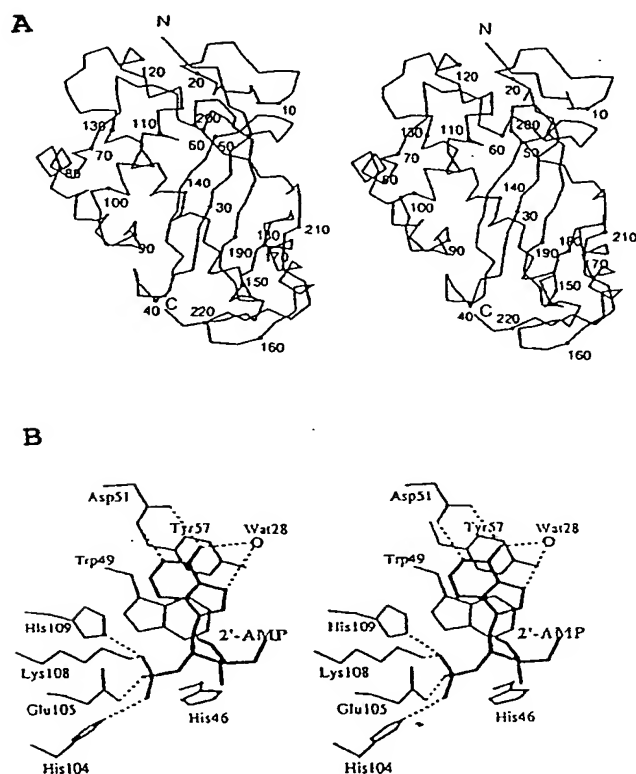


FIGURE 2. (A) Stereo view of the carbon C_{α} skeleton of RNase Rh from *Rhizopus niveus* (Kurihara *et al.*, 1992). (B) Stereo view of the RNase Rh-2'-AMP complex (Nakamura *et al.*, 1993; Hamashima, 1994).

amino acid residues presumed to constitute the active site. The mutants made were Phe-mutants of three His residues, as well as two mutants at amino acid residues with carboxylic acid groups Asp51 and Glu105. The latter two were selected by conducting a search for the commonly conserved amino acid residues among the several RNases known at that time, namely, Asp51 and Glu105.

As described below, X-ray crystallography of the RNase Rh-ligand complex (Nakamura *et al.*, 1993) revealed Lys108 to be located near the active site. Thus, several Lys mutants were prepared (Ohgi *et al.*, 1995, 1996) and their enzymatic activities measured (Table 1). The mutants of three His residues, H46F, H104F, and H109F, were virtually inactive, but the degree of inactivation was more marked for H46F and H109F (<0.02% of native RNase Rh activity). The residual activity of H104F was about 1%. Thus, His46 and His109 were thought to be more important for enzymatic activity. For the H104F mutant, the K_m for several substrates, and K_i value for 2'-AMP, increased, but those for other His-mutants were not markedly different from the native RNase Rh. Thus, H104 was considered to be a binding site for the negatively charged phosphate group of the substrate. Based on the [^1H] NMR spectra of the three His mutants, the three histidine residues were assigned. From the titration curves of each peak in various pH ranges, pK_a values of the three His residues were determined to be 6.7, 5.9, and 6.3 for His46, His104, and His109, respectively. From these data, it was tentatively concluded that His46 and His109 are general acid and base catalysts at the first stage of the reaction (Ohgi *et al.*, 1992). The E105Q mutant was markedly inactivated (activity ~1–2% of the native enzyme), while the D51N mutant was fairly active in hydrolyzing RNA. Thus, Glu105 was thought to be involved in catalysis. Since the K_m values of E105Q were very similar to those of the native enzyme, it was concluded that Glu105 is catalytically crucial and probably operates to polarize the P=O bond or to stabilize a pentacovalent intermediate (Ohgi *et al.*, 1993). The situation for the Lys108 residue was more complex. In some crystals, the side chain of Lys was directed to the active site, while in others, it was not (Kurihara *et al.*, 1992; Nakamura *et al.*, 1993). However, the enzymatic activity of K108L was very low (3.1%), while that of K108R was relatively high. Thus, there may be a relationship to the activation of the enzyme (Ohgi *et al.*, 1995, 1996). The role of these amino acid residues in enzymatic activity was confirmed by X-ray crystallographic analysis of the RNase Rh-2'-AMP complex (Nakamura *et al.*, 1993; Hamashima, 1994). The aforementioned mechanisms of RNase Rh action are summarized in Fig. 3. The enzymatic activities of His46 and His109 in the second step of the reaction were measured using four 2',3'-cyclic nucleotides as substrates. H46F was inactive towards these substrates, while H109F exhibited 5–10% activity. It was found that reversal of the second step of the reaction, i.e., the synthesis of a dinucleoside phosphate from a nucleoside and a 2',3'-cyclic nucleotide, is catalyzed by H109F rather than by H46F (Irie *et al.*, 1997). These results indicated

TABLE 1. Enzymatic Activities of Various Mutants of RNase Rh from *Rhizopus niveus*

Mutant enzyme	Relative activity of substrate (%)		
	RNA	ApU	UpU
RNase Rh	100	100	100
H46F	<0.02	0.19	
H104F	0.30	0.88	
H109F	<0.02	0.24	
E105Q	0.96	1.84	
D51N	66.0	0.19	31.0
K108R	34.0		
K108L	3.1		

that His46 is crucial for the activation of a water molecule and the 5'-hydroxy group of the nucleoside, that is, the roles of the two histidine residues in the first and second steps of the reactions are reversed. Thus, in the second step, His46 serves as the base catalyst and His109 as the acid catalyst.

The D51N mutant had about 30% of the activity of the native enzyme toward UpU, but it showed only 0.2% activity for ApU cleavage (Ohgi *et al.*, 1993). This suggested that Asp51 is related to base recognition at the B1 (major binding) site of RNase Rh. X-ray crystallographic data for the RNase Rh-2'-AMP complex (Hamashima, 1994) are shown in Fig. 2, and indicate that the adenine base is hydrogen bonded with Asp51. The other members of the B1 base recognition site are Tyr57 and Trp49. The latter is probably the amino acid oxidized first by *N*-bromosuccinimide (Ohgi and Irie, 1977). These two aromatic amino acid residues stacked with the base moiety of the nucleotide at the B1 site (Nakamura *et al.*, 1993; Hamashima, 1994).

The base recognition site (B2 site), adjacent to the 3'-side of the B1 site, was identified by X-ray crystallography of the d(ApC or ApG)-RNase Rh complex by Hamashima (1994). The B2 site consisted of Gln32, Pro92, Ser93, Asn94, Gln95, and Phe101. Among these amino acid residues, Phe101 and Pro92 are essentially conserved in all acid RNases elucidated to date (see Fig. 1), but the others have undergone substitution with other amino acid residues. Phe101 is stacked with the cytosine base of the dinucleoside phosphate dApC.

Since the two segments CAS I and CAS II, which contain the catalytic amino acid residues, are common to all acid RNases (RNase T2 family), we assume the same mechanisms prevail for all other members of this family. However, microbial RNases, as well as plant and animal RNases, contain different numbers of disulfide bridges, some of which are located at positions other than those of fungal RNases. Thus, full understanding of this mechanism awaits clarification of the structures of such RNases by X-ray crystallography.

6. PHYSIOLOGICAL FUNCTIONS OF ACID RIBONUCLEASES

6.1. Viral Surface Protein

The envelope glycoprotein (E-rns) of classical swine fever virus (CSFV) was known to have RNase activity. The pri-

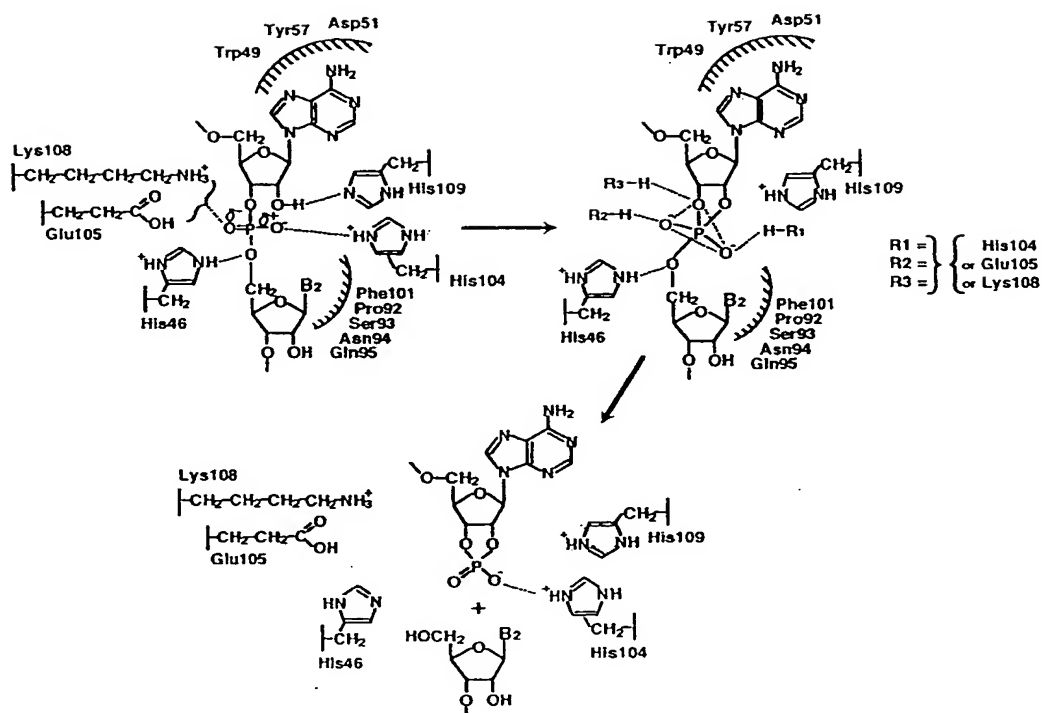


FIGURE 3. Proposed mechanism of action of RNase Rh in the first step (transphosphorylation) of the reaction. R1, R2, and R3 represent one of His104, Glu105, and Lys108.

mary structure of E-rns determined from gene cloning indicated that it was a member of the RNase T2 family (Schneider *et al.*, 1993). The E-rns inhibited the infection of porcine kidney cells with CSFV (Hulst and Moomann, 1997), and completely inhibited concanavalin A-induced proliferation of porcine, bovine, ovine, and human lymphocyte cells (immunosuppression) *in vitro*. It also inhibited protein synthesis of lymphocytes of various species without damage of the cell membrane, leading to apoptosis. These results suggest that the glycoprotein plays an important role in the pathogenesis of CSFV (Bruschke *et al.*, 1997).

6.2. Self-Incompatibility

Self-incompatibility is a mechanism that prevents pollen from one plant from fertilizing other flowers of the same plant. Self-incompatibility is often observed in plants belonging to such families as *Solanaceae* and *Rosaceae*. In these plants, the self-incompatibility is controlled by a single genetic locus with a large number of alleles, the S-locus. In self-incompatible plants, when a pollen particle lands on a style expressing the same S-allele, the pollen tube growth is stopped or retarded, and there is no delivery of sperm to the ovary.

Anderson *et al.* (1986, 1989) cloned the cDNA encoding the extracellular basic proteins S associated with the S-allele of *Nicotiana glauca*, a species of tobacco. Among these proteins, only 56% of the amino acid residues were identical.

However, there are several blocks of well-conserved sequences among all the proteins. Later, McClure *et al.* (1989) identified the CAS sequences of RNase T2 from *Aspergillus oryzae* (Kawata *et al.*, 1988) in these proteins. They also found that basic proteins associated with the S-allele exhibit RNase activity; hence, these proteins are called S-RNases. Similar S-RNases have been found by several groups in many members of the *Solanaceae* and other plants with self-incompatibility (for a review, see Parry *et al.*, 1997a).

The role of S-RNases in self-incompatibility is not adequately understood. McClure *et al.* (1989) suggested that S-RNase degrades rRNA, thus acting like a cytotoxin in the pollen tube. Evidence that the RNase activity of S-RNase is essential for self-incompatibility has been obtained in several ways. The following is an example. The S3-RNase of *Petunia inflata*, the catalytic His of which was mutated to Asn, was introduced into transgenic plants. S-RNase without activity accumulated in the plant at a level normal for self-incompatible plants. However, such a plant did not reject the pollen grain with the S3-gene. Therefore, the RNase activity of S-RNase is essential for its self-incompatibility (Huang *et al.*, 1994).

In a transgenic plant of *Nicotiana*, two RNase T2 family enzymes, S-RNase and *E. coli* RNase I, were expressed and tested for rejection by these plants of the pollen of self-compatible plants (Beecher *et al.*, 1998). Plant-expressed S-RNase rejected the pollen of self-compatible plants, but

expressed *E. coli* RNase I did not. It follows that *E. coli* RNase I cannot substitute for the role of S-RNase in pollen rejection.

6.3. Phosphate Remobilization

An increase in the S-like RNase level in response to phosphate deprivation is very often observed in the plant kingdom. This phenomenon was discovered by Nümberger *et al.* (1990) in cultured tomato cells. The induction of RNases, e.g., extracellular RNase LE, vacuolar RNase LV1-LV3, and intracellular, but extravacuolar, RNase LX, with phosphate deprivation was observed at the protein level (Löffler *et al.*, 1992). Later, Köck *et al.* (1995) demonstrated an increase in the mRNA of RNase LE and that of RNase LX with P_i deprivation. The induction of RNase activity parallels the increase of phosphatase, thus accelerating the uptake of phosphate from environmental RNA.

Vacuolar RNases might function in the uptake of phosphate by digesting intracellular RNA. Similar induction of RNases by phosphate deprivation has been observed in *Arabidopsis thaliana* (Bariola *et al.*, 1994; Tayler *et al.*, 1993) and RNase NE from *Nicotiana glauca* (Dodds *et al.*, 1996). However, not all S-like RNases are necessarily induced by phosphate deprivation. The *Arabidopsis* RNase of the RNase-related self-incompatibility encoding gene RNS3 is not inducible (Parry *et al.*, 1997b).

6.4. Defense against Pathogens

S-like RNases are found in plant seeds, especially in cucurbit species. These S-like RNases were thought to protect the seeds from pathogens. Bitter melon (*Momordica charantia*) seeds contain RNase MC1 (Ide *et al.*, 1991); sponge gourd (*Luffa cylindrica*) seeds, RNase LC1 and LC2 (K. Nakamura *et al.*, unpublished data); cucumber seeds, cusativin (Rojo *et al.*, 1994a); and melon seeds, melosin (Rojo *et al.*, 1994b), all of which belong to the RNase T2 family of RNases. Furthermore, all are self-compatible plants and thus, do not have related self-incompatibility. Cusativin, located in the coat and cotyledon of cucumber seeds, inhibits the translational step of the cell-free protein synthesis system (Rojo *et al.*, 1994a).

In the field of agriculture, it has been reported that expression of a double-stranded RNA-specific RNase in transgenic potato conferred resistance to pathogenic viroids (Sano *et al.*, 1997). A similar result was reported for plant acid RNase. A hypersensitive response and acquired resistance are induced in the tobacco plant by cryptogenin secreted by *Phytophthora cryptogea*. This conferred resistance to subsequent leaf infection by *Phytophthora parasitica* var. *nicotianae* (Galiana *et al.*, 1997). In studies on the mechanism of induction, the authors found that the cellular gene encoding the extracellular S-like RNase NE is expressed rapidly after inoculation with pathogenic fungi, and this activity proved capable of controlling fungal invasion.

The rapid increase in RNase activity in plants in response to wounding was well documented long ago (Farkas,

1982). More recently, Ye and Droste (1996) have described induction of acid RNase by wounding in *Zinnia elegans*. The result appears to be rapid death of the cells around the wound, with protection of the remaining tissues, thus serving a defense mechanism.

6.5. Senescence

During senescence of tomato leaves, two RNase genes, RNase LE and RNase Lx, are expressed, expression of the latter being more pronounced (Lers *et al.*, 1998). The two RNases have been identified in cultured tomato cells, and they are highly homologous enzymes (Löffler *et al.*, 1993). Thus, RNase Lx is related to RNA metabolism in the final stage of senescence.

6.6. Localization of Acid Ribonucleases in Eukaryotic and Prokaryotic Cells

The localization of acid RNases in animal cells is very complex. Many investigators have reported these enzymes to be localized in lysosomes, and also in cytoplasm and nuclei. Localization of acid RNase in lysosomes of rat liver cells was proposed by de Duve *et al.* (1955). Acid RNase is localized in more dense lysosomal-like particles different from those containing acid phosphatase (Rahman *et al.*, 1967; Rahman and Cerny, 1969). Futai *et al.* (1969) characterized an acid RNase from rat liver, separable from alkaline RNase by column chromatography on CM cellulose, with a pH optimum of 5–6. They confirmed that the RNase was lysosomal by isolating it from purified lysosomes. The characteristics of the enzyme, including base nonspecificity and its sharp pH optimum, are very similar to those of RNase from porcine spleen (Bernardi and Bernardi, 1966) and bovine spleen (Ohgi *et al.*, 1988).

These data all indicated that acid RNase is located in lysosomes, and, to our knowledge, only one species of acid RNase is found in animal tissues (Bernardi and Bernardi, 1966; Ohgi *et al.*, 1988). Thus, it is highly probable that acid RNase in lysosomes or lysosome-like particles is a member of the T2 family of RNases. On the other hand, Nakabayashi and Ikezawa (1979) analyzed acid RNases of vertebrate (rat, guinea pig, pig, chicken, and cow) lysosomes by isoelectric focusing, and demonstrated the presence of two or three acid RNases with different isoelectric points. These results may be interpreted in terms of the presence of multiple-sized carbohydrate chains in acid RNases among those observed in bovine and porcine spleen (Ohgi *et al.*, 1988; Kusano *et al.*, 1997). Immunochemical studies by Morikawa (1967) also suggested two acid RNases with identical immunological properties in bovine tissue.

In studies on protozoa, McKee and Prescott (1991) reported that RNase from *Tetrahymena pyriformis* is an acid RNase with a molecular mass of 26.5 kDa, which is excreted from the cells. Müller *et al.* (1966) found that intracellular RNase activity was only 17% when assayed in 0.25 M sucrose, and after exposure to low osmotic pressure, the latency was lost. This suggests that acid RNase is in the ly-

sosomes of protozoa. Localization of RNase in lysosome-like particles was also reported in *Dictyostelium discoidium* cells (Wiener and Ashworth, 1970). The N-terminal sequence of acid RNase isolated from *Dictyostelium discoidium* indicated that this RNase belongs to the RNase T2 family (N. Inokuchi *et al.*, unpublished data). We have no direct evidence as to the nature of lysosomal RNases in general. The evidence described above strongly suggests that lysosomal RNases are mostly RNase T2 family enzymes.

An age-dependent change in activity of acid RNase in rat brain tissues was reported by Nakamura *et al.* (1989). Acid RNase activity was highest in the hippocampus and the lowest activity in 18-month-old rats. On the other hand, Alberghina and Griffida Stella (1988) observed increases in acid RNase activity in the CNS with aging. A similar effect of aging on lysosomal acid RNase was observed previously in *Drosophila melanogaster* (Webster and Webster, 1978). The lysosomal acid RNase activity was also increased in chick oviduct by tissue damage or administration of actinomycin D or progesterone (Heinonen and Tuohimaa, 1979).

The distributions of acid RNases in organelles other than lysosomes have been described by many groups. An acid RNase was reported in rabbit brain nuclei (Pantopoulos and Georgatos, 1992). It had an optimum pH of ~6.0 and depolymerized four homopolynucleotides in the order poly(U) > poly(I) > poly(C) and poly(A). These properties are very similar to those of chicken liver RNase (Uchida *et al.*, 1996). The base specificity of this enzyme, with 5S RNA as a substrate, showed that it specifically cleaved -XpU- bonds, especially when X = G. This feature is similar to that of acid RNases from other animals, but we have no information on the structural relationships among these enzymes.

The presence of another acid RNase has been shown in bovine brain nuclei (Ittel *et al.*, 1975). The enzyme appears to be base nonspecific like RNase T2, but the identity with RNase T2 is not clear.

In a histochemical study with anti-acid RNase serum, Morikawa (1967) demonstrated the presence of acid RNase in the nuclei and cytoplasm of some mammalian tissues. Similarly, the presence of cytosolic acid RNases was reported in mouse liver and chick oviduct (Pantazaki and Georgatos, 1990; Heinonen and Tuohimaa, 1979). These findings suggested that lysosomes are not the sole source of acid RNases. Further information regarding the structure, function, and distribution of these acid RNases is required.

In plants, the situation is more complicated. In tomato cells, acid RNases are distributed extracellularly, in vacuoles, and probably in the endoplasmic reticulum (ER). Tomato RNase LX has a putative C-terminal signal for ER retention, while RNase LV2, which is located in vacuoles and has the same sequence as LX, does not contain this signal sequence, suggesting that RNase LV2 moves to the vacuole from the ER (Löffler *et al.*, 1993; Köck *et al.*, 1995). Further progress in gene cloning should clarify the location and function of acid RNases in eukaryotes.

7. CONCLUSIONS AND PERSPECTIVES

As described in this review, the widespread occurrence of acid RNases in various organisms has now been well documented. However, at the moment, our knowledge of the characteristics of these enzymes is limited to those that are members of the RNase T2 family. This group appears to play diverse roles, depending on the organism, as lysosomal, vacuolar, periplasmic, and cell-defense enzymes, as well as self-incompatibility factors. Further clarification of the nature of these functions is an obvious goal for further research, which should be stimulated by the remarkable advances already made in our understanding of the physiological roles and therapeutic potentials of the members of the RNase A family of enzymes.

Acknowledgement—The author thanks Professor D. Shugar, Department of Biophysics, Institute of Experimental Physics, University of Warsaw, for his advice and critical reading of the manuscript.

References

- Ai, Y., Singh, A., Coleman, C. E., Ioege, T. R., Kheyr-Pour, A. and Kao, T.-H. (1990) Self-incompatibility in *Petunia inflata*. Isolation and characterization of cDNAs encoding three S-allele associated proteins. *Sex. Plant Reprod.* 3: 130–138.
- Alberghina, M. and Griffida Stella, A. M. (1988) Age-related changes of ribonuclease activities in various regions of the rat central nervous system. *J. Neurochem.* 51: 21–24.
- Anderson, M. A., Cornish, E. C., Mau, S.-L., Williams, E. G., Hoggart, R., Atkinson, A., Böning, I., Grego, B., Simpson, R., Roche, P. J., Haley, J. D., Penschow, J. D., Niall, H. D., Tregear, G. W., Coghlan, J. P., Crawford, R. J. and Clarke, A. E. (1986) Cloning of cDNA for a stylar glycoprotein associated with expression of self-incompatibility in *Nicotiana glauca*. *Nature* 321: 38–44.
- Anderson, M. A., McFadden, G. I., Bernatzky, R., Atkinson, A., Orpin, T., Dedman, H., Tregear, G., Fernley, R. and Clarke, A. E. (1989) Sequence variability of three alleles of the self-incompatibility gene of *Nicotiana glauca*. *Plant Cell* 1: 483–491.
- Bariola, P. A., Howard, C. J., Taylor, C. B., Verburg, M., Jaglan, V. D. and Green, P. J. (1994) The *Arabidopsis* ribonuclease gene RNS1 is tightly controlled in response phosphate limitation. *Plant J.* 6: 673–685.
- Beecher, B., Murfett, J. and McClure, B. A. (1998) RNase I from *Escherichia coli* cannot substitute for S-RNase in rejection of *Nicotiana glauca* pollen. *Plant Mol. Biol.* 36: 553–563.
- Beintema, J. J., Hofsteenge, J., Iwama, M., Morita, T., Ohgi, K., Irie, M., Sugiyama, R. H., Schieven, G. L., Dekker, C. A. and Glitz, D. (1988) Amino acid sequence of the non-secretory ribonuclease of human urine. *Biochemistry* 27: 4530–4538.
- Beintema, J. J., Breukelman, H. J., Carsana, A. and Furia, A. (1997) Evolution of vertebrate ribonuclease: ribonuclease A superfamily. In: *Ribonucleases, Structures and Functions*, pp. 245–269, D'Alessio, J. and Riordan, J. F. (eds.) Academic Press, New York.
- Bernardi, A. and Bernardi, G. (1966) Studies on acid hydrolases. III. The isolation and properties of spleen acid ribonuclease. *Biochim. Biophys. Acta* 129: 23–31.
- Bruschke, C. J. M., Hulst, M. M., Moorman, R. J. M., van Rijn, P. A. and van Oorschot, J. T. (1997) Glycoprotein E-RNS of pestiviruses induces apoptosis in lymphocytes of several species. *J. Virol.* 71: 6692–6696.

- Cannistraro, V. J. and Kennell, D. (1991) RNase I*, a form of RNase I and m-RNA degradation in *Escherichia coli*. J. Bacteriol. 173: 4653-4659.
- Cannistraro, V. J. and Kennell, D. (1997) RNase YI* and RNA structure studies. Nucl. Acid Res. 25: 1405-1411.
- De, A. and Funatsu, G. (1992) Crystallization and preliminary X-ray diffraction analysis of a plant ribonuclease from the seeds of the bitter melon *Momordica charantia*. J. Mol. Biol. 228: 1271-1273.
- de Duve, C., Pressman, B. C., Glanetto, R., Wattiaux, R. and Appelmans, P. (1955) Tissue fractionation studies. 6. Intracellular distribution patterns of enzymes in rat-liver tissue. Biochem. J. 60: 604-617.
- Dodds, P. N., Clarke, A. E. and Newbigin, E. (1996) Molecular characterization of an S-like RNase of *Nicotiana glauca* that is induced by phosphate starvation. Plant Mol. Biol. 31: 227-238.
- Domachowske, J. B. and Rosenberg, H. F. (1997) Eosinophils inhibit retroviral transduction of human target cells by a ribonuclease-dependent mechanism. J. Leukoc. Biol. 62: 363-368.
- Edmonds, M. and Roth, J. S. (1960) The purification and properties of a ribonuclease from squid. Arch. Biochem. Biophys. 89: 207-212.
- Egesten, A., Dyer, K. D., Batten, D., Domachowske, J. B. and Rosenberg, H. F. (1997) Ribonuclease and host defense: identification, localization and gene expression in adherent monocytes in vitro. Biochim. Biophys. Acta 1358: 255-260.
- Farkas, G. L. (1982) Ribonuclease and ribonucleic acid breakdown. Encycl. Plant Physiol. 14B: 224-262.
- Favre, D., Ngai, P. K. and Timmis, K. N. (1993) Relatedness of a periplasmic broad-specificity RNase from *Aeromonas hydrophila* to RNase I of *Escherichia coli* and to a family of eukaryotic RNases. J. Bacteriol. 175: 3710-3722.
- Fernlund, P. and Josefsson, L. (1968) Preparation and properties of a sea-urchin ribonuclease. Biochim. Biophys. Acta 151: 373-382.
- Futai, F., Miyata, S. and Mizuno, D. (1969) Acid ribonucleases of lysosomal and soluble fractions from rat liver. J. Biol. Chem. 244: 4951-4960.
- Galiana, E., Bonnet, P., Conrod, S., Keller, H., Panabières, F., Ponchet, M., Poupet, A. and Ricci, P. (1997) RNase activity prevents the growth of a fungal pathogen in tobacco leaves and increases upon induction of systemic acquired resistance with Elicitin. Plant Physiol. 115: 1557-1567.
- Green, P. J. (1994) The ribonucleases of higher plants. Annu. Rev. Plant Physiol. Plant Mol. Biol. 45: 421-445.
- Griffiths, S. J., Adams, D. J. and Talbot, S. J. (1997) Ribonuclease inhibits Kaposi's sarcoma. Nature 390: 568.
- Hamashima, M. (1994) M.Sc. thesis (in Japanese), Nagaoka University of Science and Technology.
- Hayano, K., Iwama, M., Sakamoto, H., Watanabe, H., Sanda, A., Ohgi, K. and Irie, M. (1993) Characterization of poly(C) preferential ribonuclease from chicken liver. J. Biochem. 114: 156-162.
- Heinonen, P. K. and Tuohimaa, P. (1979) Acid ribonuclease activation in the chick oviduct by tissue damage, actinomycin D and progesterone. J. Steroid Biochem. 10: 629-631.
- Hime, G., Prior, L. and Saint, R. (1995) The *Drosophila melanogaster* genome contains a member of the Rh/TZ/S-glycoprotein family of ribonuclease-encoding genes. Gene 158: 203-207.
- Hiramaru, M., Uchida, T. and Egami, F. (1969) Studies on ribonucleases from *Physarum polycephalum*. Purification and characterization of substrate specificity. J. Biochem. 65: 693-700.
- Horiuchi, H., Yanai, K., Takagi, M., Yano, K., Wakabayashi, E., Sanda, A., Mine, S., Ohgi, K. and Irie, M. (1988) Primary structure of a base non-specific ribonuclease from *Rhizopus niveus*. J. Biochem. 103: 408-418.
- Huang, S., Lee, H.-S., Karunanandaa, B. and Kao, T.-H. (1994) Ribonuclease activity of *Petunia inflata* S proteins is essential for rejection of self-pollen. Plant Cell 6: 1021-1028.
- Hulst, M. M. and Moxmann, R. J. M. (1997) Inhibition of pestivirus infection in cell culture by envelop proteins E-RNS and E2 of classic swine virus: E-RNS and E2 interact with different receptors. J. Gen. Virol. 78: 2779-2787.
- Ide, H., Kimura, M., Arai, M. and Funatsu, G. (1991) The complete amino acid sequence of ribonuclease from the seeds of bitter melon (*Momordica charantia*). FEBS Lett. 284: 161-164.
- Inada, Y., Watanabe, H., Ohgi, K. and Irie, M. (1991) Isolation, characterization, and primary structure of a base non-specific and adenylic acid preferential ribonuclease with higher specific activity from *Trichoderma viride*. J. Biochem. 110: 896-904.
- Inokuchi, N., Koyama, T., Sawada, F. and Irie, M. (1993) Purification, some properties, and primary structure of base non-specific ribonuclease from *Physarum polycephalum*. J. Biochem. 113: 425-432.
- Inokuchi, N., Kobayashi, H., Miyamoto, M., Koyama, T., Iwama, M., Ohgi, K. and Irie, M. (1997) Primary structure of base non-specific and acid ribonuclease from bullfrog (*Rana catesbeiana*). Biol. Pharm. Bull. 20: 471-478.
- Irie, M. (1967) Isolation and properties of a ribonuclease from *Aspergillus saitoi*. J. Biochem. 62: 509-518.
- Irie, M. (1969) pH-profile of the kinetic parameters of ribonuclease from *Aspergillus saitoi*. J. Biochem. 65: 133-140.
- Irie, M., Harada, M. and Sawada, F. (1972) Studies on the state of tryptophan residues in ribonuclease from *Aspergillus saitoi*. J. Biochem. 72: 1351-1359.
- Irie, M., Watanabe, H., Ohgi, K. and Harada, M. (1986) Site of alkylation of the major ribonuclease from *Aspergillus saitoi*. J. Biochem. 99: 627-633.
- Irie, M., Ohgi, K., Iwama, M., Koizumi, M., Sasayama, E., Harada, K., Yano, Y., Udagawa, J. and Kawasaki, M. (1997) Role of histidine 46 in the hydrolysis and the reverse transphosphorylation reaction of RNase Rh from *Rhizopus niveus*. J. Biochem. 121: 849-853.
- Ishimizu, T., Miyagi, M., Norioka, S., Liu, Y.-H., Clarke, A. E. and Sakiyama, F. (1995) Identification of histidine 31 and cysteine 95 in the active site of self-incompatibility associated S6-RNase in *Nicotiana glauca*. J. Biochem. 118: 1007-1013.
- Ittel, M. E., Niedergang, C., Munoz, D., Petek, F., Okazaki, H. and Mandel, P. (1975) Partial purification and characterization of an acid ribonuclease in beef brain nuclei. J. Neurochem. 25: 171-176.
- Jost, W., Bak, H., Glund, K., Terpstra, P. and Beintema, J. J. (1991) Amino acid sequence of an extra-cellular phosphate starvation induced ribonuclease from cultured tomato (*Lycopersicon esculentum*) cells. Eur. J. Biochem. 198: 1-6.
- Kawata, Y., Sakiyama, F. and Tamaoki, H. (1988) Amino acid sequence of ribonuclease T2 from *Aspergillus oryzae*. Eur. J. Biochem. 176: 683-697.
- Kawata, Y., Sakiyama, F., Hayashi, F. and Kyogoku, Y. (1991) Identification of two essential histidine residues of ribonuclease T2. Eur. J. Biochem. 187: 253-262.
- Kobayashi, H., Inokuchi, N., Koyama, T., Watanabe, H., Iwama, M., Ohgi, K. and Irie, M. (1992) Primary structure of a base non-specific and adenylic acid preferential ribonuclease from the fruit bodies of *Lentinus edodes*. Biosci. Biotechnol. Biochem. 56: 2003-2010.

- Köck, M., Löffler, A., Abel, S. and Glund, K. (1995) cDNA structure and regulatory properties of a family of Pi-starvation induced ribonucleases from tomato. *Plant Mol. Biol.* 27: 477-485.
- Komiyama, T. and Irie, M. (1972) pH-profile of the kinetic parameters and photooxidation of ribonuclease from *Rhizopus niveus*. *J. Biochem.* 71: 973-980.
- Kurihara, H., Mitsui, Y., Ohgi, K., Irie, M., Mizuno, H. and Nakamura, K. T. (1992) Crystal and molecular structure of RNase Rh, a new class of microbial ribonuclease from *Rhizopus niveus*. *FEBS Lett.* 306: 189-192.
- Kusano, A., Iwama, M., Sanda, A., Suwa, K., Nakaizumi, E., Nakatani, Y., Ohkawa, H., Ohgi, K. and Irie, M. (1997) Primary structure of porcine spleen ribonuclease. *Acta Biochim. Pol.* 44: 689-700.
- Kusano, A., Iwama, M., Ohgi, K. and Irie, M. (1998) Primary structure of a squid acid and base-nonspecific ribonuclease. *Biochem. Biotechnol. Biochem.* 62: 87-94.
- Lehrer, R. I., Szklarek, D., Barton, A., Ganz, T., Hamann, K. J. and Gleich, G. J. (1989) Antibacterial properties of eosinophil major basic protein and eosinophil cationic protein. *J. Immunol.* 142: 4428-4434.
- Lers, A., Khalchitski, A., Lomaniec, E., Burd, S. and Green, P. J. (1998) Senescence-induced RNases in tomato. *Plant Mol. Biol.* 36: 439-449.
- Levy, C. C. and Karpetsky, T. P. (1980) The purification and properties of chicken liver RNase. An enzyme which is useful in distinguishing between cytidylic and uridylic acid residues. *J. Biol. Chem.* 255: 2153-2159.
- Lim, L. W., Mathur, S., Cannistraro, V. J. and Kennel, D. (1993) Preliminary X-ray crystallographic studies of ribonuclease I from *Escherichia coli*. *J. Mol. Biol.* 234: 499-500.
- Löffler, A., Abel, S., Jost, W., Beintema, J. J. and Glund, K. (1992) Phosphate regulated induction of intracellular ribonucleases in cultured tomato (*Lycopersicon esculentum*) cells. *Plant Physiol.* 98: 1472-1478.
- Löffler, A., Glund, K. and Irie, M. (1993) Amino acid sequence of an intracellular, phosphate-starvation-induced ribonuclease from cultured tomato (*Lycopersicon esculentum*) cells. *Eur. J. Biochem.* 214: 627-633.
- Maouri, A. and Georgatsos, J. G. (1987) Specificity and other properties of three ribonucleases of *Tetrahymena pyriformis*. *Eur. J. Biochem.* 168: 523-528.
- Maver, M. E. and Greco, A. E. (1962) The chromatographic separation and characterization of the acid and alkaline ribonucleases of bovine spleen and liver. *J. Biol. Chem.* 237: 736-741.
- McClure, B. A., Haring, V., Ebert, P. R., Anderson, M. A., Simpson, R. J., Sakiyama, F. and Clarke, A. E. (1989) Style self-incompatibility gene products of *Nicotiana glauca* are ribonuclease. *Nature* 342: 955-957.
- McKee, T. and Prescott, D. (1991) Characterization of the extracellular ribonuclease of *Tetrahymena pyriformis* W. *J. Protozool.* 38: 465-471.
- Meador, J., III and Kennell, D. (1990) Cloning and sequencing the gene encoding *Escherichia coli* ribonuclease I: exact physical mapping using the genome library. *Gene* 95: 1-7.
- Miura, K., Inoue, Y., Inoue, A. and Ueda, T. (1984) Purification of chicken liver ribonuclease by affinity chromatography with UMP-Sepharose CL. *Chem. Pharm. Bull.* 32: 4054-4060.
- Morikawa, S. (1967) Studies on alkaline, and acid ribonucleases in mammalian tissues. Immunohistochemical localization and immunohistochemical properties. *J. Histochem. Cytochem.* 15: 662-673.
- Morita, T., Niwata, Y., Ohgi, K. and Irie, M. (1986) Distribution of two urinary ribonuclease-like enzymes in human organs and body fluids. *J. Biochem.* 99: 17-25.
- Müller, M., Baudhuin, M. and de Duve, C. (1966) Lysosomes in *Tetrahymena pyriformis* I. Some properties and lysosomal localization of acid hydrolases. *Cell Physiol.* 68: 1165-1176.
- Nakabayashi, T. and Ikezawa, H. (1979) An isoelectric focusing study of acid phosphohydrolase in liver lysosomes of higher vertebrates. *Comp. Biochem. Physiol. B* 63B: 221-231.
- Nakamura, Y., Takeda, M., Suzuki, H., Morita, H., Tada, K., Horiguchi, S. and Nishimura, T. (1989) Age-dependent change in activities of lysosomal enzymes in rat brain. *Mech. Ageing Dev.* 50: 215-225.
- Nakamura, T. K., Ishikawa, N., Hamashima, M., Kurihara, H., Nonaka, T., Mitsui, Y., Ohgi, K. and Irie, M. (1993) Protein nucleic acid recognition in ribonuclease Rh-2'-adenylic acid complex. In: *The 3rd International Meeting on Ribonuclease, Chemistry, Biology, Biotechnology, Capri*, p. 5.
- Narumi, H., Ogawa, Y., Iwama, M., Kusano, A., Sanda, A., Ohgi, K. and Irie, M. (1997) Bovine spleen acid ribonuclease is a member of the RNase T2 family. *J. Biochem. Mol. Biol. Biophys.* 1: 21-26.
- Neu, H. C. and Heppel, L. A. (1964) The release of ribonuclease into the medium when *Escherichia coli* cells are converted to spheroplast. *Biochem. Biophys. Res. Commun.* 14: 109-112.
- Nürnberg, T., Abel, S., Jost, W. and Glund, K. (1990) Induction of an extracellular ribonuclease in cultured tomato cells upon phosphate starvation. *Plant Physiol.* 92: 970-976.
- Ohgi, K. and Irie, M. (1977) Circular dichroism studies on the N-bromosuccinimide oxidation of ribonuclease from *Aspergillus saitoi*. *J. Biochem.* 81: 1031-1039.
- Ohgi, K., Sanda, A., Takizawa, Y. and Irie, M. (1988) Purification of acid ribonuclease from bovine spleen. *J. Biochem.* 103: 267-273.
- Ohgi, K., Horiuchi, H., Watanabe, H., Takagi, M., Yano, K. and Irie, M. (1991) Expression of RNase Rh from *Rhizopus niveus* in yeast and characterization of the excreted protein. *J. Biochem.* 109: 776-785.
- Ohgi, K., Horiuchi, H., Watanabe, H., Iwama, M., Takagi, M. and Irie, M. (1992) Evidence that three histidine residues of a base non-specific and adenylic acid preferential ribonuclease from *Rhizopus niveus* are involved in the catalytic function. *J. Biochem.* 112: 132-138.
- Ohgi, K., Horiuchi, H., Watanabe, H., Iwama, M., Takagi, M. and Irie, M. (1993) Role of Asp51 and Glu105 in the enzymatic activity of a ribonuclease from *Rhizopus niveus*. *J. Biochem.* 113: 219-224.
- Ohgi, K., Iwama, M., Tada, K., Takizawa, R. and Irie, M. (1995) Role of Lys108 in the enzymatic activity of RNase Rh from *Rhizopus niveus*. *J. Biochem.* 117: 27-33.
- Ohgi, K., Iwama, M., Ogawa, Y., Hagiwara, C., Ono, E., Kawaguchi, R., Kanazawa, C. and Irie, M. (1996) Enzymatic activities of several K108 mutants of ribonuclease (RNase) Rh isolated from *Rhizopus niveus*. *Biol. Pharm. Bull.* 19: 1080-1082.
- Oxley, D. and Bacic, A. (1996) Disulfide bonding in a stylar self-incompatibility ribonuclease of *Nicotiana glauca*. *Eur. J. Biochem.* 242: 75-80.
- Pantazaki, A. and Georgatsos, J. G. (1990) A guanyloribonuclease of mouse liver cytosol. *Eur. J. Biochem.* 192: 115-117.
- Pantopoulos, K. and Georgatsos, J. G. (1992) Ribonucleases of diverse specificities in rabbit brain nuclei. *Eur. J. Biochem.* 207: 1045-1051.

- Parry, S. K., Liu, Y.-H., Clarke, A. E. and Newbiggin, E. (1997a) S-RNases and other plant extracellular ribonucleases. In: *Ribonuclease, Structures and Functions*, pp. 191–211, D'Alessio, G. and Riordan, J. F. (eds.) Academic Press, New York.
- Parry, S. K., Newbiggin, E., Currie, G., Bacic, A. and Oxley, D. (1997b) Identification of active-site histidine residues of a self-incompatibility ribonuclease from a wild tomato. *Plant Physiol.* 115: 1421–1429.
- Parry, S. K., Newbiggin, E., Craik, D., Nakamura, K. T., Bacic, A. and Oxley, D. (1998) Structural analysis and molecular model of a self-incompatibility ribonuclease from *Lycopersicon peruvianum*. *Plant Physiol.* 116: 463–469.
- Rahman, Y. E. and Cerny, E. A. (1969) Studies on rat liver ribonucleases. III. Further studies on heterogeneity of lysosomes. Intracellular localization of acid ribonuclease and acid phosphatase in rat liver of various ages. *Biochim. Biophys. Acta* 178: 61–67.
- Rahman, Y. E., Howe, J., Nance, S. L. and Thomson, J. F. (1967) Studies on rat liver ribonucleases. II. Zonal centrifugation of acid ribonuclease, implications for the heterogeneity of lysosome. *Biochim. Biophys. Acta* 146: 484–492.
- Riordan, J. F. (1997) Structure and function of angiogenin. In: *Ribonucleases, Structures and Functions*, pp. 446–489, D'Alessio, G. and Riordan, J. F. (eds.) Academic Press, New York.
- Rojo, M. A., Arias, F. J., Iglesias, R., Ferreras, J. M., Muñoz, R., Escarmís, C., Soriano, F., López-Fando, J., Méndez, E. and Gírbés, T. (1994a) Cusativin; a new cytidine specific ribonuclease accumulated in seeds of *Cucumis sativus* L. *Planta* 194: 328–338.
- Rojo, M. A., Arias, F. J., Iglesias, R., Ferreras, J. M., Soriano, F., Méndez, E., Escarmís, C. and Gírbés, T. (1994b) Enzymatic activity of melonin, a translational inhibitor present in dry seed of *Cucumis melo* L. *Plant Sci.* 103: 127–134.
- Sanda, A., Takizawa, Y., Iwama, M. and Irie, M. (1985) Modification of a ribonuclease from *Rhizopus* sp. with 1-cyclohexyl 3-(2-morpholinyl-(4)-ethyl) carbodiimide *p*-toluenesulfonate. *J. Biochem.* 98: 125–132.
- Sano, T., Nagayama, A., Ogawa, T., Ishida, I. and Okada, Y. (1997) Transgenic potato expressing a double-stranded RNA-specific ribonuclease is resistant to potato spindle tuber viroid. *Nature Biotech.* 15: 1291–1294.
- Sato, K. and Egami, F. (1957) Studies on ribonuclease in *Takadiastase* I. *J. Biochem.* 44: 753–767.
- Schneider, R., Unger, G., Stark, R., Schneider-Scherzer, E. and Thiele, H.-J. (1993) Identification of a structural glycoprotein of an RNA virus as a ribonuclease. *Science* 261: 1169–1171.
- Shen, V. and Schlessinger, D. (1982) RNases I, II, and IV of *Escherichia coli*. In: *The Enzymes*, pp. 501–515, Boyer, P. D. (ed.) Academic Press, New York.
- Sierakowska, H. and Shugar, D. (1977) Mammalian nucleolytic enzymes. *Prog. Nucl. Acid Res. Mol. Biol.* 20: 59–130.
- Snyder, M. R. and Gleich, G. J. (1997) Eosinophil-associated ribonucleases. In: *Ribonuclease, Structures and Functions*, pp. 425–444, D'Alessio, G. and Riordan, J. F. (eds.) Academic Press, New York.
- Taylor, C. B., Bariola, P. A., delCardayré, S. A., Raines, R. T. and Green, P. J. (1993) RNS2 A senescence-associated RNase of *Arabidopsis* that diverged from the S-RNases before speciation. *Proc. Natl. Acad. Sci. USA* 90: 5118–5122.
- Trubia, M., Sessa, L. and Taramelli, R. (1997) Mammalian Rh/T2/S-glycoprotein ribonuclease family genes: cloning of a human member located in a region of chromosome 6 (6q27) frequently deleted in human malignancies. *Genomics* 42: 342–344.
- Tsai, D.-S., Lee, H. S., Post, L. C., Kreiling, K. M. and Kao, T.-H. (1992) Sequence of an S-protein of *Lycopersicon peruvianum* and comparison with other solanaceous S-proteins. *Sex Plant Reprod.* 5: 256–263.
- Uchida, T. and Egami, F. (1971) Microbial ribonuclease with special references to RNase T1, T2, N1 and U2. In: *The Enzymes*, 3rd edn., Vol. 4, pp. 208–250, Boyer, P. D. (ed.) Academic Press, New York.
- Uchida, T., Hayano, K., Iwama, M., Watanabe, H., Sanda, A., Ohgi, K. and Irie, M. (1996) Base specificity and primary structure of poly(U)-preferential ribonuclease from chicken liver. *Biosci. Biotechnol. Biochem.* 60: 1982–1988.
- Uchiyama, S., Isobe, K. and Nagai, S. (1992) Determination of the molecular weight of ribonuclease isozymes in a cell-free crude extract of *Dictyostelium discoideum* by activity staining of gels after SDS-PAGE. *Comp. Biochem. Physiol.* 102B: 343–347.
- Watanabe, H., Naitoh, A., Suyama, Y., Inokuchi, N., Shimada, H., Koyama, T., Ohgi, K. and Irie, M. (1990) Primary structure of a base non-specific and adenylic acid preferential ribonuclease from *Aspergillus saitoi*. *J. Biochem.* 108: 303–310.
- Watanabe, H., Narumi, H., Inaba, T., Ohgi, K. and Irie, M. (1993) Purification, some properties, and primary structure of a base non-specific ribonuclease from oyster (*Crassostrea gigas*). *J. Biochem.* 114: 800–807.
- Watanabe, H., Fauzi, H., Iwama, M., Onda, T., Ohgi, K. and Irie, M. (1995) Base non-specific acid ribonuclease from *Irpex lacteus*, Primary structure and phylogenetic relationship in RNase T2 family enzyme. *Biosci. Biotechnol. Biochem.* 59: 2097–2103.
- Webster, G. C. and Webster, S. L. (1978) Lysosomal enzyme activity during aging in *Drosophila melanogaster*. *Exp. Gerontol.* 13: 343–347.
- Wiener, E. and Ashworth, J. M. (1970) The isolation and characterization of lysosomal particles from *Myxamebae* of the cellular slime mold *Dictyostelium discoideum*. *Biochem. J.* 118: 505–512.
- Wilson, C. M. (1982) Plant ribonucleases: biochemistry and development of multiple molecular forms. *Isoenzymes. Curr. Top. Biol. Med. Res.* 6: 33–54.
- Ye, Z.-H. and Droste, D. L. (1996) Isolation and characterization of cDNAs encoding xylogenesis associated and wounding induced ribonuclease in *Zinnia elegans*. *Plant Mol. Biol.* 30: 697–709.
- Youle, R. J. and D'Alessio, G. (1997) Anti-tumor RNases. In: *Ribonuclease, Structures and Functions*, pp. 491–514, D'Alessio, G. and Riordan, J. F. (eds.) Academic Press, New York.
- Zhu, L., Gangopadhyay, T., Padmanabha, K. P. and Deutscher, M. P. (1990) *Escherichia coli* rna gene encoding RNase I: cloning, overexpression, subcellular distribution of the enzyme and use of rna deletion to identify additional RNases. *J. Bacteriol.* 172: 3146–3151.

A small-molecule inhibitor of the ribonucleolytic activity of human angiogenin that possesses antitumor activity

Richard Y. T. Kao^{*†}, Jeremy L. Jenkins^{*}, Karen A. Olson^{**}, Marc E. Key[‡], James W. Fett^{**}, and Robert Shapiro^{**†}

^{*}Center for Biochemical and Biophysical Sciences and Medicine and [†]Department of Pathology, Harvard Medical School, Cambridge, MA 02139; and [‡]Dako Corporation, Carpinteria, CA 93013

Communicated by Bert L. Vallee, Harvard Medical School, Boston, MA, June 7, 2002 (received for review April 29, 2002)

The results of previous preclinical and clinical studies have identified angiogenin (ANG) as a potentially important target for anticancer therapy. Here we report the design and implementation of a high-throughput screening assay to identify small molecules that bind to the ribonucleolytic active site of ANG, which is critically involved in the induction of angiogenesis by this protein. Screening of 18,310 compounds from the National Cancer Institute (NCI) Diversity Set and ChemBridge DIVERSet yielded 15 hits that inhibit the enzymatic activity of ANG with K_i values <100 μ M. One of these, NCI compound 65828 [8-amino-5-(4'-hydroxybiphenyl-4-ylazo)naphthalene-2-sulfonate; $K_i = 81$ μ M], was selected for more detailed studies. Minor changes in ANG or ligand structure markedly reduced potency, demonstrating that inhibition reflects active-site rather than nonspecific binding; these observations are consistent with a computationally generated model of the ANG-65828 complex. Local treatment with modest doses of 65828 significantly delayed the formation of s.c. tumors from two distinct human cancer cell types in athymic mice. ANG is the likely target involved because (i) a 65828 analogue with much lower potency against the enzymatic activity of ANG failed to exert any antitumor effect, (ii) tumors from 65828-treated mice had fewer interior blood vessels than those from control mice, and (iii) 65828 appears to have no direct effect on the tumor cells. Our findings provide considerable support for the targeting of the enzymatic active site of ANG as a strategy for developing new anticancer drugs.

Angiogenin (ANG), a 14.1-kDa monomeric protein, was originally isolated as a human tumor-derived angiogenesis factor (1), and has since been identified as a potentially important target for anticancer therapy. Monoclonal antibodies and an antisense oligonucleotide directed against ANG are highly effective at inhibiting the establishment of s.c. human colon, prostate, breast, lung, and fibroblast tumors in athymic mice (2–4). These antagonists also protect mice from regional iliac lymph node metastases after implantation of human prostate cancer cells directly in the prostate gland (3, 5). Strikingly, the metastasis experiments with antisense reveal a strict correlation between the extent of reduction in ANG expression in the primary tumors and the degree of protection achieved (3). Another ANG antagonist, an 11-amino acid peptide, dramatically reduces liver metastases in mice injected with human colorectal carcinoma cells (6).

An association between ANG and cancer has been observed in more than 20 clinical studies to date. ANG mRNA and/or protein was elevated in colorectal (7, 8), gastric (7), pancreatic (9), breast (10, 11), prostate (5), melanoma (12), and urothelial (13) cancer lesions compared with the corresponding nonneoplastic tissues. In some cases, high tissue ANG was shown to correlate with cancer progression or poor prognosis (8, 9, 14). ANG levels in serum were significantly increased in patients with colorectal (15), gastric (16), pancreatic (9), ovarian (17), renal cell (18), and urothelial (13) cancer and with melanoma (19). Moreover, ANG was shown to be up-regulated by hypoxia in cultured melanoma cells but not in normal melanocytes, and the

degree of induction correlated with the metastatic potential of the cell line used (12).

As ANG antagonists for clinical use, low molecular weight compounds would offer tremendous advantages over the agents (proteins, oligonucleotides, and peptides) tested thus far in mice. One attractive strategy for developing such inhibitors is to exploit a unique feature of ANG: it possesses a ribonucleolytic activity that is essential for angiogenicity (20–22). In general, targeting of enzymatic active sites has proved to be particularly successful for drug development, especially when, as in the case of ANG, the three-dimensional structure is known (23) and “rational” approaches can be incorporated. ANG is a member of the pancreatic RNase superfamily, with 33% sequence identity to bovine pancreatic RNase A (24). Although it contains analogues of the catalytic triad and the major substrate-binding residues of RNase A, it exhibits only weak ribonucleolytic activity toward standard RNase substrates (25). Its natural substrate has not been determined, but may reside in the nucleolus of vascular endothelial cells, where ANG accumulates after binding to the cell surface (26).

Previous efforts to identify small active-site-directed inhibitors of ANG have focused on nucleotides (27, 28). Although some of the compounds tested had mid-to-upper nanomolar K_i values with RNase A, K_i values with ANG were no better than ~ 500 μ M under physiological conditions. This unfavorable starting point, together with obstacles to the crystallographic study of ANG-nucleotide complexes that have been encountered (29), make the development of nucleotide-based ANG inhibitors a daunting prospect. As an alternative, we have now devised a high-throughput screening (HTS) assay for ANG and used it to conduct a wider search for low molecular weight inhibitors. This approach has yielded two potential leads that bind an order of magnitude more tightly than any of the nucleotides; one of these is here demonstrated to have antitumor activity in mice at modest doses. Thus small molecules directed at the active site of ANG may constitute a previously unrecognized class of anticancer agents.

Materials and Methods

Materials. Human ANG and its R5A (Arg-5 \rightarrow Ala) variant were prepared as described (30). Oligonucleotides were from Integrated DNA Technologies (Coralville, IA). Chemical libraries were from the National Cancer Institute (NCI; Bethesda, MD) and ChemBridge Corporation (San Diego), as were all compounds denoted with prefixes N and C, respectively. Tyger Scientific (Princeton, NJ) resynthesized compound N-65828 and provided the analytical information cited below except for the

Abbreviations: ANG, angiogenin; HTS, high-throughput screening; NCI, National Cancer Institute; 6-FAM, 6-carboxyfluorescein.

[†]Present address: Department of Microbiology, University of Hong Kong, Hong Kong.

[‡]To whom reprint requests should be addressed at: One Kendall Square, Building 600, Third Floor, Cambridge, MA 02139. E-mail: Robert.Shapiro@hms.harvard.edu.

MS data, which were collected by the authors with a Micromass Platform LCZ instrument and electrospray ionization. $[M - H]^-$ was 418.0 Da vs. 418.1 Da (calc). Sodium 6-amino-5-(2-benzenesulfonylphenylazo)-4-hydroxynaphthalene-2-sulfonate (catalog no. S321443) and DMSO (Hybri-Max grade) were purchased from Sigma-Aldrich. 5'-Phosphothymidine 3'-pyrophosphate ($P' \rightarrow 5'$) adenosine 3'-phosphate was from earlier studies (27). Rabbit reticulocyte lysate *in vitro* translation system, luciferase assay system, and luciferase mRNA were from Promega; the translation and assay systems were used according to the manufacturer's recommendations. Precautions for minimizing RNase contamination were described previously (31).

Kinetic Analyses. Fluorimetric assays. A modification of an earlier method (32) was used with the fluorogenic substrate 6-FAM-(mA)₂rC(mA)₂-Dabcyl, where 6-FAM is the fluorophore 6-carboxyfluorescein, mA is 2'-O-methylriboadenosine, rC is ribocytidine, and Dabcyl is the quencher 4-(4-dimethylaminophenylazo)benzoic acid. The fluorescence increase accompanying substrate cleavage at 37°C was monitored with a Jobin-Yvon-Spex (Longjumeau, France) FluoroMax-2 fluorimeter (λ_{ex} = 495 nm; λ_{em} = 525 nm). Assay mixtures contained 20 nM substrate, 400 nM ANG, and 10 μ g/ml BSA in buffer A (20 mM Hepes-NaOH/100 mM NaCl, pH 7.0). Values of k_{cat}/K_m were determined from initial velocities as described (33).

HPLC assays. Reaction mixtures (30 μ l) containing ANG (5 μ M) and substrate [20 μ M (dA)₅rC(dA)₂, a concentration expected to be $\ll K_m$ (33, 34)] in buffer A were incubated for 2 hr at 37°C and then injected onto a Mono Q HR5/5 (Amersham Pharmacia) column. Products and substrate were separated with a 9-min linear gradient from 0.19 M to 0.28 M NaCl in 10 mM Tris-HCl, pH 8.0, at ambient temperature at a flow rate of 1.5 ml/min. Peak areas at 254 nm for substrate and the product (dA)₅rC cyclic 2',3'-phosphate were used to calculate k_{cat}/K_m values (35). Test compounds were assayed initially at a concentration of 25 μ M; those that inhibited by >10% were investigated further. K_i values were calculated from the dependence of k_{cat}/K_m on free inhibitor concentration, [I] (31); typically, at least four concentrations of inhibitor (10–100 μ M) were used. R5A-ANG was assayed in 0.2 M Mes, pH 5.9, because activity in buffer A is too low for accuracy; R5A data are compared with those for ANG under the same conditions.

HTS. HTS was performed in black polypropylene 384-well plates (Nalge Nunc). Twenty microliters of 800 nM ANG in 40 μ g/ml BSA were delivered into each well with a Multidrop liquid dispenser (Labsystems, Chicago). Test compounds (100 nl) were then added with a solid pin array device (V & P Scientific, San Diego); stock solutions were 10 mM (NCl) or 5 mg/ml (Chem-Bridge) in DMSO. The reaction was initiated by addition of substrate (20 μ l of 50 nM 6-FAM-(mA)₂rC(mA)₂-Dabcyl) in 2 \times buffer A with the Multidrop dispenser. The plates were film-sealed and incubated for 1.5–2 hr at 37°C in the dark, and fluorescence was then measured with a Wallac 1420 Victor² multilabel counter (excitation: 485 nm; emission: 535 nm) (Perkin-Elmer Life Sciences). The median value for each plate (\sim 1,500 counts per second) was normalized to fluorescence intensity of 1.0; this value was similar to that measured when no library compound was added.

Luciferase mRNA Cleavage Assay. Pretranslation assay mixtures contained 50 ng of luciferase mRNA, 50 μ M test compound, 60 nM ANG, and buffer A in a total volume of 5 μ l. After 15 min of incubation at 30°C, 45 μ l of translation mixture was added. After another 90 min at 30°C, the amount of luciferase produced was determined by transferring 5 μ l of sample to wells containing 95 μ l of luciferase substrate on a 384-well plate. Luminescence was measured with the Wallac counter described above.

Modeling of ANG-Inhibitor Complex Structures. Ligand docking to the ANG (PDB ID code 1B1I) active site was carried out in AUTODOCK 3.0 (36) as described for RNase A (31). Docking was constrained to a 22.5-Å cubic grid whose origin corresponds to the position of the phosphorus atom in the superimposed coordinates of free ANG and the ANG-phosphate complex (PDB ID code 1H52) (29).

Antitumor Activity in Mice. Effects of test compounds on the establishment of tumors from PC-3 and HT-29 cells were determined as described previously (2, 3). Cells (1×10^4 and 1.25×10^5 for PC-3 and HT-29, respectively) were injected s.c. in the shoulder of 6- to 7-week old athymic mice on day 0; in the protocols used, these numbers of cells have been shown to be sufficient to produce tumors in all mice given PC-3 cells (3, 5) and >97% of mice injected with HT-29 cells (2). Treatment or control solutions (100 μ l) were administered locally s.c. six times per week until day 35; the first dose was given 5–10 min before injection of the cells. Test compounds were 400, 80, and 16 μ g/ml in PBS containing 4%, 0.8%, and 0.16% DMSO (from 10 mg/ml stock solutions in DMSO), respectively. Control groups were injected with PBS containing the same concentration of DMSO. *P* values for statistical significance were from Mantel-Cox tests performed on Kaplan-Meier survivor functions; results for treatment groups were compared with those for appropriate DMSO control groups. There were no detectable differences in the survivor functions for control groups given PBS alone and those injected with PBS containing up to 4% DMSO.

Histology. Tissue sections from tumors (weight range: 18–89 mg; average: 47 mg) were examined for blood vessel content by factor VIII staining (2).

Results

HTS Development. Until recently, no assays for the ribonucleolytic activity of ANG were available that could be adapted for use in HTS. Because activity toward common small RNase substrates such as dinucleotides is extremely low (25), kinetic measurements typically required \sim 10 μ M ANG, and it was necessary to monitor the reaction by HPLC. Assays with polynucleotide substrates (37) used somewhat lower enzyme concentrations, but would be problematic to implement on microtiter plates. In 1999, Kelemen *et al.* (32) reported an assay for RNase A and ANG that appeared to have sufficient sensitivity and other characteristics compatible with HTS. The substrates are small oligonucleotides containing a single ANG-cleavable bond, a fluorophore at the 5' end, and a quencher at the 3' end. Cleavage relieves the internal quenching and produces a substantial increase in fluorescence.

For HTS, we opted to use the substrate 6-FAM-(mA)₂rC(mA)₂-Dabcyl and to conduct assays at pH 7 rather than the less physiological, but more kinetically optimal, pH value of \sim 6 used in previous studies (28, 32). Initial rate assays in cuvettes yielded a k_{cat}/K_m value of $34 \pm 1 \text{ M}^{-1} \text{ s}^{-1}$. On this basis, an ANG concentration of 400 nM, sufficient to cleave \sim 5% of the substrate in 1 hr, was selected for HTS. Testing in microtiter plates showed that the fluorescence increase during this reaction could be quantitated with good precision by using 20 nM substrate; the fluorescence reading after 2 hr of incubation was 5-fold higher than the background from buffer and uncleaved substrate.

An important consideration that must be taken into account for the HTS assay is the extent to which the ANG preparation used is free of adventitious RNases. As with all other substrates reported, RNase A cleaves 6-FAM-(mA)₂rC(mA)₂-Dabcyl several orders of magnitude more rapidly than does ANG [$k_{cat}/K_m = (3.1 \pm 0.1) \times 10^7 \text{ M}^{-1} \text{ s}^{-1}$]. Therefore, the presence of less than 0.0001% of this common laboratory contaminant in an ANG



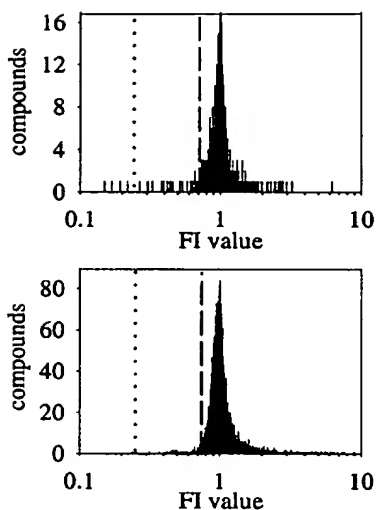


Fig. 1. Frequency of fluorescence readings from HTS of NCI (Upper) and ChemBridge (Lower) libraries. Readings are normalized to the median value for each plate (fluorescence intensity FI = 1). The dotted line indicates the background value, and the dashed line shows the cutoff for classification as a hit.

preparation would invalidate any results obtained. We established that our ANG did not contain any significant amount of RNase A by demonstrating that activity was decreased by <10% upon addition of the inhibitor 5'-phosphothymidine 3'-pyrophosphate ($P' \rightarrow 5'$) adenosine 3'-phosphate at a concentration of 1 μM , well above the K_i for RNase A but >100-fold below that for ANG (27).

HTS and Follow-Up Assays to Eliminate False Positives. The NCI Diversity Set (1,990 compounds) and ChemBridge DIVERset E (16,320 compounds) were screened at concentrations of 25 μM or 12.5 $\mu\text{g}/\text{ml}$ (20–70 μM), respectively. The results are shown in Fig. 1. Twenty-nine NCI compounds and 173 ChemBridge compounds reduced the fluorescence readings by at least 33% compared with the median value for each plate (minus background) and were classified as hits.

Some of the hits were expected to be false positives because of delivery errors, light scattering, or optical absorbance of test compounds. The final evaluation of inhibitors was to be performed with a rigorous HPLC assay that is not subject to these artifacts. However, this assay is time-consuming and the number of hits obtained from HTS is fairly large. Therefore, we first used a rapid secondary screening method, independent of that used for HTS, as a filter. In this method, luciferase mRNA is incubated with ANG in the presence and absence of putative inhibitor and then added to an *in vitro* translation system; the dilution used (10-fold) is sufficient to prevent any significant further RNA degradation by ANG and minimizes any influence of the test compounds on translation. After translation, the sample is diluted another 20-fold into a luciferase substrate mixture for quantification of protein product by luminescence. ANG concentrations of 30 and 60 nM in the absence of inhibitor commonly result in luminescence reductions of 38% and 70%, respectively, compared with the level measured when ANG is omitted. Sixty nanomolar ANG was used for inhibitor testing, and compounds were designated as hits if they appeared to rescue more than 50% of mRNA (i.e., if the readings were higher than that measured for 30 nM ANG without inhibitor) when

used at 50 μM . Twelve compounds from each library satisfied this criterion and were investigated further by HPLC.

Previous HPLC assay methods with dinucleotide substrates (34) were deemed unsuitable for studying the secondary screening hits because (i) ANG activity in the pH 7 buffer is too low and (ii) test compounds might not separate adequately from substrate or products. These problems were averted by using the substrate (dA)₅rC(dA)₂ and a modified anion-exchange HPLC procedure. The k_{cat}/K_m value for this octanucleotide is $27.0 \pm 1.1 \text{ M}^{-1} \text{ s}^{-1}$, severalfold higher than for any dinucleotide. The substrate and its hexanucleotide cleavage product have considerably greater net charge than any of the test compounds and were well resolved in all cases.

Of the 24 compounds assayed by HPLC, 15 had apparent K_i values <100 μM (Fig. 2), and 5 produced no detectable inhibition. The 4 that inhibited most effectively ($K_i < 11 \mu\text{M}$) all contained copper complexes. These were dismissed from further consideration because development of such hits would be difficult and because ANG is known to be inhibited effectively by free cupric ions (37), which might be present in these samples. N-13778 ($K_i = 42 \mu\text{M}$) was rejected because it contains antimony. C-181431, C-180582, C-180553, and C-216112 are structurally related. C-181431 has the lowest K_i value of any inhibitor lacking metal ions ($41 \pm 7 \mu\text{M}$), and its structure seems particularly amenable to both rational design and combinatorial approaches for improving affinity, suggesting that this compound may have promise as a potential lead. Similar considerations apply to N-65828 ($K_i = 81 \pm 7 \mu\text{M}$), which has greater aqueous solubility than C-181431 and was more readily available. Therefore, this latter inhibitor was selected for further studies, including testing for antitumor activity *in vivo*.

Interaction of N-65828 with ANG. Before proceeding with animal studies, we considered it critical to establish that inhibition by N-65828 reflects active-site rather than nonspecific binding. The plot of k_{cat}/K_m vs. [I] for N-65828 conformed well to the theoretical shape for simple inhibition ($r^2 = 0.99$), as was the case for all of the inhibitors examined; this observation already suggests that binding is specific. More conclusive evidence was obtained by measuring the effects of minor changes in enzyme and/or ligand structure on K_i . Many active-site variants of ANG and analogues of N-65828 were available for this purpose. The choice of which to use was guided by a model for the complex of ANG with N-65828 generated by AUTODOCK 3.0. In this model (Fig. 3), the azo group sits in the catalytic center with His-13 and His-114 on either side, the substituted naphthalene component forms four hydrogen bonds (two between the sulfonate and the side chain of Arg-5, and two involving the amino group and the main-chain O of Arg-5 and the imidazole of His-8), and the OH of the biphenyl component hydrogen bonds with Asp-41 and Arg-121. In view of the apparent prominence of the interactions involving Arg-5 and the sulfonate group, we examined the effect of replacing Arg-5 with Ala. R5A was not inhibited detectably by 250 μM N-65828, indicating that the K_i value is >1 mM (compared with 58 μM for ANG under the same conditions).

Findings with analogues of N-65828 are also consistent with specific binding at the active site (Fig. 4). The compounds tested retain the 5-phenylazonaphthalene core of N-65828, but differ in the substitutions on the rings. In N-45571, the phenol is replaced by an *N*-acetamide that, according to the model, would not interact with ANG; K_i is increased by ≈ 4 -fold. N-45557, which lacks the 2-sulfonate on the naphthalene ring, and contains a sulfo rather than an amino group at position 8 and a hydroxyl instead of the phenol group, has a K_i value >10-fold higher than for N-65828. S321443 also binds at least 10-fold less tightly than N-65828. This compound retains the 2-sulfo group on the naphthalene ring and has 6-amino and 4-hydroxyl groups, both of which might form hydrogen bonds with ANG according to the

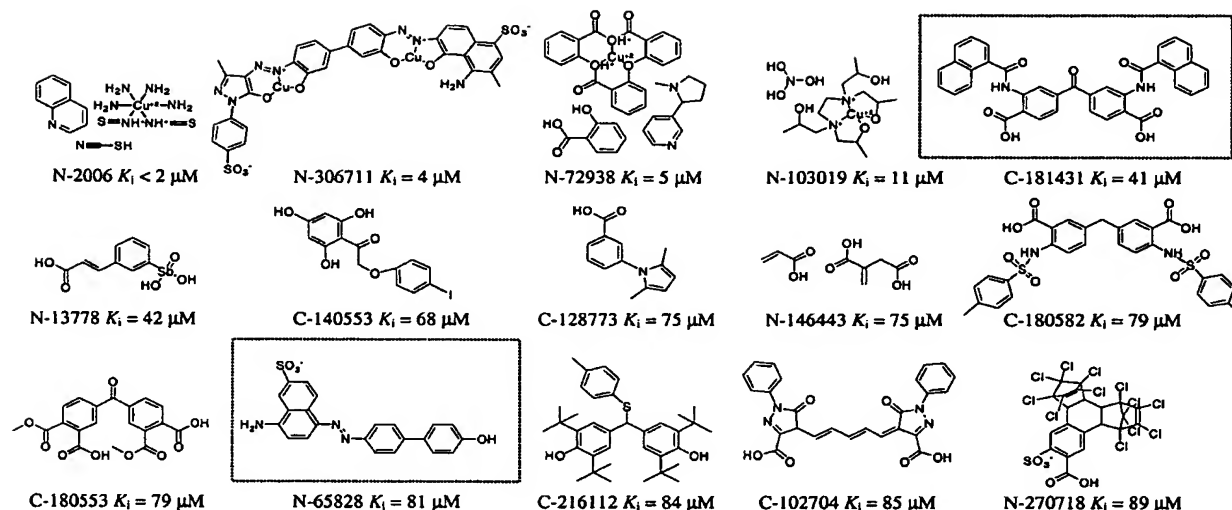


Fig. 2. Chemical structures and K_i values of ANG inhibitors identified by HTS of the NCI and ChemBridge libraries. The two compounds considered to be potential leads are boxed.

AUTODOCK model. However, the benzenesulfonyl group would be expected to clash with His-13, Lys-40, and Gln-117.

Antitumor Activity of N-65828. The efficacy of N-65828 *in vivo* was examined by using s.c. human tumor xenograft models in athymic mice (2, 3) and local administration of the inhibitor. In the initial test, PC-3 prostate cancer cells were used with three doses of inhibitor (40, 8, and 1.6 $\mu\text{g}/\text{day}$, corresponding to ≈ 1.4 , 0.3, and 0.06 mg/kg per day on average) and four mice per group. Mice receiving the higher two doses developed tumors more slowly than those in the corresponding vehicle control groups. This experiment was then repeated with a larger number of mice (Fig. 5 A and B). Again there was an appreciable delay in the appearance of tumors in the groups receiving 40 μg and 8 $\mu\text{g}/\text{day}$ of N-65828 (P values for the two combined experiments are <0.0001 and 0.0003 , respectively). Two mice were still tumor-free 25 days after all of the mice in the vehicle control groups had tumors and 14 days after treatment had ceased on day 35. We also included groups of mice treated with 40 μg and 8 $\mu\text{g}/\text{day}$ of N-45557, one of the N-65828 analogues shown to be ineffective as an inhibitor of ANG's ribonucleolytic activity. The rates of

tumor appearance in these mice were very similar to those in the vehicle control groups (Fig. 5 A and B).

It is well known that some compounds in the NCI libraries are impure or have even been misidentified (38). To ensure that the observed antitumor activity of N-65828 was actually due to the compound listed, additional tests were performed with newly synthesized material whose structure and purity ($>95\%$) were established by NMR, MS, elemental analysis, TLC, and C_{18} HPLC. The K_i for inhibition of the enzymatic activity of ANG was identical to that for the NCI preparation. Direct comparison in mice ($n = 8$ and $n = 12$, respectively, with $n = 8$ for vehicle controls) showed that the resynthesized material is at least as effective as that from NCI (P values for doses of 8–40 $\mu\text{g}/\text{day}$ vs. vehicle controls are 0.0037 – 0.0008). The resynthesized inhibitor was also tested for efficacy *in vivo* against a second human

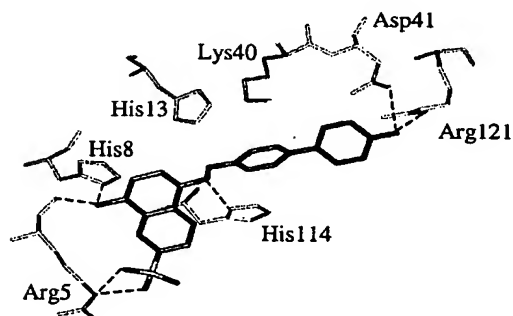


Fig. 3. Structure of the complex of ANG (light) with N-65828 (dark) as predicted by AutoDock. Hydrogen bonds are denoted with broken lines. The figure was drawn with INSIGHT II (Accelrys; Burlington, MA).

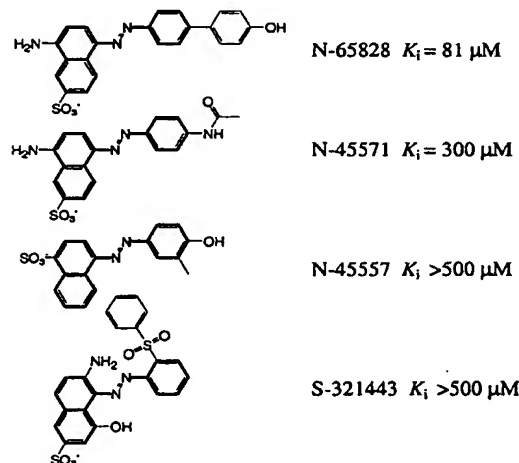


Fig. 4. Chemical structures and K_i values of N-65828 and three analogues predicted to bind less tightly on the basis of the modeled complex.

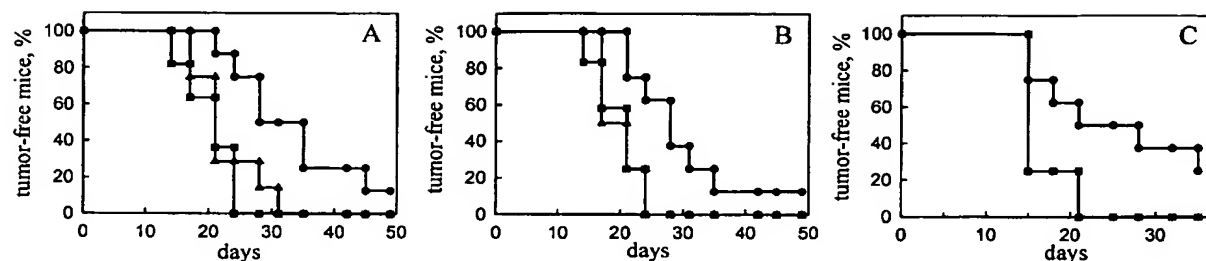


Fig. 5. Prevention of PC-3 (A and B) and HT-29 (C) tumor formation by N-65828. Cells were injected s.c. on day 0, and treatment or control solutions (●, N-65828; ■, vehicle; ▲, N-45557) were administered locally s.c. six times per week starting on the same day. Mice were examined twice per week for palpable tumors. Treatment doses: 40 µg/day (A and C); 8 µg/day (B). $n = 8$ for all groups except the vehicle controls in A and B, where $n = 12$.

tumor cell line, HT-29 (colon adenocarcinoma) (Fig. 5C). The compound again caused a significant delay in the appearance of tumors ($P = 0.02$), and 2 of the 8 mice in the treatment group were still tumor-free at sacrifice (14 days after all animals in the control group had tumors).

The mice in all of the treatment groups gained weight normally and had no apparent liver or kidney abnormalities at necropsy, suggesting that N-65828 is not toxic.

Effects of N-65828 on Tumor Vasculature. The extent and pattern of vascularization in PC-3 tumors from mice treated with N-65828 (40 or 8 µg/day; $n = 7$) were compared with those in weight-matched tumors from mice treated with the corresponding vehicle control solutions ($n = 9$). The average number of interior blood vessels was 53% lower in the treatment groups than in the controls, although the numbers of peripheral vessels were similar. These differences are not statistically significant, but follow the same trend observed previously for prostate tumors in mice treated with anti-ANG antibody or antisense vs. vehicle-treated mice (3, 5). As noted in the earlier reports, the development of interior vessels is thought to reflect true angiogenesis, whereas peripheral vessels might originate by co-option of preexisting vasculature (39).

Discussion

In recent years, inhibition of tumor angiogenesis has become one of the most active avenues for development of new anticancer drugs, and more than 30 anti-angiogenesis agents have entered clinical trials (40). Some of these antagonists have been directed at individual molecules, including several of the many known inducers of angiogenesis and their receptors and proteins that participate in downstream processes such as tissue remodeling. Others have targeted endothelial cells more generally, often without any defined mechanism of inhibition. As of this writing, no resounding successes have been reported in these trials, and it is too early to discern which, if any, of the specific approaches already being tested will yield drugs that are both effective and safe for human therapy.

Considerable evidence from preclinical and clinical studies, summarized above, suggests that ANG plays an important role in the establishment, progression, and metastatic dissemination of numerous types of human cancers. Yet no agent known to interfere, either directly or indirectly, with the actions of ANG has been tested in humans. Indeed, the ANG antagonists that have been amply demonstrated to be active in mice have potentially formidable drawbacks as drugs. The mAbs would probably need to be administered at relatively large doses: the vasculature in an adult cancer patient contains anywhere from ~1 mg of ANG to more than twice this amount (9), requiring from 6 to >12 mg of mAb for neutralization of the protein in this compartment alone. Long-term treatment with high doses of

protein can be problematic in terms of both practical considerations and side-effects, although immunogenicity can be minimized by using chimeric (4) or more fully "humanized" versions of the antibody. The other ANG antagonist investigated extensively in mice belongs to a class of compounds, antisense oligonucleotides, whose use in humans remains experimental (41).

The present work now provides a pathway for the development of small-molecule inhibitors of ANG for anticancer therapy, using the ribonucleolytic active site of ANG as the target and HTS as the starting point for lead identification. The viability of this approach depends, in part, on the strength of one of its underlying hypotheses: that the catalytic center of ANG is critically involved in the induction of angiogenesis by this protein. The results of mutational studies have provided considerable support for this view. ANG variants with markedly decreased enzymatic activity invariably have reduced angiogenic activity as well. These include the catalytically inactive derivatives H13A, H13Q, H114A, H114N, and K40Q, as well as others (K40R and T44H) showing less extensive losses of enzymatic activity (20–22). The properties of T44H are particularly noteworthy because a different replacement of Thr-44 (by Asp) has essentially no impact on either activity (22). Crystal structures of the K40Q and H13A variants show no significant changes beyond the site of the substitution, establishing that the loss of angiogenicity is directly attributable to disruption of the catalytic apparatus (23). In addition, parallel increases in catalytic efficiency and angiogenic potency have been observed with some ANG variants (42).

These mutational findings establish that the angiogenic action of ANG requires an intact catalytic site, and thereby suggest that molecules directed at this site would have antitumor activity. However, at least two plausible scenarios can be envisioned in which this would not be the case. First, the antitumor effects of antibodies and antisense DNA might be due not to interference with angiogenesis [although a reduction in tumor vasculature has indeed been observed (2, 3, 5)] but to inhibition of some other activity of ANG, independent of the active site. Tumor cells are known to secrete several additional angiogenesis factors (43), and it is possible that the vascularization induced by these molecules is sufficient to foster growth and metastasis when ANG is inhibited. Moreover, ANG has at least one cancer-promoting activity unrelated to its angiogenic and ribonucleolytic actions: it can serve as an adhesion molecule for tumor cells (44). If this is the property of ANG that is most critical for tumor formation, then active-site-directed inhibitors might not be effective anticancer agents. Second, it is possible that the role of the active site of ANG in the angiogenic mechanism does not involve catalysis, but binding of some activating ligand that potentiates cellular interactions such as receptor binding. In this case, compounds that bind to this site and inhibit ribonucleolytic activity might even enhance the biological actions of the protein.

The results of the study reported here largely allay these theoretical concerns and provide considerable support for targeting of the enzymatic active site of ANG as a strategy for developing new anticancer drugs. N-65828, a compound selected purely on the basis of a screen for ribonucleolytic activity inhibitors, was shown to significantly delay the formation of tumors from two distinct human cancer cell types. Although we cannot exclude the possibility that N-65828 acts on other molecules critical for tumor establishment, three lines of evidence, taken together, point to ANG as the target most likely involved. (i) An analogue of this compound that has greatly reduced potency against the enzymatic activity of ANG also fails to exert any protective effect against PC-3 tumors (Fig. 5). (ii) Tumors from mice treated with N-65828 have fewer interior (but not peripheral) blood vessels than tumors from the control groups, a trend seen previously for two antagonists that were demonstrably ANG specific (mAb and antisense) (3, 5). (iii) Data listed at an NCI web site (http://dtp.nci.nih.gov/docs/cancer/searches/cancer_open_compounds.html) show that N-65828, at concentrations up to 100 μ M, does not inhibit the growth in culture of PC-3, HT-29, or any of 57 other human tumor cell lines tested. These data suggest that the antitumor activity of this compound does not derive from a direct effect on tumor cells, and are consistent with inhibition of angiogenesis or some other process involving interactions with the host as the basis for protection.

The utility of ANG inhibitors N-65828 and C-181431 as leads that can ultimately be developed into anticancer agents for human therapy is unclear at this stage. The requisite affinity

improvements (probably more than two orders of magnitude) can potentially be achieved by structure-based design and/or combinatorial methods. For optimization of N-65828, the computational model of the ANG complex may already serve as a useful guide; results with N-65828 analogues and ANG variants described above, and other findings in these areas to be reported elsewhere (J.L.J. and R.S., unpublished data), are in complete agreement with this model. These follow-up studies have already yielded several analogues that have 4- to 20-fold greater potency *in vitro*. Crystallographic and NMR experiments are needed to determine actual complex structures. Along with increasing affinity, lead optimization will also likely involve making the compounds more "drug-like" (45, 46)—e.g., replacing the azo group of N-65828 or adding some hydrophilic substituents to C-181431. Finally, we note that application of the HTS method developed here to additional libraries might well yield leads that already have more favorable K_i values and/or physical properties than do the compounds thus far identified.

The excellent technical assistance of Shannon Sabbar and Najat Ziyadeh is gratefully acknowledged. This work was supported by the NCI (Grant CA88738 to R.S.) and the Endowment for Research in Human Biology, Inc. We thank the Harvard Institute of Chemistry and Cell Biology, and Dr. Randall King in particular, for providing HTS facilities and libraries, and for valuable advice and discussions. The Harvard Institute of Chemistry and Cell Biology is supported by NCI Program Project CA78048, National Institute of General Medical Sciences Program Project GM62566, Merck & Company, Inc., and Merck KGaA. We also thank the Developmental Therapeutics Program at NCI for samples of their compounds.

- Fett, J. W., Strydom, D. J., Lobb, R. R., Alderman, E. M., Bethune, J. L., Riordan, J. F. & Vallee, B. L. (1985) *Biochemistry* 24, 5480–5486.
- Olson, K. A., Fett, J. W., French, T. C., Key, M. E. & Vallee, B. L. (1995) *Proc. Natl. Acad. Sci. USA* 92, 442–446.
- Olson, K. A., Byers, H. R., Key, M. E. & Fett, J. W. (2001) *Clin. Cancer Res.* 7, 3598–3605.
- Piccoli, R., Olson, K. A., Vallee, B. L. & Fett, J. W. (1998) *Proc. Natl. Acad. Sci. USA* 95, 4579–4583.
- Olson, K. A., Byers, H. R., Key, M. E. & Fett, J. W. (2002) *Int. J. Cancer* 98, 923–929.
- Gho, Y. S., Yoon, W. H. & Chae, C. B. (2002) *J. Biol. Chem.* 277, 9690–9694.
- Li, D., Bell, J., Brown, A. & Berry, C. L. (1994) *J. Pathol.* 172, 171–175.
- Etoh, T., Shibuta, K., Barnard, G. F., Kitano, S. & Mori, M. (2000) *Clin. Cancer Res.* 6, 3545–3551.
- Shimoyama, S., Gansauge, F., Gansauge, S., Negri, G., Oohara, T. & Beger, H. G. (1996) *Cancer Res.* 56, 2703–2706.
- Eppenberger, U., Kueng, W., Schlaeppli, J. M., Roessel, J. L., Benz, C., Mueller, H., Matter, A., Zuber, M., Luescher, K., Litschgi, M., et al. (1998) *J. Clin. Oncol.* 16, 3129–3136.
- Blaser, J., Thomssen, C., Schmitt, M., Pache, L., Janicke, F., Graeff, H. & Tschesche, H. (1994) in *Prospects in Diagnosis and Treatment of Breast Cancer*, ed. Schmitt, M. (Elsevier Science, Amsterdam), pp. 223–227.
- Hartmann, A., Kunz, M., Kostlin, S., Gillitzer, R., Toksoy, A., Brocker, E. B. & Klein, C. E. (1999) *Cancer Res.* 59, 1578–1583.
- Miyake, H., Hara, I., Yamanaka, K., Gohji, K., Arakawa, S. & Kamidono, S. (1999) *Cancer* 86, 316–324.
- Eberle, K., Oberpichler, A., Trantakis, C., Krupp, W., Knupfer, M., Tschesche, H. & Seifert, V. (2000) *Anticancer Res.* 20, 1679–1684.
- Shimoyama, S., Yamasaki, K., Kawahara, M. & Kaminishi, M. (1999) *Clin. Cancer Res.* 5, 1125–1130.
- Shimoyama, S. & Kaminishi, M. (2000) *J. Cancer Res. Clin. Oncol.* 126, 468–474.
- Barton, D. P., Cai, A., Wendt, K., Young, M., Gamero, A. & De Cesare, S. (1997) *Clin. Cancer Res.* 3, 1579–1586.
- Wechsel, H. W., Bichler, K. H., Feil, G., Loeser, W., Lahme, S. & Petri, E. (1999) *Anticancer Res.* 19, 1537–1540.
- Ugurel, S., Rappl, G., Tilgen, W. & Reinhold, U. (2001) *J. Clin. Oncol.* 19, 577–583.
- Shapiro, R. & Vallee, B. L. (1989) *Biochemistry* 28, 7401–7408.
- Shapiro, R., Fox, E. A. & Riordan, J. F. (1989) *Biochemistry* 28, 1726–1732.
- Curran, T. P., Shapiro, R. & Riordan, J. F. (1993) *Biochemistry* 32, 2307–2313.
- Leonidas, D. D., Shapiro, R., Allen, S. C., Subbarao, G. V., Veluraja, K. & Acharya, K. R. (1999) *J. Mol. Biol.* 285, 1209–1233.
- Strydom, D. J., Fett, J. W., Lobb, R. R., Alderman, E. M., Bethune, J. L., Riordan, J. F. & Vallee, B. L. (1985) *Biochemistry* 24, 5486–5494.
- Shapiro, R., Riordan, J. F. & Vallee, B. L. (1986) *Biochemistry* 25, 3527–3532.
- Moroi, J. & Riordan, J. F. (1994) *Proc. Natl. Acad. Sci. USA* 91, 1677–1681.
- Russo, A., Acharya, K. R. & Shapiro, R. (2001) *Methods Enzymol.* 341, 629–648.
- Russo, N., Acharya, K. R., Vallee, B. L. & Shapiro, R. (1996) *Proc. Natl. Acad. Sci. USA* 93, 804–808.
- Leonidas, D. D., Chavali, G. B., Jardine, A. M., Li, S., Shapiro, R. & Acharya, K. R. (2001) *Protein Sci.* 10, 1669–1676.
- Shapiro, R. & Vallee, B. L. (1992) *Biochemistry* 31, 12477–12485.
- Jardine, A. M., Leonidas, D. D., Jenkins, J. L., Park, C., Raines, R. T., Acharya, K. R. & Shapiro, R. (2001) *Biochemistry* 40, 10262–10272.
- Kelemen, B. R., Klink, T. A., Behlke, M. A., Eubanks, S. R., Leland, P. A. & Raines, R. T. (1999) *Nucleic Acids Res.* 27, 3696–3701.
- Leland, P. A., Staniszewski, K. E., Park, C., Kelemen, B. R. & Raines, R. T. (2002) *Biochemistry* 41, 1343–1350.
- Russo, N., Shapiro, R., Acharya, K. R., Riordan, J. F. & Vallee, B. L. (1994) *Proc. Natl. Acad. Sci. USA* 91, 2920–2924.
- Shapiro, R., Fett, J. W., Strydom, D. J. & Vallee, B. L. (1986) *Biochemistry* 25, 7255–7264.
- Morris, G. M., Goodsell, D. S., Halliday, R. S., Huey, R., Hart, W. E., Belew, R. K. & Olson, A. J. (1998) *J. Comput. Chem.* 19, 1639–1662.
- Lee, F. S. & Vallee, B. L. (1989) *Biochem. Biophys. Res. Commun.* 161, 121–126.
- Enyedy, I. J., Ling, Y., Nacro, K., Tomita, Y., Wu, X., Cao, Y., Guo, R., Li, B., Zhu, X., Huang, Y., et al. (2001) *J. Med. Chem.* 44, 4313–4324.
- Pezzella, F., Pastorino, U., Tagliabue, E., Andreola, S., Sozzi, G., Gasparini, G., Menard, S., Gatter, K. C., Harris, A. L., Fox, S., et al. (1997) *Am. J. Pathol.* 151, 1417–1423.
- Matter, A. (2001) *Drug Discov. Today* 6, 1005–1024.
- Flaherty, K. T., Stevenson, J. P. & O'Dwyer, P. J. (2001) *Curr. Opin. Oncol.* 13, 499–505.
- Harper, J. W. & Vallee, B. L. (1988) *Proc. Natl. Acad. Sci. USA* 85, 7139–7143.
- Carmeliet, P. & Jain, R. K. (2000) *Nature (London)* 407, 249–257.
- Soncina, F., Strydom, D. J. & Shapiro, R. (1997) *J. Biol. Chem.* 272, 9818–9824.
- Oprea, T. I., Davis, A. M., Teague, S. J. & Leesons, P. D. (2001) *J. Chem. Inf. Comput. Sci.* 41, 1308–1315.
- Sheridan, R. P. (2002) *J. Chem. Inf. Comput. Sci.* 42, 103–108.



Amino-acid sequence of ribonuclease T₂ from *Aspergillus oryzae*

Yasushi KAWATA, Fumio SAKIYAMA and Hidetsune TAMAOKI
Institute for Protein Research, Osaka University

(Received April 12, 1988) – EJB 88 0420

The amino acid sequence of ribonuclease T₂ (RNase T₂) from *Aspergillus oryzae* has been determined. This has been achieved by analyzing peptides obtained by digestions with *Achromobacter lyticus* protease I, *Staphylococcus aureus* V8 protease, and α -chymotrypsin of two large cyanogen bromide peptides derived from the reduced and S-carboxymethylated or S-aminoethylated protein. Digestion with *A. lyticus* protease I was successfully used to degrade the N-terminal half of the S-aminoethylated protein at cysteine residues.

RNase T₂ is a glycoprotein consisting of 239 amino acid residues with a relative molecular mass of 29155. The sugar content is 7.9% (by mass). Three glycosylation sites were determined at Asns 15, 76 and 239. Apparently RNase T₂ has a very low degree of sequence similarity with RNase T₁, but a considerable similarity is observed around the amino acid residues involved in substrate recognition and binding in RNase T₁. These similar residues may be important for the catalytic activity of RNase T₂.

RNase T₂ was first reported by Sato and Egami [1] as a ribonuclease in Takadiastase produced from a culture extract of *Aspergillus oryzae* and purified independently by Rushizky and Sober [2] and by Uchida [3]. The relative molecular mass, M_r , of RNase T₂ was estimated to be 30500 [2] or 36000 [3] including about 10% sugars. RNase T₂ exerts its catalytic activity on the phosphodiester bonds of RNA with a preference for adenylic acid residues without an absolute base specificity [2, 3]. In addition to RNase T₂, RNase T₁ was also purified from Takadiastase. RNase T₁, a small protein with an M_r 11000, has a strict substrate specificity for guanylic acid, and Glu58 [4], His40 and His92 [5] have been shown to be essential for catalysis. It is therefore important to examine the similarity and dissimilarity of the structure and function of RNases T₂ and T₁, which are produced by the same fungus but differ from each other with respect to molecular size and substrate specificity.

Although the primary structures of several smaller ribonucleases including RNase T₁ are known [6], there is no known primary structure of a single-chain ribonuclease with M_r = 20000–30000. We have undertaken the elucidation of the primary structure of RNase T₂ as the first step toward gaining an insight into the molecular basis of catalysis with a ribonuclease of the above size. In this paper, we describe the complete amino acid sequence of RNase T₂ and compare its primary structure with those of other ribonucleases.

MATERIALS AND METHODS

Materials

Achromobacter lyticus protease I and ethyleneimine were kindly donated by Dr T. Masaki (Faculty of Agriculture,

Correspondence to F. Sakiyama, Institute for Protein Research, Osaka University, Yamada-oka, Suita, Osaka-fu, Japan 565

Abbreviations. AcCys, S-aminoethylcysteine; Cm-Cys, S-carboxymethylcysteine.

Enzymes. *Achromobacter lyticus* protease I (EC 3.4.21.50); α -chymotrypsin (EC 3.4.21.1); *Staphylococcus aureus* V8 protease (EC 3.4.21.19); RNase T₂ (EC 3.1.27.1); RNase T₁ (EC 3.1.27.3).

Ibaraki University). The following materials were purchased from the indicated sources: *Staphylococcus aureus* V8 protease from Miles Laboratories; α -chymotrypsin from Sigma; 4 M methanesulfonic acid containing 0.2% 3-(2-aminoethyl)indole from Pierce; yeast RNA from Tokyo Kasei. All other chemicals were of the highest grade commercially available.

Preparation of RNase T₂

RNase T₂ was prepared from Takadiastase Sankyo by the method of Uchida [3] with modification. The detail of the procedure is documented in the Supplement. Purified RNase T₂ gave a single band on sodium dodecyl sulfate/polyacrylamide gel electrophoresis [7] (0.1% sodium dodecyl sulfate, 7.5% polyacrylamide) and eluted as a single peak on a reverse-phase HPLC (Synchrom RP-P) column (4.6 mm \times 300 mm) with a linear concentration gradient of 0.1% F₃CCOOH in water to 0.1% F₃CCOOH in isopropanol/acetonitrile (7:3 by vol.). The specific activity was the same as reported by Uchida [3].

Assay for RNase T₂

RNase activity was assayed, with yeast RNA as a substrate, according to the method of Uchida [3] and expressed as enzyme units and specific activity according to the method described by Takahashi for RNase T₁ [8].

Determination of protein concentration

Protein concentration was determined by taking an absorption coefficient of 2.16 at 280 nm with a 10-mm cell for RNase T₂ at a concentration of 1 mg/ml.

Amino acid analysis

Protein or peptides were hydrolyzed in evacuated, sealed glass tubes with twice-distilled constantly boiling HCl, containing 0.2% phenol, or with 4 M methanesulfonic acid and 0.2% 3-(2-aminoethyl)indole [9], for 24 h at 110°C. The amino

acid analysis was performed with a Hitachi amino acid analyzer (model KLA-5, 835-S or 835-S-30).

Enzymatic digestion

Digestion with *A. lyticus* protease I was performed in 0.05 M Tris/HCl buffer, pH 9.0, for 6–8 h at 37°C at a substrate/enzyme ratio of 400:1 (mol/mol). Digestions with *S. aureus* V8 protease and α -chymotrypsin were performed in 0.1 M ammonium bicarbonate, pH 8.0, for 6–8 h at 37°C at a substrate/enzyme ratio of 100:1 (mol/mol).

Cyanogen bromide cleavage

RNase T₂ (40 mg) was treated with cyanogen bromide (17 mg, a 120-fold molar excess over methionine) in 2.2 ml 70% formic acid at 20°C overnight, then diluted with distilled water and lyophilized. Lyophilization was repeated three times after dissolving the reaction mixture in deionized water.

In manual Edman degradation, Lys was the only amino acid detected in addition to Glu, the N-terminal residue of intact RNase T₂. The extent of the CNBr degradation was about 95% in terms of Pth N⁶-phenylthiocarbamoyllysine estimated.

Reduction and S-carboxymethylation or S-aminoethylation

CNBr-cleaved RNase T₂ was reduced and S-carboxymethylated according to the method of Crestfield et al. [10] or S-aminoethylated according to the method of Rall et al. [11]. The S-alkylated derivative of CNBr-cleaved RNase T₂ was finally obtained as a lyophilizate after desalting on Sephadex G-25 into 0.1 M NH₄OH.

HPLC separation of peptides

HPLC was carried out with a Gilson HPLC system using TSK ODS-120A (4.6 mm × 250 mm, 5 μ m, Toyo Soda) or ODS-LiChrospher (4.6 mm × 300 mm, 5 μ m, 50-nm pore size, Merck) columns at a flow rate of 1 ml/min. Reverse-phase chromatography was performed with a linear concentration gradient using the following combination of solvents: A, 0.1% F₃CCOOH in water/0.1% F₃CCOOH in isopropanol-acetonitrile (7:3 by vol.); B, 0.1% F₃CCOOH in water/0.1% F₃CCOOH in acetonitrile; C, 0.1 M ammonium formate (pH 6.4)/60% acetonitrile in 0.1 M ammonium formate. Peptides were usually separated with solvent system A or B and those not resolved were rechromatographed with solvent system C.

Sequence analysis

Sequence analysis was performed by manual Edman degradation [12] and with a model 470A gas-phase sequencer (Applied Biosystems). The amounts of sample used for manual and automated Edman degradation were 5–10 nmol and 1–2 nmol, respectively. In the automated degradation, the carryover of phenylthiohydantoins from previous cycles was about 15% at the most; they were determined by isocratic reverse-phase HPLC [13] and by modification of the method of Zimmermann et al. [14] with a Zorbax CN column (4.6 mm × 250 mm), a buffer system of methanol/acetonitrile (85:15 by vol.) and sodium acetate, and an eight-channel stepwise elution system.

Similarity of amino acid sequence between RNase T₂ and other nucleases was tested by using a DNASIS/PROTES software developed to search for the similarity of two sequences (Hitachi Software Engineering Co.).

Sugar analysis

Sugar analysis was performed according to the method of Mega and Ikenaka [15]. Methanolysis with 1.5 M hydrogen chloride in methanol was performed at 90°C for 4 h in sealed glass tubes. Glucosamine was determined with an amino acid analyzer, after hydrolysis in evacuated, sealed glass tubes in 4 M methanesulfonic acid containing 0.2% 3-(2-aminoethyl)indole at 110°C for 24 h.

Molecular mass determination

The molecular mass of RNase T₂ was determined by the sedimentation equilibrium method at 21.5°C with a Beckman Spinco Model E analytical ultracentrifuge, equipped with ultraviolet-scanning optics. The protein was dissolved in 50 mM Tris/HCl containing 0.1 M NaCl, pH 7.5. The partial specific volume was assumed as 0.712 ml/g on the basis of the amino-acid and sugar compositions [16].

Nomenclature of peptides

Peptides were numbered according to their final alignments in the sequence of RNase T₂. AP, V and Ch stand for peptides digested with *A. lyticus* protease I, *S. aureus* V8 protease and α -chymotrypsin, respectively.

RESULTS

Determination of the primary structure of CMF-2 (C-terminal half of RNase T₂)

When RNase T₂ was degraded with CNBr, followed by reduction and S-carboxymethylation, two peptide fragments were obtained, as expected from the presence of a single methionine residue. These two peptides, designated CMF-2 and CMF-3, were separated on Sephadex G-100 (Fig. 1s). In this gel filtration, a fraction (CMF-1), containing RNase T₂, uncleaved at either the single methionyl residue or at disulfide linkage(s) connecting the N- and C-terminal halves of the molecule, was also eluted (data not shown). The mass of the peptide CMF-1 was about 10% of that of the protein loaded onto the column. Table 1 summarizes the amino acid compositions of RNase T₂, CMF-2 and CMF-3. It is seen that CMF-2 and CMF-3 are composed of 146 and 93 amino acids, respectively. Homoserine is present in CMF-3 only, indicating that CMF-3 and CMF-2 are aligned in this order from the N-terminus in the intact polypeptide chain. Detection of glucosamine in acid hydrolyzates suggested the presence of N-glycosylation sites in both peptide fragments.

Fragmentation was performed separately for CMF-2 and CMF-3. CMF-2 containing 17 lysines was digested with *A. lyticus* protease I and separated to small peptides (Figs 2s and 4s) and subsequently sequenced completely (Fig. 1). These peptides were obtained by the hydrolysis of lysyl bonds, except Lys94-Lys95, Lys186-Pro187 and Lys236-Ser237 bonds. The insensitivity of these three bonds to this protease digestion is understandable: Lys94 is the N-terminus of CMF-2 and the rate of hydrolysis at the unacylated lysyl bond is very low [17]. The same occurred in the cases of the Lys186-Pro187 bond

Table 1. Amino acid compositions of RNase T₂, CMF-2, and CMF-3. Values were calculated by assuming the number of leucine residues as 14 in RNase T₂, alanine as 8 in CMF-2 and 4 in CMF-3, and are expressed as mol/mol polypeptide. Values in parentheses were calculated from the established sequence

Amino acid	Amount in		
	RNase T ₂	CMF-2	CMF-3
CysO ₃ H ^a	9.9 (10)		
Cm-Cys		3.4 (4)	5.0 (6)
Asx (Asp)	28.6 (17)	17.0 (10)	12.1 (7)
Asn (Asn)	(12)	(7)	(5)
Thr ^b	13.5 (14)	8.2 (8)	6.1 (6)
Ser ^b	22.8 (24)	12.3 (12)	11.3 (12)
Glx (Glu)	25.6 (17)	16.0 (13)	10.0 (4)
Gln (Gln)	(9)	(3)	(6)
Pro	15.8 (16)	8.3 (8)	8.0 (8)
Gly	17.8 (18)	11.3 (11)	7.3 (7)
Ala	11.9 (12)	8.0 (8)	4.0 (4)
1/2Cys ^c	9.2 (10)		
Val	3.9 (4)	2.9 (3)	1.0 (1)
Met	0.9 (1)	0 (0)	0 (0)
Ile	14.6 (15)	10.7 (11)	4.1 (4)
Leu	14.0 (14)	8.2 (8)	6.1 (6)
Tyr	14.7 (15)	12.0 (12)	3.1 (3)
Phe	7.8 (8)	3.0 (3)	5.1 (5)
Lys	17.8 (19)	16.4 (17)	1.7 (2)
His	3.9 (4)	2.9 (3)	1.0 (1)
Trp ^c	6.8 (7)	3.5 (4)	2.5 (3)
Arg	3.1 (3)	1.1 (1)	2.0 (2)
Hse/Hsl			0.7 (1)
GlcN	+	+	+
Total	(239)	(146)	(93)

^a Value after performic acid oxidation.

^b Value after extrapolation to zero hour for 24-h, 48-h and 72-h hydrolyzates.

^c Value after 4 M methanesulfonic acid hydrolysis.

preceded by Lys185 and the Lys236-Ser237 bond preceded by Lys235. That is, in the former case, *A. lyticus* protease I hydrolyzes Lys-Pro bonds at a much slower rate than the Lys-Lys bond, predominantly forming a peptide with the N-terminal Lys-Pro sequence. In the case of the Lys-Ser bond, Ser is followed by a dipeptide containing *N*-glycosylated Asn, giving rise to the slow hydrolysis of the Lys-Ser bond compared with the preceding Lys-Lys bond. Although *A. lyticus* protease I has been known to be extremely specific for lysyl bonds [18], partial cleavages took place at Gly194-Ala195 and Glu198-Ile199, peptides AP-20 and AP-21 being formed in 10–15% yield. However, these cleavages were not serious problems in the present sequencing because AP-19, which escaped from the unusual fragmentation of the peptide chain, was isolated in a higher yield (27.5%) and sequenced without any ambiguities.

In contrast to CMF-2, CMF-3 was only partially degraded with *A. lyticus* protease I. Therefore we performed automated and manual Edman degradation exclusively for AP peptides of CMF-2; the results are shown in Fig. 1. The C-terminal Asn(CHO) residue in peptide AP-24 was determined on the basis of results of amino acid analysis and sequencing data, including identification of glucosamine in the acid hydrolyzate (2 M HCl for 4 h at 110°C) of the water-soluble phenylthiohydantoin obtained at the fourth cycle of manual Edman degradation.

To obtain overlaps for AP peptides, CMF-2 was digested with *S. aureus* V8 protease. In this digestion, Glu101-Gly102, Glu105-Glu106, Glu123-Pro124 and Glu238-Asn(CHO)239 bonds were quite insensitive to proteolysis. Peptides digested were separated by reverse-phase HPLC and each peptide was sequenced (Figs 3s, 4s and Fig. 1). Peptide Ile81-Glu82 was not recovered by HPLC. Nevertheless, the peptides thus sequenced enabled all AP peptides to be aligned unequivocally and generate the sequence of 146 amino acids (Fig. 1). In particular, it was important that peptide V-10, which was unambiguously placed at the C-terminal part of CMF-2 by comparing with sequences of AP-22, AP-23 and AP-24, had *N*-glycosylated asparagine as the C-terminus. Neither denatured RNase T₂ nor CMF-2 afforded any radioactive amino acid by tritium labeling [19]. Carboxypeptidase Y digestion and hydrazinolysis did not directly liberate any amino acids detectable as the C-terminus. These findings are compatible with the presence of *N*-glycosylated asparagine at the C-terminus of RNase T₂.

Determination of the primary structure of AEF-3 (N-terminal half of RNase T₂)

By *A. lyticus* protease digestion, CMF-3 liberated a small peptide (CMF-3-AP-1) and a large peptide (CMF-3-AP-3) (Fig. 5s), which were individually sequenced. CMF-3-AP-1, containing the N-terminal sequence identical to that of intact RNase T₂, and CMF-3-AP-3, containing the C-terminal homoserine residue, were located at the N- and C-terminal portions of CMF-3, respectively. However, a large central core (CMF-3-AP-2) of CMF-3 remained undigested. Since CMF-3 had been shown to contain two arginine residues, a tryptic digestion was attempted. However the hydrolysis pattern was almost same as that obtained in the case of digestion with *A. lyticus* protease I, indicating no fragmentation of the central core peptide (data not shown).

Our next attempt was to *S*-aminoethylate the six half-cystine residues of RNase T₂, since it was anticipated that *S*-(2-aminoethyl)cysteine (AcCys), isosteric to lysine, was sensitive to *A. lyticus* protease I. Two fragments, AEF-2 and AEF-3, were obtained by reduction and *S*-aminoethylation subsequent to CNBr cleavage of RNase T₂ and separated by reverse-phase HPLC on a C₁₈ wide-pore column (Fig. 6s). AEF-3 thus obtained was digested with *A. lyticus* protease I and the peptides produced were fractionated by reverse-phase HPLC (Figs 7s, 9s). The isolated peptides were analyzed for their amino acid composition and sequence. Peptide AP-8 was eluted as several peaks but shown to have the same amino acid sequence, probably owing to microheterogeneity of the sugar moiety and/or a *cis/trans* isomerization of a peptide bond at a proline residue. Peptide AP-6 (Phe25–AcCys60) was also eluted differently. This peptide includes three tryptophan and five proline residues, which might be responsible for the elution of this peptide in three peaks. *N*-Glycosylated asparagine residues at positions 15 and 76 were determined in the same way as described previously for Asn(CHO)239 of peptide AP-24. It is interesting to note that all AP peptides bearing the C-terminal Lys or AcCys residue were sequenced completely with an automated gas-phase sequencer in the present experiment.

In order to overlap the AP peptides, AEF-3 was digested with α -chymotrypsin; twentythree peptides were separated by HPLC and their amino acid sequences were determined (Figs 8s, 9s and Fig. 1). Although a peptide of Ser75-Leu81 was not isolated, all the Ch peptides overlapping the AP

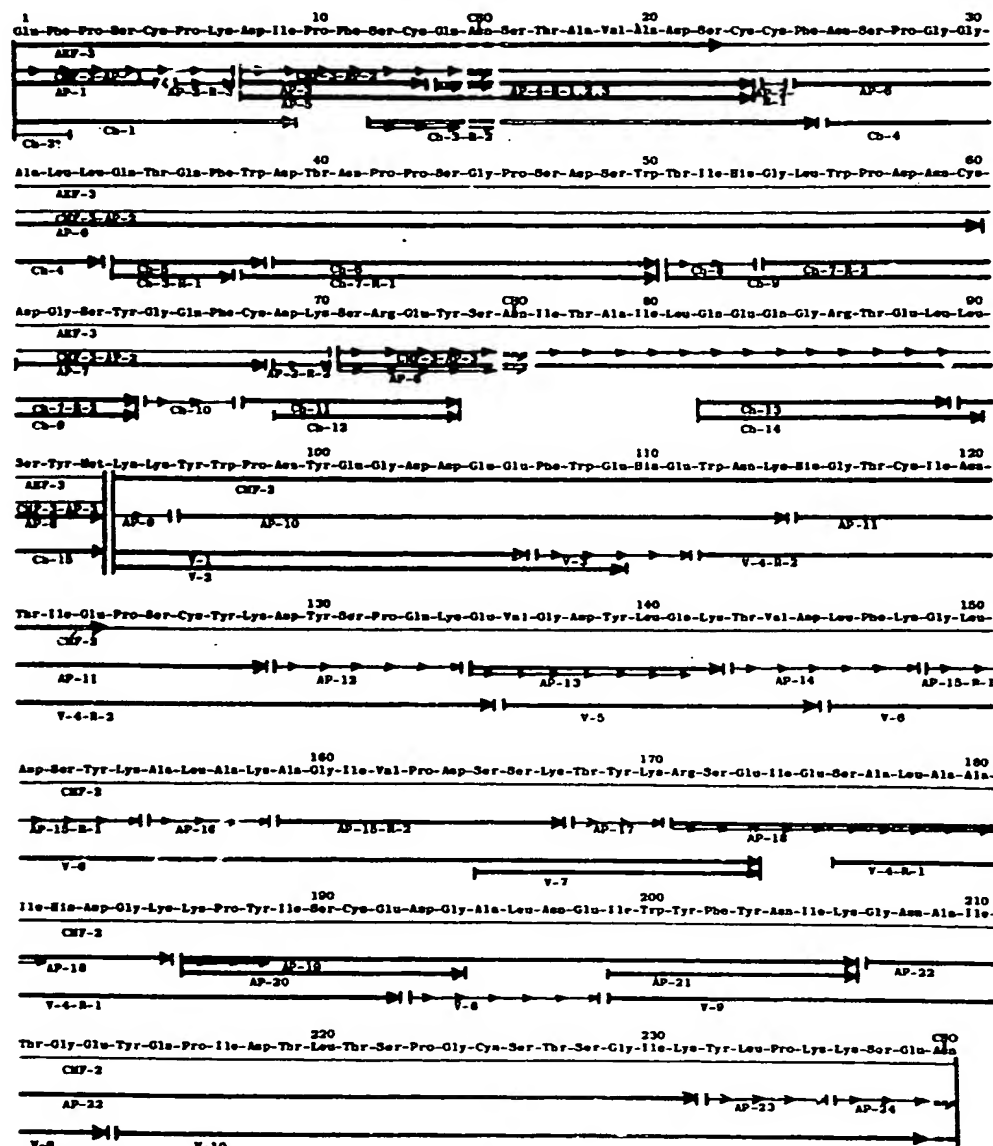


Fig. 1. Amino acid sequence of RNase T₂. Solid, thin lines with bars on both ends (|—|) indicate peptides whose amino acid compositions have been determined; short arrows (→) and long thick arrows (⇒) are sequences identified by manual and automated Edman degradation, respectively. Asn-CHO not identified by the automated degradation are shown by thick broken lines; those not identified as Pth-Asn, but detected as aspartic acid and glucosamine on acid hydrolysis of the product of manual Edman degradation, are shown by broken lines over half arrows (⇌). CHO represent sugars. Two S-S linkages established are Cys68-Cys118 and Cys191-Cys225.

peptides were obtained (Fig. 1). For a sequence of 93 residues, lysine and arginine residues are located at positions 7 and 70 and positions 72 and 86, respectively, whereas the six half-cystine residues are widely distributed at positions 5, 13, 23, 24, 60 and 68.

The amino acid sequence of RNase T₂

The amino acid sequence of RNase T₂ was derived by placing AEF-3 with the C-terminal homoserine before CMF-2, as shown in Fig. 1. The total amino-acid residues are 239, and the sole methionine residue is located around the middle of the peptide chain. The sugar moieties are present at Asns 15, 76 and 239. The relative molecular mass, M_r , of

RNase T₂ including the five disulfide bonds and the sugar moieties is 29155, which is in good agreement with 29200 determined by sedimentation equilibrium [20]. The sedimentation velocity pattern gave a single symmetrical peak and its sedimentation coefficient was estimated as 3.16 S at 21.5°C. The apparent M_r , estimated by the method of Weber and Osborn [7] was 31500.

RNase T₂ has ten half-cystine residues located at positions 5, 13, 23, 24, 60, 68, 118, 126, 191 and 225. To determine the positions of disulfide bonds, RNase T₂ was digested with pepsin and cystine-containing peptides were isolated by reverse-phase HPLC followed by amino acid analysis after performic acid oxidation. Two peptides were purified which were identified as (Gly65-Glu73)-(Trp112-Thr121) con-

Table 2. Sugar composition of RNase T₂ and its glycopeptides

The values are expressed as mol sugar/mol protein or peptide. The values in parentheses are the nearest integer. GlcN was obtained from amino acid analysis, and all other values from gas-chromatographic analysis. — = not detected. Values obtained from Klemer et al. [21] and Kanaya and Uchida [22] are expressed as molar ratios

Peptide	Location of sugar moiety	GlcN	Man	Glc	Fuc	Gal	Xyl
CMF-2	Asn239	0.8 (1)	0.1 (0)	—	—	—	—
AEF-2	Asn239	0.9 (1)	0.1 (0)	—	—	—	—
CMF-3-AP-3 (Ser 71 ~ Hse 93)	Asn76	2.1 (2)	2.9 (3)	—	—	—	—
CMF-3-AP-2 (Asp 8 ~ Lys 70)	Asn15	2.1 (2)	3.7 (3–4)	—	—	—	—
CMF-3	Asns 15, 76	3.7 (4)	6.2 (6)	—	—	—	—
RNase T ₂	Asns 15, 76, 239	4.8 (5)	7.5 (7–8)	—	—	—	—
RNase T ₂ [21]		6	14	8	6	4	1
RNase T ₂ [22]		—	24	3.5	—	4	1

taining Cys68–Cys118 and (Ala179–Gly194)–(Leu220–Gly229) containing Cys191–Cys225 (data not shown). Peptides related to the three other S-S linkages were not purified, and their locations remain to be determined. Nevertheless, the presence of a Cys68–Cys118 disulfide is compatible with the failure in dissociating the two peptide fragments produced by CNBr cleavage of RNase T₂.

Analysis of sugars at Asns 15, 76 and 239

RNase T₂ had three sugar moieties at Asns 15, 76 and 239. Each glycopeptide was isolated by reverse-phase HPLC from their parental CNBr fragments by digestion with *A. lyticus* protease I (Fig. 5s) and the sugar composition of the individual peptides was determined. For Asn15 and Asn76, two glucosamines and three to four mannoses were obtained, suggesting the existence of a sugar containing a high level of mannose. The C-terminal Asn239 was shown to have only one glucosamine residue (Table 2). It is interesting to note that the sugar content of RNase T₂ used in the present experiment is much lower than that reported by Klemer et al. [21] and Kanaya and Uchida [22].

DISCUSSION

Fragmentation of CMF-3

In sequencing RNase T₂, we have encountered some difficulty in fragmenting a cyanogen bromide peptide, CMF-3. In this peptide, all the sites sensitive to trypsin and *A. lyticus* protease I were localized in the N- and C-terminal region. To overcome this difficulty, we have introduced S-aminoethylation to provide new cleavage sites for *A. lyticus* protease I. Digestion with this protease was so effective that the core peptide, which remained uncleaved in the *A. lyticus* protease I digest of CMF-3, could be fragmented to peptides of appropriate size. Moreover, this digestion was extremely favorable for carrying out automated Edman degradation because almost all peptides bearing lysine or S-aminoethylcysteine at the C-terminus were completely sequenced.

Accuracy of amino acid sequence

It should be noted that each amino acid in the established sequence was determined at least twice by manual and/or automated Edman degradation. In particular, the amino acid

sequence determined by both manual and automated Edman degradation is devoid of ambiguity since the phenylthiohydantoin released were identified by two HPLC analyses performed by different elution systems. It should also be noted that the position of tryptophan residue(s) in the peptide chain was determined at least three times, since in peptides obtained by protease digestion the content of tryptophan was not quantitatively determined due to decomposition during the hydrolysis with HCl. The total number of this aromatic residue, thus determined, was identical with that observed for the native protein. This was also confirmed in the case of CMF-2 and CMF-3.

Non-specific partial cleavages of two peptide bonds were observed in the digestion with *A. lyticus* protease I and *S. aureus* V8 protease bearing narrow substrate specificities. Fortunately, these cleavages caused no ambiguity in generating the whole polypeptide chain from all the peptide fragments sequenced.

The only possible ambiguity is with the C-terminal Asn. As shown in Table 2 and Fig. 1, sugar moieties are attached to Asns 15, 76 and 239. Asn15 and Asn76 actually exist in the consensus sequence for an N-glycosylation site Asn-Xaa-Thr (or Ser), where Xaa represents one of 20 amino acids [23]. Asn239 is the C-terminus and the Xaa-Thr(Ser), found adjacent to the two other Asn residues, is therefore absent. However, the presence of an Asn bearing one N-glycosidic glucosamine has been reported for the glycosylation site (Asn197) of Taka-amylase A purified from Takadiastase (*Aspergillus oryzae*) [24]. Both RNase T₂ and Taka-amylase A are extracellular proteins and are likely to be processed by some glycolytic and/or proteolytic enzymes present in the culture medium. It is possible that intact, secreted RNase T₂ has the structure Asn(CHO)-Xaa-Thr (or Ser) at or close to the C-terminus. In Takadiastase, endo- β -1,4-N-acetylglucosaminidase [25] and endo- α -1,2-mannosidase [26] are present. Therefore it can be speculated that these glycosidases could cleave their preferred glycosidic linkages in the sugar moiety of Asn239 near the C-terminus. However, the possibility of acid hydrolysis of the glycosidic linkage during the preparation of RNase T₂ ($\approx 80^\circ\text{C}$ for 5 min at pH 1.5) cannot be ruled out. In any case, an endopeptidase and/or an exopeptidase would then be able to cleave the peptide bond at the asparagine residue. In fact, it is known that *A. oryzae* produces proteases [27]. Hence, the amino acid sequence at the C-terminus of RNase T₂ might differ according to the different purification procedures.



Fig. 2. Alignment of Pro42-Ser166 in RNase T₂ with the whole amino acid sequences of RNase T₁ and other RNases. Asterisks show His53 and His115 which are reactive to iodoacetic acid. Residues which are identical (solid line) or similar (dotted line) in six or more sequences are boxed. The similarity relationships used are: T = S, G = A, V = L = I, Y = F = W, D = N = E = Q, R = K. The origin of each RNase is as follows: RNase T₂ and T₁ from *Aspergillus oryzae*, RNase Ms from *Aspergillus saitoi*, RNase C₂ from *Aspergillus clavatus*, RNase F₁ from *Fusarium moniliforme*, RNase Pch₁ from *Penicillium chrysogenum* 152A, RNase St from *Streptomyces erythraeus*, RNase Sa from *Streptomyces aureofaciens*, RNase Bi from *Bacillus intermedius*, RNase Ba from *Bacillus amyloliquefaciens*.

Molecular mass and sugar composition

The *M_r* of RNase T₂ was calculated as 29155, on the basis of the primary structure which includes three sugar moieties. These are assumed to be composed of a total of five *N*-acetylglucosamine and eight mannose residues. This value is in good agreement with 29200 estimated by the sedimentation equilibrium experiment and close to the 30500 reported by Rushizky and Sober [2]. However, a higher *M_r* (36000) has been reported by Uchida [3]. Perhaps a higher content of sugar in the enzyme preparation might have been responsible for the higher estimation of the molecular mass. In fact, recently, Kanaya and Uchida reported that RNase T₂, purified by affinity chromatography, is a multiple-form enzyme with respect to sugar content [22]. As shown in Table 2, the sugar composition of native RNase T₂ given by those authors, differs considerably. It should be noted that we could not detect glucose by sugar analysis in contrast to the results presented by Klemer et al. [21] and Kanaya and Uchida [22].

Structural characteristics and sequence similarity to RNase T₁ and other ribonucleases

In the amino acid sequence of RNase T₂, there are two distinct clusters of particular amino acids: one is an acidic cluster composed of Glu-Gly-Asp-Asp-Glu-Glu (positions 101–106) and the other is an aromatic one composed of Trp-Tyr-Phe-Tyr (positions 200–203). The acidic cluster is followed by an α -helix (Glu105–Glu111) predicted by the methods of Chou and Fasman [28] and Garnier et al. [29]. Three other helical regions are predicted for Glu88–Tyr96, Lys154–Val162 and Ser176–Lys186 and β -sheets for Ala31–Thr40, Glu141–Leu150 and Asn208–Glu213.

When we compare the primary structure of apparently non-specific RNase T₂ with that of guanylic-acid-specific RNase T₁ [30] which is also derived from *A. oryzae*, several interesting features are found even for an amino acid sequence with a very low degree of similarity. One is the presence of a similar sequence between Ser91–Asp104 in RNase T₂ and Ser37–Asp49 in RNase T₁. In this region, nine of fourteen amino acids are identical. This local but high similarity was observed between RNase T₂ and other fungal RNases: Ms (*Aspergillus saitoi*) [31], C₂ (*Aspergillus clavatus*) [32], F₁ (*Fusarium moniliforme*) [33] and Pch₁ (*Penicillium chrysogenum* 152A) [34]. The bacterial ribonucleases St (*Streptomyces erythraeus*) [35, 36], Sa (*Streptomyces aureofaciens*) [37], Bi (*Bacillus intermedius*) [38] and Ba (*Bacillus amyloliquefaciens*) [39] are less similar even in this region. Comparison of the amino acid sequence around the central part of RNase T₂ with these ribonucleases is shown in Fig. 2. It can be seen that Glu101 and Glu111 in RNase T₂ are consistent in all the ribonucleases aligned. Glu111 corresponds to reactive Glu58 of RNase T₁. X-ray [40] and NMR [41] analyses suggested that in RNase T₁ the main chain of Tyr42 and the side chain of Tyr45 interact with the guanine residue of the substrate in the bound state. Moreover, very recently Ikehara et al. reported that Asn44 rather than Asn43 plays an important role in the maintenance of the function of the active site of RNase T₁ [42]. It appears likely that in RNase T₂ Tyr96–Gly102 takes the place of Tyr42–Gly47 in RNase T₁. In this regard, it is interesting to note that the presence of Trp97–Pro98 as seen in RNase T₂, in place of Asn43 in RNase T₁, might be related to the broadened base specificity in the latter enzyme compared with the narrow specificity of the former. However, we have to wait for the elucidation

of the tertiary structure of RNase T₂ in order to test this hypothesis.

The second site with a considerable similarity is the region of Phe107–Trp112, which possibly aligns with Tyr56–Trp59 in RNase T₁ by the insertion of Glu109 and His110 in RNase T₂. This region of RNase T₁ includes Glu58, which is reactive to iodoacetic acid [4]. In RNase T₂, Glu111 and Trp112 are aligned with Glu58 and Trp59, respectively, in RNase T₁ which are proposed to be part of the active site of RNase T₁ [41, 43]. However, the reaction of RNase T₂ with iodoacetic acid involved His53 and His115, with accompanying inactivation, but not Glu111 (unpublished data). Recently, Irie et al. [44] reported that RNase M from *Aspergillus saitoi*, related to *A. oryzae*, was inactivated by the reaction with iodoacetic acid. They also determined the structures around the two modified histidine residues responsible for inactivation. The sequences are Thr-Ile-His-Gly-Leu-Trp-Pro-Asn-Cys-Asp-Gly-Ser-Tyr and His-Gly-Thr-Cys-Ile-Asn-Thr-Ile-Asp-Pro-Ser-Cys-Tyr. Therefore it is reasonable to assume that the two histidine residues of these peptides correspond to His53 and His115, respectively, in RNase T₂. This is because the amino acid residues around each histidine residue are identical in both RNase T₂ and RNase M, as underlined. Although, very recently, Nishikawa et al. reported that Glu58 is important but not essential for catalysis [45], the position of this acidic amino acid, close to His40 in the tertiary structure of RNase T₁, was obvious from crystallographic data [40]. Therefore it can be assumed that the residues Glu58 and His40 in RNase T₁ are replaced by Glu111 and His115 in RNase T₂, since these residues are still close to each other in the primary structure. If this assumption is correct, His53 of RNase T₂ would be assumed to correspond to His92 of RNase T₁. It should be noted that the same amino acids appear around these two histidine residues (RNase T₂: Thr51-Ile52-His53 and RNase T₁: Ile90-Thr91-His92).

The similarity of the amino acid sequence discussed above concerns only a limited part of RNase T₂. However, this part might be also important to the function of the enzyme because a highly similar sequence is integrated to the site involving in substrate binding in RNase T₁. Moreover, it is interesting that the sequences around the two histidine residues reactive to iodoacetic acid are also similar in RNase T₂ (Trp50-Thr51-Ile52-His53-Gly54 and Trp112-Asn113-Lys114-His115-Gly116). It would appear that RNase T₂ may have evolved by gene duplication. No distinct sequence similarity was found in bovine pancreatic [46] and microbial ribonucleases listed in Fig. 2, bovine [47], ovine [47] and porcine [48] DNases I, 5'-exonuclease from bacteriophage T7 [49] and of *E. coli* DNA polymerase I [50], *Staphylococcus aureus* nuclease [51], endonucleases *EcoRI* [52] and *HhaI* [53].

We are grateful to Miss Y. Yagi of this Institute for amino acid analysis, to Dr S. Tsunasawa and Dr K. Kakiuchi of this Institute for discussion of amino acid sequence determination and sedimentation analysis, respectively. We also thank to Professor T. Ikenaka and Dr T. Mega (Faculty of Science, Osaka University) for sugar analysis, Mr A. Hirai (The Hiratsuka Factory of Sankyo Co., Ltd) for technical support for the RNase T₂ purification, and Dr E. Appella (National Institutes of Health, Maryland) for reading the manuscript.

REFERENCES

1. Sato, K. & Egami, F. (1957) *J. Biochem. (Tokyo)* **44**, 753–767.
2. Rushizky, G. W. & Sober, H. A. (1963) *J. Biol. Chem.* **238**, 371–376.
3. Uchida, T. (1966) *J. Biochem. (Tokyo)* **60**, 115–132.

4. Takahashi, K., Stein, W. H. & Moore, S. (1967) *J. Biol. Chem.* **242**, 4682–4690.
5. Takahashi, K. (1973) *J. Biochem. (Tokyo)* **74**, 1279–1282.
6. Hill, C., Dodson, G., Heinemann, U., Saenger, W., Mitsui, Y., Nakamura, K., Borisov, S., Tischenko, G., Polyakov, K. & Pavlovsky, S. (1983) *Trends Biochem. Sci.* **8**, 364–369.
7. Weber, K. & Osborn, M. (1969) *J. Biol. Chem.* **244**, 4406–4412.
8. Takahashi, K. (1961) *J. Biochem. (Tokyo)* **49**, 1–8.
9. Simpson, R. J., Neuberger, M. R. & Liu, T.-Y. (1976) *J. Biol. Chem.* **251**, 1936–1940.
10. Crestfield, A. M., Moore, S. & Stein, W. H. (1963) *J. Biol. Chem.* **238**, 622–627.
11. Rall, S. C., Bolinger, R. E. & Cole, R. D. (1969) *Biochemistry* **8**, 2486–2496.
12. Edman, P. & Henschen, A. (1975) *Protein sequence determination* (Needleman, S. B., ed.) pp. 232–279, Springer-Verlag, Berlin, Heidelberg, New York.
13. Tsunasawa, S., Kondo, J. & Sakiyama, F. (1985) *J. Biochem. (Tokyo)* **97**, 701–704.
14. Zimmerman, C. L., Appella, E. & Pisano, J. J. (1977) *Anal. Biochem.* **77**, 569–573.
15. Mega, T. & Ikenaka, T. (1982) *Anal. Biochem.* **119**, 17–24.
16. Darchschlag, H. (1986) *Thermodynamic data for biochemistry and biotechnology* (Hinz, H.-J., ed.) pp. 17–128, Springer-Verlag, Heidelberg.
17. Masaki, T., Nakamura, K., Isono, M. & Soejima, M. (1978) *Agric. Biol. Chem.* **42**, 1443–1445.
18. Masaki, T., Tanabe, M., Nakamura, K. & Soejima, M. (1981) *Biochim. Biophys. Acta* **660**, 44–50.
19. Matsuo, H. & Narita, K. (1975) *Protein sequence determination* (Needleman, S. B., ed.) pp. 104–113, Springer-Verlag, Berlin, Heidelberg, New York.
20. Kakiuchi, K. & Williams, J. W. (1966) *J. Biol. Chem.* **241**, 2781–2786.
21. Klemer, A., Künemeyer, H.-M. & Matern, H. (1981) *Z. Naturforsch. B Chem. Sci.* **36**, 1163–1168.
22. Kanaya, S. & Uchida, T. (1981) *J. Biochem. (Tokyo)* **90**, 473–481.
23. Eylar, E. H. (1965) *J. Theor. Biol.* **10**, 89–113.
24. Hase, S., Fujimura, K., Kanoh, M. & Ikenaka, T. (1982) *J. Biochem. (Tokyo)* **92**, 265–270.
25. Mega, T., Ikenaka, T. & Matsushima, Y. (1970) *J. Biochem. (Tokyo)* **68**, 109–117.
26. Yamamoto, K., Hitomi, J., Kobatake, K. & Yamaguchi, H. (1982) *J. Biochem. (Tokyo)* **91**, 1971–1979.
27. Matsubara, H. & Feder, J. (1971) *The enzymes*, vol. III (Boyer, P. D., ed.) pp. 721–795, Academic Press, New York, London.
28. Chou, P. Y. & Fasman, G. D. (1978) *Annu. Rev. Biochem.* **47**, 251–276.
29. Garnier, J., Osguthorpe, D. J. & Robson, B. (1978) *J. Mol. Biol.* **120**, 97–120.
30. Takahashi, K. (1985) *J. Biochem. (Tokyo)* **98**, 815–817.
31. Watanabe, H., Ohgi, K. & Irie, M. (1982) *J. Biochem. (Tokyo)* **91**, 1495–1509.
32. Bezborodova, S. I., Khodova, O. M. & Stepanov, V. M. (1983) *FEBS Lett.* **159**, 256–258.
33. Hirabayashi, J. & Yoshida, H. (1983) *Biochem. Int.* **7**, 255–262.
34. Shlyapnikov, S. V., Bezborodova, S. I., Kulikov, V. A. & Yakovlev, G. I. (1986) *FEBS Lett.* **196**, 29–33.
35. Yoshida, N., Sakei, A., Rashid, M. A. & Otsuka, H. (1976) *FEBS Lett.* **64**, 122–125.
36. Nakamura, K. T., Iwahashi, K., Yamamoto, Y., Iitaka, Y., Yoshida, N. & Mitsui, Y. (1982) *Nature (Lond.)* **299**, 564–566.
37. Shlyapnikov, S. V., Both, V., Kulikov, V. A., Dementiev, A. A., Ševčík, J. & Zelinka, J. (1986) *FEBS Lett.* **209**, 335–339.
38. Aphanasenko, G. A., Dudkin, S. M., Kaminir, L. B., Leshchinskaya, I. B. & Severin, E. S. (1979) *FEBS Lett.* **97**, 77–80.
39. Hartley, R. W. & Barker, E. A. (1972) *Nat. New Biol.* **235**, 15–16.
40. Heinemann, U. & Saenger, W. (1982) *Nature (Lond.)* **299**, 27–31.

41. Nagai, H., Kawata, Y., Hayashi, F., Sakiyama, F. & Kyogoku, Y. (1985) *FEBS Lett.* 189, 167–170.
42. Ikchara, M., Ohtsuka, E., Tokunaga, T., Nishikawa, S., Uesugi, S., Tanaka, T., Aoyama, Y., Kikyodani, S., Fujimoto, K., Yano, K., Fuchimura, K. & Morioka, H. (1986) *Proc. Natl. Acad. Sci. USA* 83, 4695–4699.
43. Tamaoki, H., Sakiyama, F. & Narita, K. (1978) *J. Biochem. (Tokyo)* 83, 771–781.
44. Irie, M., Watanabe, H., Ohgi, K. & Harada, M. (1986) *J. Biochem. (Tokyo)* 99, 627–633.
45. Nishikawa, S., Morioka, H., Fuchimura, K., Tanaka, T., Uesugi, S., Ohtsuka, E. & Ikchara, M. (1986) *Biochem. Biophys. Res. Commun.* 138, 789–794.
46. Smyth, D. G., Stein, W. H. & Moore, S. (1963) *J. Biol. Chem.* 238, 227–234.
47. Paudel, H. K. & Liao, T.-H. (1986) *J. Biol. Chem.* 261, 16012–16017.
48. Paudel, H. K. & Liao, T.-H. (1986) *J. Biol. Chem.* 261, 16006–16011.
49. Kaliman, A. V., Krutilina, A. I., Kryukov, V. M. & Bayev, A. A. (1986) *FEBS Lett.* 195, 61–64.
50. Joyce, C. M., Kelsey, W. S. & Grindley, N. D. F. (1982) *J. Biol. Chem.* 257, 1958–1964.
51. Shortle, D. (1983) *Gene* 22, 181–189.
52. Greene, P. J., Gupta, M., Boyer, H. W., Brown, W. E. & Rosenberg, J. M. (1981) *J. Biol. Chem.* 256, 2143–2153.
53. Schoner, B., Keliy, S. & Smith, H. O. (1983) *Gene* 24, 227–236.

Supplementary material to
Amino-acid sequence of ribonuclease T₂
from *Aspergillus oryzae*

Yasushi KAWATA, Fumio SAKIYAMA and Hidetsune TAMAOKI

Large-scale preparation of RNase T₂

All experiments were carried out at 4°C unless otherwise specified.

Step 1. Extraction of RNase T₂ and removal of RNase T₁ and Taka-amylase A. 2 kg of Takadiastase powder (Sanzyme R, a commercial product of Sankyo Co., Ltd) was extracted with 4 l 0.1 M calcium acetate overnight. After the insoluble materials had been filtered off, the filtrate was adjusted to pH 5.0 with lactic acid and dialyzed against running tap water for 72 h. The dialyzed solution was passed through a Duolite A-2 column (8 cm × 60 cm), previously equilibrated with 0.1 M sodium lactate buffer, pH 5.0, and the column was thoroughly washed with 3 l of the same buffer. On this column RNase T₁ was adsorbed but RNase T₂ not. The fractions which passed through the column were pooled, diluted with two volumes of cold ethanol and allowed to stand overnight to precipitate the proteins. The supernatant was discarded by decantation, and the collected precipitates were dissolved in 5 l tap water and dialyzed thoroughly against running tap water. To the dialyzed solution, saturated 2-ethoxy-6,9-diaminoacridine lactate solution was added under stirring to attain 2–3% dye concentration. By this treatment Taka-amylase A was precipitated as a 2-ethoxy-6,9-diaminoacridine adduct and collected by filtration. Cold acetone was then added to the filtrate to the final concentration of 55%. After standing overnight, the precipitate was collected, dissolved in 0.5 l deionized water and dialyzed against deionized water.

Step 2. DEAE-Sephadex A-25 chromatography. The dialyzed solution was loaded into a DEAE-Sephadex A-25 column (5 cm × 25 cm), previously equilibrated with 0.05 M sodium acetate buffer, pH 5.5, and chromatographed with a linear concentration gradient of 0.05–0.4 M sodium acetate buffer (1.5 l of each buffer at the extreme concentration), pH 5.5, at a flow rate of 2 ml/min. The RNase activity which was eluted in fractions 45–120 (fractions of 20 ml) was pooled and the pH was adjusted to 4.0 with concentrated HCl after the eluents had been diluted with deionized water to give an total absorbance at 280 nm of less than 10 in a 1-cm path-length cuvette. The dilution was necessary to minimize inactivation of RNase T₂. The crude en-

zyme was then collected by precipitation with acetone (final concentration, 55%), followed by centrifugation and dialyzed against deionized water for half a day after being dissolved in water (200 ml).

Step 3. SP-Sephadex C-50 chromatography and heat treatment. Crude RNase T₂ preparation, thus obtained, was adsorbed to an SP-Sephadex C-50 column (4 cm × 32 cm), previously equilibrated with 0.01 M ammonium acetate buffer, pH 4.0 and washed with 400 ml of the same buffer. Chromatography was performed with a linear concentration gradient of 0.01–0.06 M ammonium acetate buffer (0.5 l of each buffer at the extreme concentration), pH 5.5, at a flow rate of 40 ml/h. RNase T₂ was eluted in fractions 60–120 (fractions of 10 ml), pooled and heated carefully at 78–80°C for 5 min at pH 1.5. This pH had been adjusted with concentrated HCl after keeping the RNase T₂ solution at pH 10.5 (with 30% NaOH) for 1 h at room temperature. The heat-treated solution was cooled with ice and diluted with an equal volume of cold acetone to precipitate RNase T₂ after the pH was adjusted to 5.0 with 30% NaOH. The precipitate of RNase T₂ was then collected by centrifugation.

Step 4. Gel-filtration on Sephadex G-100. The precipitate obtained above was dissolved in 15–20 ml of 0.1 M ammonium acetate buffer, pH 5.5, and gel-filtered on a Sephadex G-100 column (2 cm × 190 cm) using the same buffer at a flow rate of 10 ml/h. RNase T₂ was eluted in fractions 83–94 (fractions of 4 ml) and stored at –20°C after precipitation with 80% ammonium sulfate or lyophilization after dialysis against deionized water.

RNase T₂ used in the present sequence analysis was further purified by repeating gel-filtration on Sephadex G-100 three times. Yield was 79 mg from 2 kg Takadiastase.

Data obtained during the present experiment are summarized in Table 1s.

Data of amino acid analyses presented in Tables 2s–5s are presented according to the following format. The numerical values of the amount of amino acids are uncorrected and shown as mol/mol peptide. Hydrolysis of the samples was routinely performed in constantly boiling HCl containing 0.2% phenol at 110°C for 24 h.

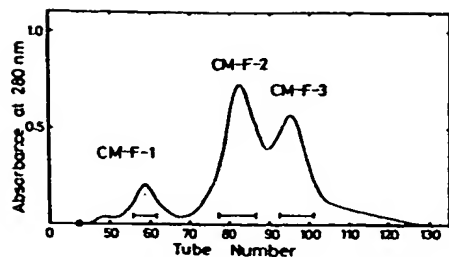


Fig. 1s. Separation of peptides produced by CNBr cleavage of reduced and S-carboxymethylated RNase T₂. The reduced and S-carboxymethylated derivative of CNBr-cleaved RNase T₂ (40 mg) was dissolved in 7 ml 1 M Tris/HCl buffer (pH 8.6) containing 6 M urea and 5% EDTA, and loaded on a Sephadex G-100 column (2.8 cm × 175 cm), previously equilibrated with 0.1 M NH₄OH containing 0.2 M NaCl. CMF-1 (5.0 mg), CMF-2 (16 mg) and CMF-3 (13.5 mg) were lyophilized after collection of the peptide from the fractions shown by bars and subsequent dialysis against deionized water. 5-ml fractions were collected into each tube

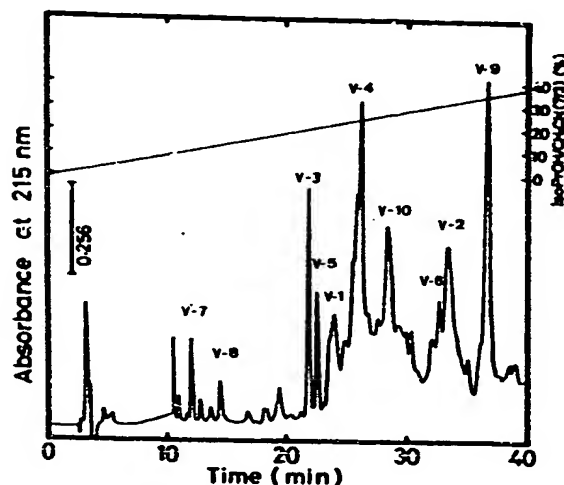


Fig. 3s. Separation of V peptides of CMF-2. CMF-2 (100 nmol) was dissolved in 200 μ l 0.1 M NH₄HCO₃ and digested with *S. aureus* V8 protease for 8 h at 37°C. After lyophilization, one fifth of the sample was dissolved in 40 μ l 0.1% F₃CCOOH and chromatographed. The conditions for chromatography and unnamed peaks were the same as described in the legend to Fig. 2s

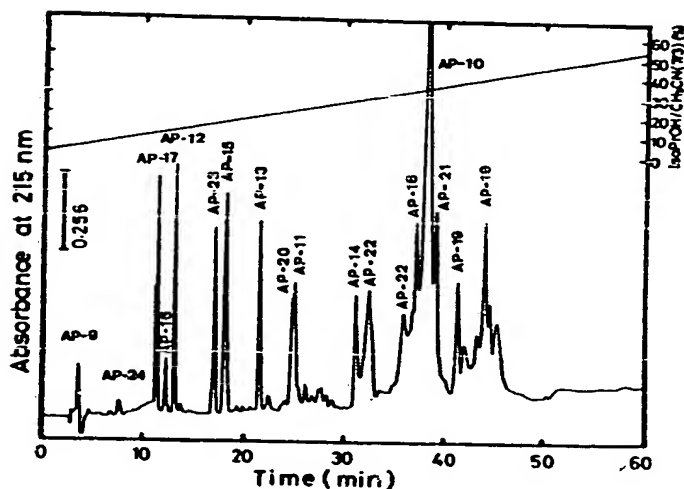


Fig. 2s. Separation of AP peptides of CMF-2. CMF-2 (100 nmol) was dissolved in 200 μ l 50 mM Tris/HCl buffer (pH 9.0) and digested with *A. lyticus* protease I for 8 h at 37°C. Digestion was halted by heating on a boiling bath for 10 min; a 40- μ l portion of the digest was chromatographed on an ODS-120A column (4.6 mm × 250 mm) with solvent system A (see Materials and Methods) at a flow rate of 1 ml/min. Unnamed peaks contained no detectable peptides. A sharp peak at 11 min is a noise due to the start of a concentration gradient of acetonitrile

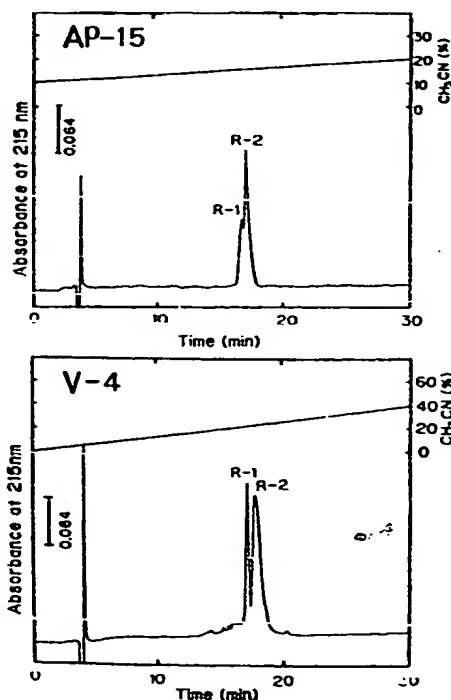


Fig. 4s. Rechromatography of peptides AP-15 and V-4 from CMF-2. AP-15 and V-4 were rechromatographed under the same conditions except for the use of solvent system B for developing as described in the legend to Fig. 2s

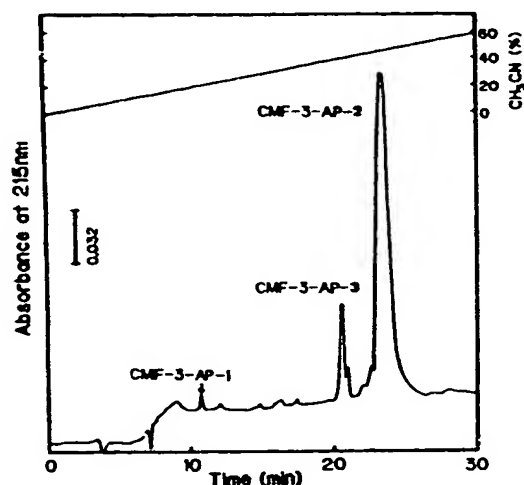


Fig. 5s. Separation of AP peptides of CMF-3. CMF-3 (30 nmol) was digested with *A. lyticus* protease I under the same conditions as described in the legend to Fig. 2s. A 50- μ l portion was chromatographed on ODS-120A (4.6 mm \times 250 mm) with solvent system B at a flow rate of 1 ml/min

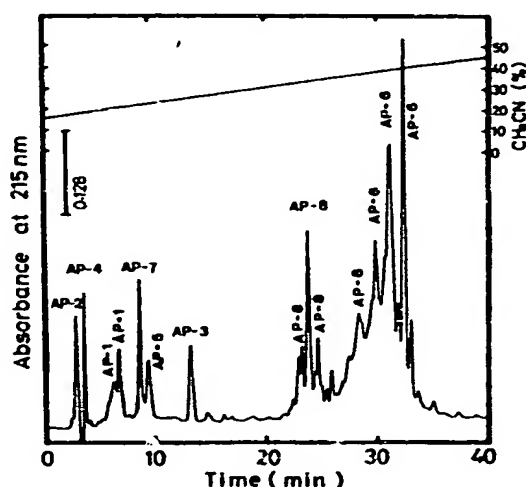


Fig. 7s. Separation of AP peptides of AEF-3. AEF-3 (100 nmol) was dissolved in 250 μ l 50 mM Tris/HCl buffer (pH 9.0) and digested with *A. lyticus* protease I for 6 h at 37°C. Digestion was halted by heating on a boiling bath for 10 min and a 20- μ l portion of the digest was chromatographed under the same conditions as described in the legend to Fig. 2s

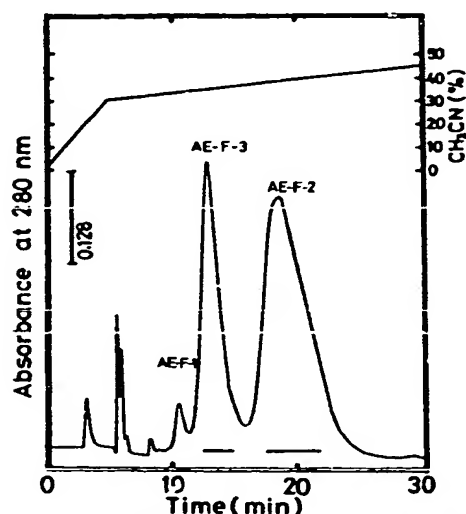


Fig. 6s. Separation of peptides produced by CNBr cleavage of reduced and S-aminoethylated RNase T₂. CNBr-cleaved reduced and aminoethylated RNase T₂ (10 mg) was dissolved in 3 ml 0.1% F₃CCOOH and 1 ml of the sample was chromatographed on an ODS-LiChrospher column (pore size 50 nm, 4.6 mm \times 300 mm) with solvent system B at a flow rate of 1 ml/min. AEF-2 (2.5 mg) and AEF-3 (1.9 mg) were obtained from the fractions shown by bars after lyophilization. Unnamed peaks eluted before AEF-1 were non-peptide origin

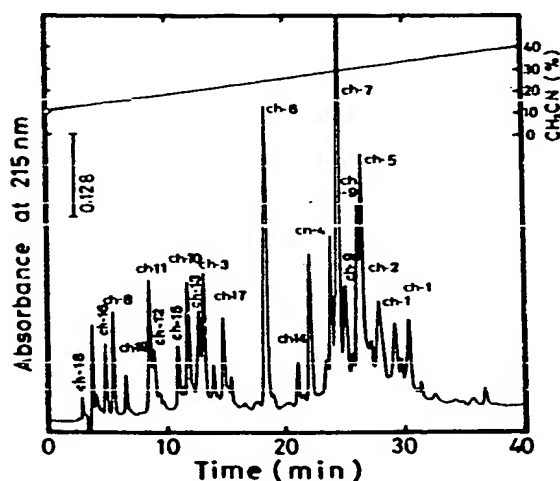


Fig. 8s. Separation of Ch peptides of AEF-3. AEF-3 (100 nmol) was digested with α -chymotrypsin under the same conditions as described in the legend to Fig. 3s. After lyophilization, half of the sample was dissolved in 100 μ l 0.1% F₃CCOOH and chromatographed. The conditions for chromatography were the same as described in the legend to Fig. 2s

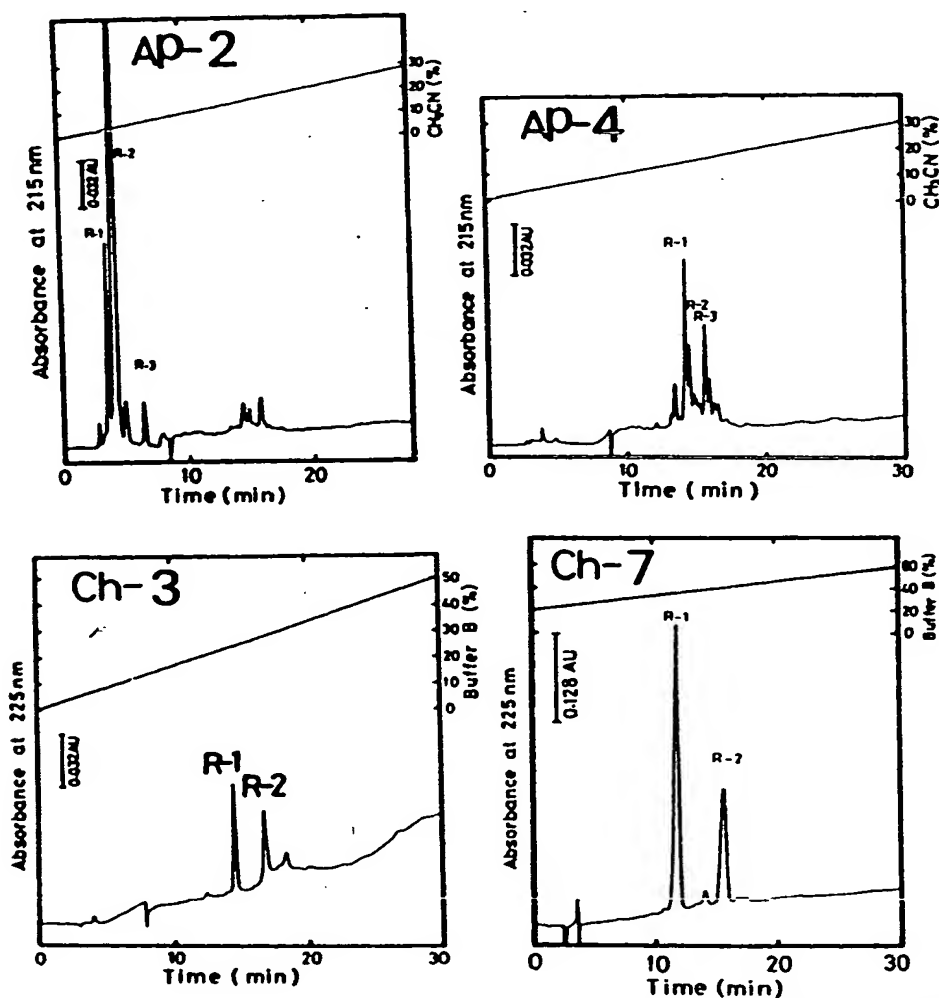


Fig. 9s. Rechromatography of peptides AP-2/4 and Ch-3/7 from AEF-3. Chromatography was performed under the same conditions as described in the legend to Fig. 2s. The solvent system was B for AP-2/4 and C for Ch-3/7

Table 1s. Purification of RNase T₂

Total protein is expressed as total absorbance at 280 nm. Total activity is expressed according to the method described by Takahashi for RNase T₁ [8]

Step	Total protein (A ₂₈₀ × 10 ⁻³)	Total activity kU	Specific activity U/A ₂₈₀	Yield %
1 Crude extract (Takadiastase 2 kg)	1293.6	14787.0	0.14	100
2 Passed fraction through Duolite A-2	823.5	1667.0 ^a	0.12 ^a	90.5
3 Ethanol precipitation	686.9	1362.3	0.20	81.7
4 2-Ethoxy-6,9-diaminoacridine lactate treatment	— ^b	508.8	— ^b	54.6
5 Chromatography on DEAE-Sephadex A-25	7.05	592.0	8.40	35.5
6 Chromatography on SP-Sephadex C-50	1.00	407.0	40.8	24.4
7 Heat treatment	1.04	231.8	22.2	13.9
8 3rd gel-filtration on Sephadex G-100	0.17	102.4	60.2	6.1

^a RNase T₂ activity corrected for contaminating RNase T₁ activity.

^b Not estimated because of the presence of 2-ethoxy-6,9-diaminoacridine lactate.

Table 2s. *Amino acid composition of AP peptides from CMF-2*
 Values in parentheses are from the established amino acid sequence. The presence of glucosamine is indicated by (+) since this was not quantifiable due to the hydrolysis conditions of the analysis. The yields of peptides calculated on the basis of data from amino acid analysis are shown

Amino acid	AP-9	AP-10	AP-11	AP-12	AP-13	AP-14	AP-15-R-1	AP-15-R-2	AP-16	AP-17	AP-18	AP-19	AP-20	AP-21	AP-22	AP-23	AP-24
Cm-Cys																	
Asp		3.8 (4)	1.2 (2)	1.0 (1)	1.0 (1)	1.0 (1)	1.0 (1)	1.0 (1)			1.1 (1)	2.9 (3)	0.8 (1)	1.0 (1)	0.6 (1)	2.0 (2)	1.0 (1)
Thr			1.6 (2)	0.9 (1)	0.9 (1)	0.9 (1)	0.9 (1)	1.7 (2)		0.9 (1)	1.5 (2)	0.8 (1)	0.9 (1)		3.4 (4)	2.6 (3)	0.9 (1)
Ser		4.7 (5)	1.0 (1)	1.0 (1)	1.9 (2)						2.1 (2)	2.0 (2)	1.0 (1)		2.1 (2)	2.1 (2)	1.0 (1)
Glu		1.1 (1)	1.0 (1)	1.0 (1)				1.1 (1)			1.0 (1)	1.0 (1)	0.8 (1)		1.9 (2)	1.9 (2)	1.0 (1)
Pro		1.2 (1)	1.0 (1)	1.0 (1)	1.0 (1)			1.0 (1)			1.0 (1)	1.1 (1)	1.0 (1)		3.7 (4)	1.2 (1)	
Gly								2.1 (2)			2.7 (3)	1.0 (1)					
Ala								0.6 (1)*			1.4 (2)	2.4 (3)	0.8 (1)	1.3 (2)	2.4 (3)		
Val			1.4 (2)					0.6 (1)*			0.8 (1)	0.9 (1)	0.9 (1)	1.6 (2)	1.0 (1)	0.8 (1)	
Ile									0.8 (1)			2.7 (3)	0.9 (1)	0.8 (1)	0.9 (1)	1.0 (1)	
Leu		1.9 (2)	0.8 (1)	1.0 (1)	0.8 (1)	0.8 (1)				1.0 (1)		1.0 (1)	0.9 (1)	0.8 (1)	1.1 (1)	1.0 (1)	0.9 (1)
Tyr		0.9 (1)															
Phe		2.0 (2)	1.1 (1)	0.9 (1)	0.9 (1)	1.0 (1)	1.0 (1)	1.0 (1)	1.0 (1)	1.0 (1)	1.0 (1)	2.0 (2)	0.9 (1)	1.0 (1)	1.1 (1)	1.0 (1)	0.9 (1)
Lys																	
His																	
Trp ^b			0.8 (1)														
Arg																	
Glc ^a																	(+)
Total	2	19	14	6	8	6	6	9	4	3	15	21	9	8	25	4	4
Yield (%)	32.2	58.7	28.3	46.9	53.0	48.4	12.1	28.9	45.5	50.8	42.2	27.5	10.0	15.0	44.8	43.7	40.5
Residue no. from sequence	94-95	96-114	115-128	129-134	135-142	143-148	149-154	159-167	155-158	168-170	171-185	186-206	186-194	199-206	207-231	232-235	236-239

^a Low recovery is due to the incomplete hydrolysis of an Ile-Val bond.

^b Low recovery is due to the HCl hydrolysis.

Table 3s. Amino acid composition of V peptides from CMF-2
For an explanation of this table see the legend to Table 2s

Amino acid	V-1	V-2	V-3	V-4-R-1	V-4-R-2	V-5	V-6	V-7	V-8	V-9	V-10
Cm-Cys				0.7 (1)	1.3 (2)						0.5 (1)
Asp	3.0 (3)	3.0 (3)		1.1 (1)	3.0 (3)	1.9 (2)	2.1 (2)		1.9 (2)	1.9 (2)	2.1 (2)
Thr					1.7 (2)	0.8 (1)	0.9 (1)	0.9 (1)		0.9 (1)	2.5 (3)
Ser				1.6 (2)	1.6 (2)		3.3 (4)	2.5 (3)			3.4 (4)
Glu	3.0 (3)	3.9 (4)	2.0 (2)	1.1 (1)	3.0 (3)	1.0 (1)	1.1 (1)	1.0 (1)	1.0 (1)	1.0 (1)	2.1 (2)
Pro	1.2 (1)	1.1 (1)		1.1 (1)	1.8 (2)		1.1 (1)				3.1 (3)
Gly	1.2 (1)	1.1 (1)		1.0 (1)	1.1 (1)	1.0 (1)	2.0 (2)		1.0 (1)	1.8 (2)	2.0 (2)
Ala				2.6 (3)			2.8 (3)		1.0 (1)	1.0 (1)	
Val						1.7 (2)	0.6 (1)*				
Ile				1.6 (2)	1.8 (2)		0.6 (1)*			2.3 (3)	1.9 (2)
Leu				0.9 (1)		0.8 (1)	2.6 (3)		0.8 (1)		2.1 (2)
Tyr	2.0 (2)	2.0 (2)		1.0 (1)	1.9 (2)	0.9 (1)	2.0 (2)	0.8 (1)		1.8 (2)	1.8 (2)
Phe		1.0 (1)	0.9 (1)				0.9 (1)			0.9 (1)	
Lys	2.0 (2)	2.0 (2)		2.0 (2)	2.9 (3)	1.0 (1)	4.6 (5)	1.7 (2)		1.0 (1)	2.8 (3)
His			0.8 (1)	0.8 (1)	1.0 (1)						
Trp ^b	0.2 (1)	0.6 (2)	0.2 (1)		0.3 (1)					0.3 (1)	
Arg							0.8 (1)	0.7 (1)			
Gln											(+)
Total	13	16	5	17	24	10	28	9	6	15	26
Yield (%)	23.0	30.3	17.3	23.0	6.3	35.0	10.9	14.0	39.1	54.5	40.5
Residue no. from sequence	94-106	94-109	107-111	176-192	112-135	136-145	146-173	165-173	193-198	199-213	214-239

* Low recovery is due to the incomplete hydrolysis of an Ile-Val bond.

^b Low recovery is due to the HCl hydrolysis.

BEST AVAILABLE COPY

Table 4s. Amino acid composition of AEF-2, AEF-3 and AP peptides from AEF-3 and CMF-3
For an explanation of this table see the legend to Table 2s

Amino acid	AP-1	AP-2-R-1	AP-2-R-2	AP-2-R-3	AP-3	AP-4 R-1,2,3	AP-5	AP-6	AP-7	AP-8	CMF-3- AP-1	CMF-3- AP-2	CMF-3- AP-3	AEF-3	AEF-2
Cm-Cys	0.9 (1)	1.0 (1)			1.0 (1)	0.9 (1)	1.6 (2)	0.9 (1)	0.8 (1)		0.9 (1)	4.3 (5)		5.3 (6)	3.4 (4)
Asp			0.9 (1)		0.8 (1)	0.9 (1)	3.0 (3)	6.0 (6)	0.9 (1)	1.1 (1)		10.7 (11)	1.1 (1)	12.0 (12)	16.2 (17)
Thr						0.9 (1)	1.0 (1)	2.8 (3)	0.9 (1)	1.9 (2)		3.5 (4)	1.7 (2)	5.7 (6)	6.7 (8)
Ser	1.1 (1)				1.0 (1)	1.8 (2)	2.8 (3)	3.8 (4)	1.0 (1)	2.9 (3)	0.9 (1)	7.0 (8)	2.4 (3)	10.5 (12)	10.2 (12)
Glu	1.0 (1)					1.0 (1)	1.3 (1)	2.1 (2)	1.0 (1)	5.0 (5)	1.0 (1)	4.1 (4)	5.1 (5)	9.8 (10)	16.2 (16)
Pro	1.2 (1)			1.0 (1)	1.1 (1)		1.1 (1)	5.1 (5)			2.0 (2)	5.8 (6)		8.0 (8)	7.3 (8)
Gly								4.1 (4)	1.7 (2)	1.2 (1)		6.1 (6)	1.0 (1)	7.0 (7)	11.1 (11)
Ala						2.0 (2)	2.0 (2)	1.0 (1)		1.0 (1)		2.7 (3)	1.0 (1)	4.0 (4)	8.0 (8)
Val						1.0 (1)	0.9 (1)					0.9 (1)		0.9 (1)	2.7 (3)
Ile					0.9 (1)		1.1 (1)	0.9 (1)		1.8 (2)		1.9 (2)	1.6 (2)	3.9 (4)	9.7 (11)
Leu								2.8 (3)		2.7 (3)		3.0 (3)	2.8 (3)	5.7 (6)	7.4 (8)
Tyr									0.8 (1)	1.9 (2)		0.9 (1)	1.9 (2)	3.2 (3)	11.2 (12)
Phc	1.0 (1)				0.9 (1)		1.1 (1)	2.0 (2)	1.1 (1)		1.0 (1)	3.7 (4)		4.8 (5)	2.8 (3)
Lys			1.0 (1)	0.8 (1)							1.0 (1)	1.0 (1)		1.5 (2)	15.5 (17)
His								0.8 (1)				0.8 (1)		0.8 (1)	2.6 (3)
Trp*								0.9 (3)				0.9 (3)		0.8 (3)	1.5 (4)
Arg										1.9 (2)			1.7 (2)	1.9 (2)	1.0 (1)
Hse(Hsl)										0.7 (1)			0.8 (1)	0.9 (1)	
GlcN						(+)	(+)			(+)			(+)	(+)	(+)
Total	5	1	2	2	6	10	16	36	8	23	7	63	23	93	146
Yield (%)	32.9	26.8	55.4	43.6	36.8	38.7	10.0	41.1	30.0	69.0	30.0	36.0	41.0	44.4	45.2
Residue no. from sequence	1-5	24	69-70	6-7	8-13	14-23	8-23	61-68	71-93	25-60	1-7	8-70	71-93	1-93	94-239

* Low recovery is due to the HCl hydrolysis.

Table 5s. Amino acid composition of *Ch* peptides from AEF-3
For an explanation of this table see the legend to Table 2s

Amino acid	Ch-1	Ch-2	Ch-3- R-1	Ch-3- R-2	Ch-4	Ch-5	Ch-6	Ch-7- R-1	Ch-7- R-2	Ch-8	Ch-9	Ch-10	Ch-11	Ch-12	Ch-13	Ch-14	Ch-15	Ch-16	Ch-17	Ch-18	Ch-19
Ac-Cys	0.5 (1)			2.9 (3)					0.9 (1)		1.2 (1)		0.9 (1)								
Asp	1.0 (1)			1.7 (2)	1.0 (1)		3.0 (3)	2.7 (3)	2.8 (3)		3.1 (3)		1.0 (1)	1.0 (1)							
Thr			0.8 (1)	0.9 (1)		0.9 (1)	0.9 (1)	0.9 (1)		1.0 (1)	0.9 (1)				0.9 (1)	0.9 (1)					
Ser	0.8 (1)			2.3 (3)	0.9 (1)		2.8 (3)	2.6 (3)	0.9 (1)		1.0 (1)		0.9 (1)	0.9 (1)			1.1 (1)	0.9 (1)	1.1 (1)		1.1 (1)
Glu	0.8 (1)	0.9 (1)	2.0 (2)	1.2 (1)		2.0 (2)						1.0 (1)	1.0 (1)	1.1 (1)	3.7 (4)	4.0 (4)					
Pro	2.1 (2)				1.0 (1)		3.2 (3)	3.0 (3)	1.1 (1)		1.3 (1)										
Gly					1.9 (2)		1.1 (1)	1.0 (1)	2.0 (2)		2.1 (2)	1.0 (1)									
Ala				1.8 (2)	0.9 (1)																
Val				0.5 (1)																	
Ile	0.6 (1)									0.8 (1)	1.0 (1)										
Leu					1.8 (2)				1.0 (1)		1.0 (1)				1.0 (1)	1.6 (2)	0.9 (1)		0.8 (1)		
Tyr									1.1 (1)		1.0 (1)				0.9 (1)	0.8 (1)	1.0 (1)	1.0 (1)	1.0 (1)		1.0 (1)
Phe	1.1 (1)	1.0 (1)	0.9 (1)	1.1 (1)		1.0 (1)						1.0 (1)									
Lys	1.0 (1)																				
His										1.0 (1)	0.8 (1)				0.9 (1)	0.7 (1)					
Trp*																					
Arg						0.4 (1)	0.4 (1)	1.2 (2)	0.2 (1)		0.4 (1)						0.8 (1)	0.7 (1)		1.0 (1)	
Hse (Hsl)																					
Gln																					
				(+)																	
Total	9	2	4	14	8	5	12	13	11	3	14	3	7	6	8	9	4	3	3	1	2
Yield (%)	38.1	34.0	41.0	10.0	94.2	34.9	40.9	15.7	9.2	43.3	16.0	91.0	47.2	24.2	47.5	20.6	19.6	33.4	23.8	13.8	
Residue no. from sequence	1-9	1-2	34-37	12-25	26-33	34-38	39-50	38-50	54-64	51-53	51-64	65-67	68-74	69-74	82-89	82-90	90-93	91-93	90-92	93	91-92

* Low recovery is due to the HCl hydrolysis.

Characterization of *Aspergillus niger* B-1 RNase and Its Inhibitory Effect on Pollen Germination and Pollen Tube Growth in Selected Tree Fruit

Levava Roiz, Uzi Ozeri, Raphael Goren, and Oded Shoseyov

The Kennedy Leigh Centre for Horticultural Research, The Faculty of Agriculture, The Hebrew University of Jerusalem, P.O. Box 12, Rehovot 76100, Israel

ADDITIONAL INDEX WORDS. RNase B1, *Citrus reticulata*, peach, pollen tube growth, *Prunus persica* (Peach Group), tangerine

ABSTRACT. *Aspergillus niger* B-1 (CMI CC 324626) extracellular RNase (RNase B1) was purified to homogeneity. It was found to contain two isoforms of 32- and 40-kDa glycoproteins, sharing a 29-kDa protein moiety. Optimal RNase activity was observed at 60 °C and pH 3.5. In 'Almog' peach [*Prunus persica* (L.) Batsch (Peach Group) 'Almog'] and 'Murcott' tangerine (*Citrus reticulata* Blanco 'Murcott') the enzyme inhibited pollen germination and pollen tube growth in vitro as well as in vivo. In field experiments, spray application of the RNase caused a reduction in 'Fantasia' nectarine [*Prunus persica* (L.) Batsch (Nectarine Group) 'Fantasia'] fruit set and interfered with embryo development. The biological effect of the RNase may be of horticultural value, due to its potential to control fertilization.

In self-incompatible plants, growth of self-pollen is arrested in the stigma or style, before fertilization occurs. Self-incompatibility is often controlled by a single multiallelic S-gene (de Jettancourt, 1977). A common outbreeding mechanism is gametophytic self-incompatibility, in which a pollen tube bearing an S-allele identical to one of the two alleles of the pistil fails to achieve fertilization (Clarke and Newbigin, 1993; Haring et al., 1990; Linata et al., 1993; Newbigin et al., 1994; Singh and Kao, 1992). In members of Solanaceae and Rosaceae, the S-alleles have been found to encode stylar-specific S-glycoproteins exhibiting ribonuclease (RNase) activity, as well as the ability to inhibit the growth of self-pollen tubes (Clarke et al., 1990; Kaufmann et al., 1991; Kirch et al., 1989; McClure et al., 1989; Sassa et al., 1992). Two domains in the primary structure of these S-glycoproteins, containing one histidine residue each show strong homology to *Aspergillus oryzae* (Ahlburg) Cohn RNase T₂, *Rizopus niveus* Yamazaki IFO 4810 RNase Rh (McClure et al., 1989), and *A. taipei* Sakaguchi et al. RNase M (Watanabe et al., 1990).

In some plants non-S-allele-specific ribonucleases were found to be produced by the female organs. For example, RNase X has been reported to be shared by both self-incompatible *Nicotiana glauca* Link et Otto and self-compatible *N. tabacum* (L.) (McClure et al., 1989). In self-incompatible *Petunia inflata* Fries RNase X₂ shares homology with S-RNases, yet its gene is not located on the S-locus (Lee et al., 1992). The biological traits and function of these RNases were not fully determined yet. In self-compatible peach [*Prunus persica* (Peach Group)] and calamondin (*Citrus reticulata* 'Austera' × *Fortunella* sp. Swingle) the stigmatic diffusate contains RNase activity (Roiz and Shoseyov, 1995; Roiz et al., 1995). These stigmatic RNases inhibit pollen germination and tube elongation in vitro in a dose-responsive manner. Furthermore, it was shown in the above studies that bovine pancreatic RNase A and *A. oryzae* RNase T₁, which are nonspecific, had similar inhibitory effect in peach and calamondin, respectively. In both species in vitro studies suggest that non-S-allele RNases play a role in the pollination process.

The effect of nonspecific RNase may be of horticultural value.

In many deciduous fruit trees, yields of commercial value depend upon massive thinning of the flowers and fruitlets. In stone fruits [peach, plum (*Prunus domestica* L.), etc.] the thinning process is currently performed manually. In *Citrus* L. trees, on the other hand, seedless fruits are desirable. Therefore, a further step in this research was to examine an effective RNase that can be produced in large amounts. Species of *Aspergillus* have been reported to produce extracellular RNases (Egami and Nakamura, 1969). *Aspergillus niger* is also used as a source for important materials and enzymes in the food industry, such as citric acid and pectinases (Kerns et al., 1987; Li and King, 1963; Rombout and Pilnik, 1978). In the present work we describe production, purification, and partial characterization of *A. niger* B-1 extracellular RNase (RNase B1) and its effect on in vitro and in vivo pollen germination and pollen tube growth.

Materials and Methods

PREPARATION AND PURIFICATION OF *A. niger* EXTRACELLULAR RNASE. *Aspergillus niger* B1 (CMI CC 324626) was grown in liquid culture containing 1% (w/v) wheat flour and 0.05% (w/v) (NH₄)₂SO₄. The mixture was adjusted to pH 3.5 with HCl and autoclaved. An inoculum of ≈10⁶ spores was suspended in 100 mL of medium and incubated at 30 °C in an orbital shaker, at 200 rpm for 100 h. The growth medium was passed through a 0.2-μm membrane and dialyzed three times against 10 volumes of 2 mM sodium acetate pH 6. Two liters of dialyzed solution were loaded onto a Fractogel EMD-TMAE 650 (M) 26/10 (Merck, Darmstadt, Germany) column, equilibrated with 20 mM sodium acetate pH 6. Bound proteins were eluted with a 500-mL linear gradient of 0 to 1.0 M NaCl in the same buffer, using a fast protein liquid chromatography (FPLC) system (Amersham Pharmacia Biotech, Buckinghamshire, U.K.) at a flow rate of 5 mL·min⁻¹. The fractions exhibiting the highest RNase activity were pooled and dialyzed against 2 mM sodium acetate pH 6, and a 50-mL aliquot was loaded onto a Mono Q 5/5 HR (Amersham Pharmacia Biotech) column, equilibrated with 20 mM sodium acetate pH 6. The elution was performed as with the EMD-TMAE column, except that only 10 mL of a 0 to 1.0 M salt gradient were used, at a flow rate of 1 mL·min⁻¹.

Proteins were monitored at 280 nm and measured according to

Received for publication 14 Jan. 1999. Accepted for publication 7 Oct. 1999. The cost of publishing this paper was defrayed in part by the payment of page charges. Under postal regulations, this paper therefore must be hereby marked advertisement solely to indicate this fact.

Bradford (1976), using bovine serum albumin (BSA) as a standard. Different fractions were analyzed by 12.5% sodium dodecyl sulfate-polyacrylamide gel electrophoresis (SDS-PAGE; Laemmli, 1970). An RNase activity gel was run according to Roiz and Shoseyov (1995).

The purified RNase B1 was deglycosylated enzymatically according to the procedure of Broothaerts et al. (1991). The enzyme was mixed with 0.5% (w/v) SDS and 5% (w/v) β -mercapthoethanol and heated at 100 °C for 5 min. Once cooled, the reaction mixture was diluted 2.5-fold with buffer containing 50 mM sodium phosphate pH 7.5, 25 mM EDTA, 1% (w/v) Triton X-100, and 0.02% (w/v) sodium azide. Peptide-N-glycosidase F (PNGase F, Boehringer-Mannheim GmbH, Mannheim, Germany) was added to a final concentration of 20 units/mL and incubated overnight at 37 °C. The sample was then mixed with sample application buffer, heated at 100 °C for 5 min, and analyzed by 12.5% SDS-PAGE.

RNase ASSAYS. The optimal conditions for RNase activity were determined within a range of temperatures from 20 to 100 °C at 10 °C intervals, and across a pH range from 2.5 to 7 at 0.5 pH units intervals, using phosphate-citrate buffer (50 and 12 mM, respectively). The RNase activity assay was modified from Brown and Ho (1986). Samples of 10 μ L were added each to 490 μ L of ice-cold buffer, containing 4 mg·mL⁻¹ yeast RNA (Sigma, St. Louis, Mo). Half of the mixture was moved immediately to another tube containing 50 μ L 0.75% (w/v) uranyl sulfate in 25% (w/v) perchloric acid (stop mixture), for use as a blank. The rest was incubated for 10 min, then 50 μ L of stop mixture were added. Following centrifugation at 15,000 g_n for 5 min, the supernatant was diluted 20-fold with distilled water and absorbance was determined at 260 nm. One unit of RNase activity was determined as the amount of enzyme releasing soluble nucleotides at a rate of one A 260 nm·min⁻¹.

RNase B1 was visualized by an activity gel, as modified from Roiz and Shoseyov (1995). An SDS gel containing RNase B1 was renatured by washing twice for 15 min each with 20 mM sodium acetate pH 3.5 containing 25% (v/v) isopropanol and then twice for 15 min each with buffer alone. The renatured gel was laid over a plate containing 0.1% RNA and 0.8% agarose in 20 mM sodium acetate and incubated at 37 °C for 30 min. The gel was then removed and the agarose plate was stained with 0.02% (w/v) toluidine blue in water to visualize RNase activity.

EFFECT OF RNase B1 ON POLLEN TUBE GROWTH. Pollen of 'Almog' Peach germinated in vitro in liquid culture, as described by Roiz and Shoseyov (1995). Pollen grains were suspended in aliquots containing 100 μ L 15% (w/v) sucrose, 100 μ g·mL⁻¹ boric acid, 200 μ g·mL⁻¹ magnesium sulfate, 200 μ g·mL⁻¹ calcium nitrate and different concentrations of RNase B1. After incubation overnight at 25 °C in a dark chamber, percent germination was recorded. Pollen tube length was examined by light microscopy with an eyepiece micrometer.

The effect of RNase B1 treatment on pollen tube growth was tested also in vivo. In peach and in tangerine (*Citrus reticulata* 'Murcott') intact flowers at the very beginning of anthesis, were sprayed with RNase B1 diluted in 20 mM citrate buffer pH 3.5 to a concentration of 0.2 mg·mL⁻¹ protein, having 100 units/mL RNase activity. In each species additional flowers at the same stage, on different branches, were sprayed with buffer alone or remained nontreated as controls. After exposure to open pollination for 48 h, the styles were fixed in 3 acetic acid : 1 ethanol (by volume) for 24 h, washed with distilled water and imbibed overnight in 8 M NaOH. Following thorough washes in distilled

water, the styles were cut longitudinally, immersed each in a drop of 0.1% (w/v) aniline blue in 0.1 M potassium phosphate on a slide and carefully squashed with a cover slip. Pollen tubes were observed by epifluorescence microscopy (model BX40, equipped with WIB cube; Olympus Optical Co., Hamburg, Germany).

THE EFFECT OF RNase B1 ON FRUIT SET. Field experiments were conducted in April 1994 using trees of 'Fantasia' nectarine [*Prunus persica* (Nectarine Group) 'Fantasia'] growing in Rosh Zurim, Israel. Branches 30 to 40 cm long, bearing \approx 10% open flowers, were sprayed with different concentrations of RNase B1 in 20 mM citrate buffer pH 3.5 and 0.025% triton-X 100. Nontreated branches, and branches sprayed with only buffer and triton-X 100, served as controls. The branches were sprayed at 2- to 3-d intervals during the blooming period (14 d). A month later, the number of fruit per branch was examined. For viability tests, seeds were cut longitudinally through the embryo and immersed in one percent 2,3,5-triphenyl tetrazolium chloride in water for 4 h at 20 °C in the dark. Red staining indicated viable tissues.

Results

PURIFICATION AND CHARACTERIZATION OF RNase B1. *Aspergillus niger* grown in liquid culture produced considerable amounts of extracellular RNase. A temperature of 60 °C and pH 3.5 were found optimal for RNase activity (Fig. 1), and were adopted as the standard conditions for RNase assays.

Purification of RNase B1 consisted of two steps (Table 1). The crude filtrate contained 1000 units/mL and 0.05 mg·mL⁻¹ protein. The pooled fractions around the active RNase peak eluting at 0.62 M NaCl (Fig. 2A) from an EMD-TMAE column, contained 0.1 mg·mL⁻¹ protein, with an RNase activity of 40,000 units/mL. In the final step, the RNase was eluted from a Mono Q column at 0.5

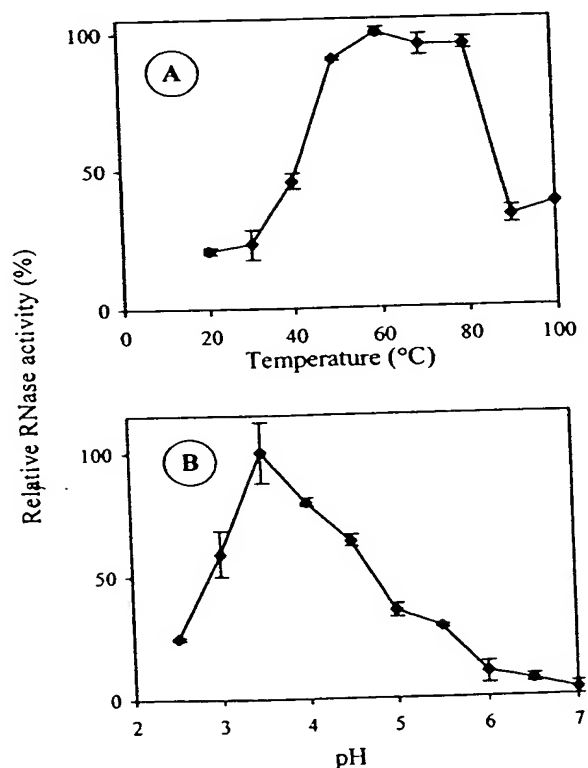


Fig. 1. Activity plots of RNase B1 as a function of (A) temperature and (B) pH.

Fig. 1. Purification of RNase B1 from growth medium filtrate of *A. niger* B-1. Protein concentration and RNase activity were monitored during enzyme purification.

Purification-step	Total vol of extract (mL)	Total RNase activity (units × 10 ³)	Protein concn (mg·mL ⁻¹)	Recovery (%)	Specific activity units × 10 ³ /mg protein)
Crude filtrate	2000	2000	0.05	100	20
EMD-TMAE column	28	1120	0.1	56	400
Mono-Q column	1.2	652	1.05	32.6	517

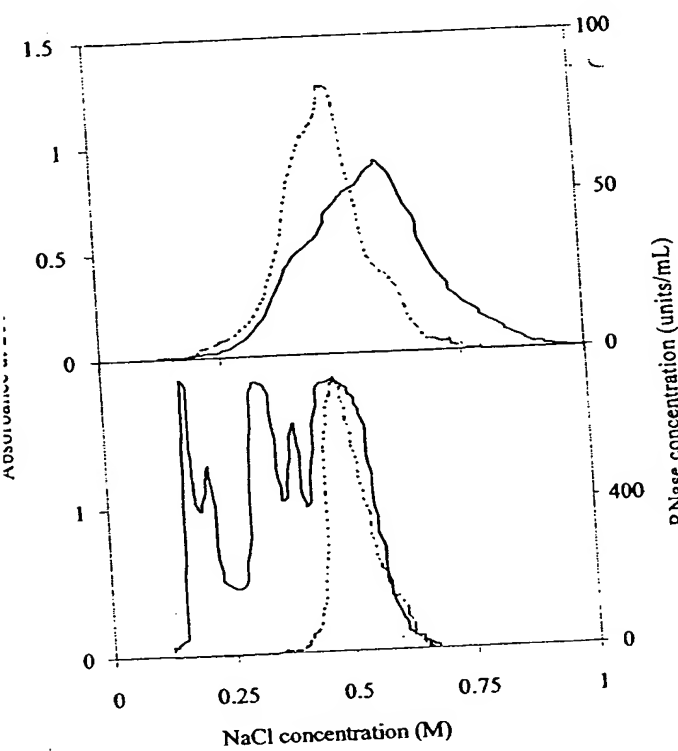


Fig. 2. Anion exchange chromatography of RNase B1. The solid line = absorbance at 280 nm and the dashed line = RNase activity. (A) The crude filtrate was dialyzed and loaded onto an EMD-TMAE column. Each 7-mL fraction was located in a separate tube. (B) Fractions eluted in 0.55 to 0.65 M NaCl (A), showing highest RNase activity, were pooled and loaded onto a Mono-Q column. Each 0.5-mL fraction was collected in a separate tube.

0.5 M NaCl (Fig. 2B); the eluant had protein concentration and RNase activity of 1.05 mg·mL⁻¹ and 543,000 units/mL, respectively. Two major protein bands, of 40 and 32 kDa, were observed following SDS-PAGE of the purified RNase B1 (Fig. 3). An RNase activity gel showed active bands corresponding to the 32 and the 40 kDa proteins. When subjected to PNGase F, a single protein band appeared at 29 kDa. RNase activity was retained after PNGase digestion (data not presented).

EFFECT OF RNASE B1 ON POLLEN TUBES AND FRUIT SET. Seventy five percent of the control peach pollen grains germinated in vitro and the pollen tubes reached 0.48 ± 0.03 mm in length. Addition of RNase B1 to the growth medium reduced percentage germination and the length of the pollen tubes, in a dose responsive manner (Fig. 4). RNase B1 had a pronounced inhibitory effect, considering that 50 units/mL, representing 0.1 mg·mL⁻¹ (2.8 × 10⁻³ mM) protein, were found lethal, whereas BSA at a 680-fold higher concentration of 125 mg·mL⁻¹ (1.9 mM) protein, reduced only 50% of pollen germinability and tube growth.

Control pollen tubes of peach were observed growing in vivo

through the stigmatic tissue directed into the style, 48 h after pollination (Fig. 5A). A similar picture was observed in styles treated with buffer only. In contrast, pollen grains germinated on stigmas treated with RNase B1 produced short pollen tubes, which appeared to lack any growth orientation, and failed to penetrate the stylar tissue (Fig. 5B). In tangerine only a small portion of the stigmatic tissue, of which the diameter was 2 to 3 mm, could be observed in the microscopic field. Therefore, only a few pollen tubes were captured in the microscopic field, as shown in Fig. 6. However, the difference between the normal growth of the control pollen tubes (Fig. 6A) and the irregular growth of the RNase-treated pollen tubes (Fig. 6B), was observed clearly.

In 'Fantasia' nectarine RNase B1 caused a reduction in fruit set (Table 2). In nontreated branches or branches sprayed with buffer containing triton X-100, fruit set was 48.3% and 36.3%, respectively. It seemed that the low pH-buffer had some inhibitory effect on fruit set, however branches treated with 500 and 1000 units/mL of RNase B1 set 23.3% and 18.4% fruit, respectively, indicating a significant thinning effect of the RNase, with a dose dependent response.

In RNase B1 treated branches, many undeveloped fruitlets were observed. Viability tests showed that in nontreated flowers or flowers sprayed with buffer, most embryos cut surfaces were stained red, whereas embryos born in RNase-treated flowers, unevenly stained cut surfaces with brown necrotic tissues were found.

Discussion

An effective fermentation and purification process was developed for production of RNase B1 (Ozeri, 1995). A temperature of 60 °C and a pH of 3.5, values which were optimal for RNase B1

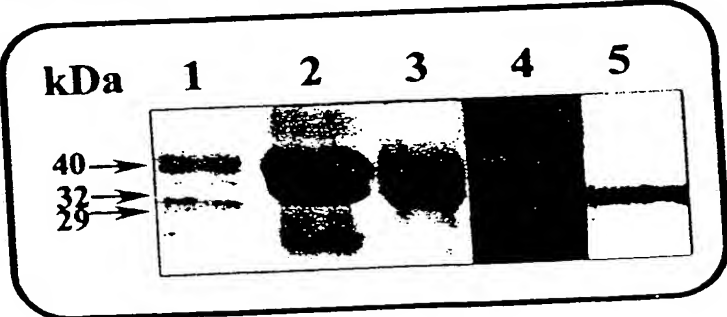


Fig. 3. SDS-PAGE zymogram of the RNase B1 purification steps. Lane 1 = crude filtrate; lane 2 = proteins eluted from the EMD-TMAE column at 0.62 M NaCl; lane 3 = proteins eluted from the Mono-Q column at 0.5 M NaCl; lane 4 = same as lane 3, except the proteins were assayed for RNase activity in situ and stained with toluidine blue; lane 5 = purified RNase after deglycosylation by PNGase; lanes 1 to 3 and 5 were stained with coomassie blue.

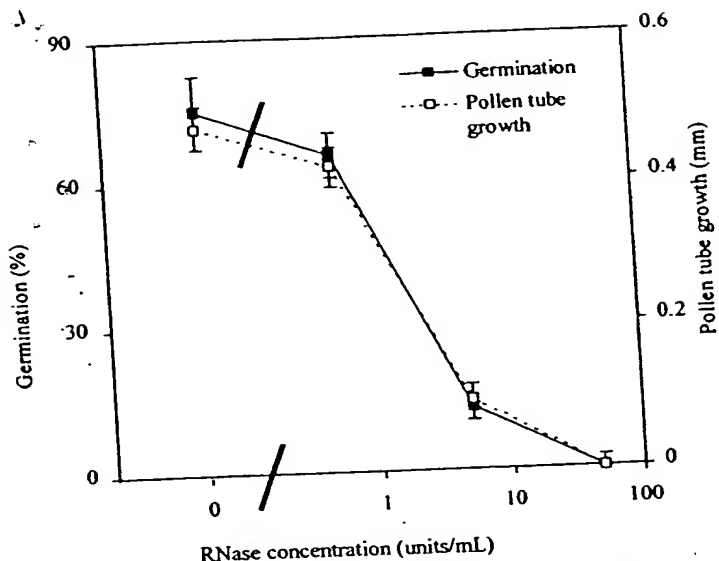


Fig. 4. Effect of different concentrations of *A. niger* B-1 RNase on peach pollen germination and pollen tube growth in vitro. For percentage germination, at least 100 pollen grains in each sample were monitored. For pollen tube growth, 10 pollen tubes in each sample were measured. Each point is the mean of three replications. Vertical bars = \pm SE.

activity, are also optimal for the activity of β -glucosidase produced by this strain (Shoseyov et al., 1988). In related species, extracellular RNases have been found to require similar conditions for optimal activity. For example, Horitzu et al. (1974) reported on *A. niger* NCR-A-1-233 RNase (50 °C, pH 3.5) and RNase T₂ (pH 4.5) and Irie (1967) reported on *A. saitoi* RNase M (50 °C, pH 4) and *Rhizopus niveus* RNase Rh (50 °C, pH 5). All these RNases have molecular weights between 24 and 34 kDa. They are also base-nonspecific enzymes with a preference to adenilic acid (Ohgi et al., 1991; Watanabe et al., 1990).

Secretion of considerable amounts of RNase should have a substantial biological role. In microorganisms, extracellular RNases are accepted generally to contribute to digestion of polyribonucleotides present in the growth medium, thereby giving rise to diffusible nutrients (Egami and Nakamura, 1969). These so-called nutritive characteristics of RNases have also been described in plants: cells of tomato (*Lycopersicon esculentum* Mill.) suspension cultures secreted RNase into the growth medium in response to phosphate starvation (Nurnberger et al., 1990). Nevertheless, more research is needed for a complete understanding of the physiological role of fungal extracellular RNases.

RNase B₁ was purified to homogeneity. PNGase deglycosylation, followed by appearance of a single 29-kDa band, indi-



Fig. 5. Effect of RNase B1 on peach pollen tube growth in the stigma and the upper part of the style. (A) Control flower that was exposed to open pollination for 48 h. (B) Flower that was treated with RNase B1 before pollination. Scale bars = 0.2 mm.

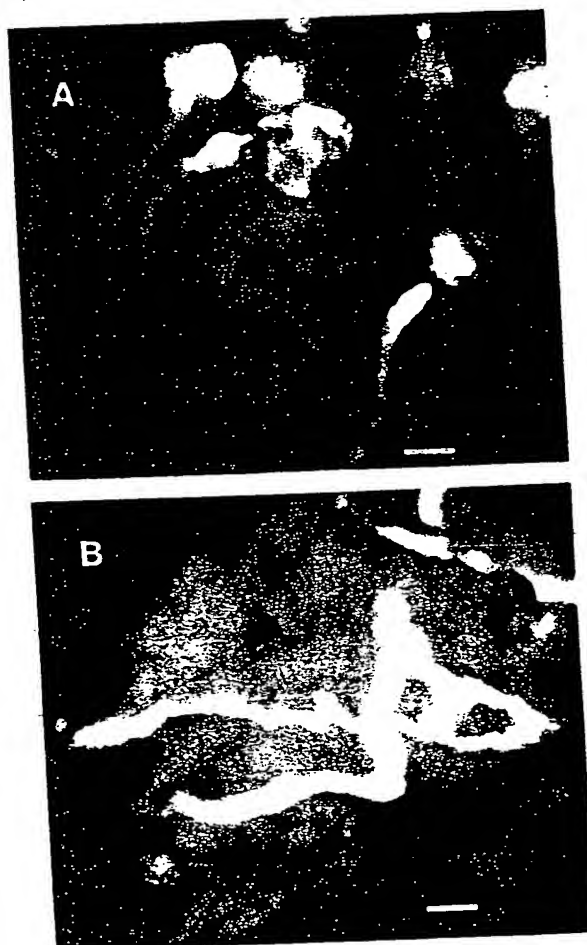


Fig. 6. Effect of RNase B1 on tangerine pollen tube growth in the stigma. (A) Control flower that was exposed to open pollination for 48 h. (B) Flower that was treated with RNase B1 before pollination. Scale bars = 0.1 mm.

BEST AVAILABLE COPY

J. AMER. SOC. HORT. SCI. 125(1):9-14, 2000.

Table 2. Fruit set of 'Fantasia' nectarine in Rosh Zurim, Israel. The buffer was sodium citrate, pH 3.5, containing 0.025% triton X-100. Fruit set is expressed as the percentage of developed fruit per flower.

treatment	Flowers (total no.)	Fruit set (%)
control nontreated	169 ^a	48.3 a ^a
control buffer	143	36.3 b
100 units/mL RNase B1	148	23.3 bc
1000 units/mL RNase B1	106	18.4 c

Each value is the mean of 10 replications.
Mean separation by Tukey-Kramer multiple range test, *P* ≤ 0.05.

ates heteroglycosylation of this protein. RNase T₂ (Kanaya and Ichida, 1981) and RNase M (Ohgi et al., 1983; Watanabe 1990) have also been found to contain different isoforms, sharing the same protein moiety, but differing in carbohydrate content. In RNase T₂, the occurrence of different-size glycan chains has been suggested to be due to enzymatic degradation by glycosidases, which are also present in *A. oryzae* medium-filtrate (Kanaya and Ichida, 1981). In *P. inflata*, S₃ protein, which normally has a single glycan chain, was mutagenized and gave rise to S₃(N29D), a nonglycosylated protein. The ability of S₃(N29D) protein to gain complete inhibition of S₃ pollen indicates that the carbohydrate moiety is not necessarily required for the self-incompatibility reaction (Karunanandaa et al., 1994). In *Lycopersicon peruvianum* (L.) Mill. the S₃-RNase has a single N-glycosylation site to which one of three n-glycans is attached (Parry et al., 1998). The exact biological role of the glycans is not understood. The molecular model of Parry et al. (1998) suggest that the glycans are not involved in determining the self-incompatibility phenotype. It is possible the glycans play a role in the maintenance of glycoprotein stability and in improving their solubility (Rademacher et al., 1988; Parry et al., 1998).

In the present work, RNase B1 had a clear inhibitory effect on pollen germination and tube growth, in vitro as well as in vivo. The optimal temperature for RNase B1 activity is 60 °C, however, at 25 °C the enzyme still possesses 25% of it's activity. In both peach and tangerine the appearance of the RNase-treated pollen tubes resembled the morphological features described in incompatible pollen tubes for *Petunia hybrida* Hort. Vilm.-Andr. (Herrero and Dickinson, 1980) and *Papaver rhoeas* L. (Franklin-Tong and Franklin, 1992). The pollen tubes were short, burst easily, had irregularities in wall deposition, and lacked a definite growth orientation. In gametophytic self-incompatible plants, the S-RNases have been found to share homology with RNase T₂, RNase Rh, and RNase M (Haring et al. 1990; McClure et al., 1989). In previous work we described intensive callose deposition in RNase-inhibited pollen tubes in calamondin in response to stigmatic RNase and RNase T1 (Roiz et al., 1995). The inhibitory effect of RNase B1 on pollen tube growth appears to resemble that of the other RNases.

In nectarine, RNase B1 treatment reduces fruit set, indicating that its ability to inhibit pollen tube growth in the style may lead to a decrease in the fertilization rate. During the first month following blooming period, fruitlets born on RNase-treated branches were smaller and showed larger falling ratio than the controls. The fact that RNase B1 affected the embryos viability, may indicate its potential to interfere with fertilization.

In conclusion, *A. niger* B1 was found to be an efficient source of RNase. The RNase B1 inhibited pollen germination and pollen tube growth nonspecifically, but pollen tubes of treated pollen

displayed morphological traits similar to those in gametophytic self-incompatibility. Much work is still needed to formulate RNase B1 as an effective control agent. However, based on this work the potential of its biological effect is clear, with its additional advantage of being environmentally safe.

Literature Cited

Bradford, M.M. 1976. A rapid sensitive method for the quantification of microgram quantities of protein utilizing the principle of protein-dye binding. *Anal. Biochem.* 72:248-245.

Broothaerts, W., P. Vanvinckenroye, B. Decock, J. Van Damme, and J.C. Vendrig 1991. *Petunia hybrida* S-proteins: Ribonuclease activity and the role of their glycan side chains in self-incompatibility. *Sexual Plant Reprod.* 4:258-266.

Brown, P.H. and T.-H.D. Ho. 1986. Barley aleurone layers secrete a nuclease in response to gibberellic acid. *Plant Physiol.* 82:801-806.

Clarke, A.E. and E. Newbigin. 1993. Molecular aspects of self-incompatibility in flowering plants. *Annu. Rev. Genet.* 27:257-279.

Clarke, K.R., J.J. Okuley, P.D. Collins, and T.L. Sims. 1990. Sequence variability and developmental expression of S-alleles in self-incompatible and pseudo self-incompatible *Petunia*. *Plant Cell* 2:815-826.

de Nettancourt, D. 1977. Incompatibility in Angiosperms, p. 28-57. In: R. Frankel, G.A.E. Gall, M. Grossmanand, and H.F. Linskens (eds.). *Monographs on theoretical and applied genetics*. vol. 3. Springer-Verlag, Berlin.

Egami, F. and K. Nakamura. 1969. *Microbial ribonucleases*. Springer-Verlag, Berlin.

Franklin-Tong, V.E. and F.C. Franklin. 1992. Gametophytic self-incompatibility in *Papaver rhoeas* L. *Sexual Plant Reprod.* 5:1-7.

Haring, V., J.E. Gray, B.A. McClure, M.A. Anderson, and A.E. Clarke. 1990. Self-incompatibility: A self-recognition system in plants. *Science* 250:937-941.

Herrero, M. and H.G. Dickinson. 1980. Pollen tube growth following compatible and incompatible intraspecific pollinations in *Petunia hybrida*. *Planta* 148:217-221.

Hinata, K., M. Watanabe, K. Toryama, and A. Isogai. 1993. A review of recent studies on homomorphic self-incompatibility. *Intl. Rev. Cytol.* 143:257-296.

Horitsu, H., Y. Higashi, and M. Tomoyedo. 1974. Production, purification and properties of ribonucleases from *Aspergillus niger*. *Agr. Biol. Chem.* 38:933-940.

Irie, M. 1967. Isolation and properties of a ribonuclease from *Aspergillus saitoi*. *J. Biochem.* 62:509-518.

Kanaya, S. and T. Uchida. 1981. An affinity adsorbent, 5'-adenylate aminohexyl-Sepharose. II. Purification and characterization of multi-forms of RNase T₂. *J. Biochem.* 90:473-481.

Karunanandaa, B., S. Huang, and T-h. Kao. 1994. Carbohydrate moiety of the *Petunia inflata* S3 protein is not required for self-incompatibility interactions between pollen and pistil. *Plant Cell* 6:1933-1940.

Kaufmann, H., F. Salamini, and R.D. Thompson. 1991. Sequence variability and gene structure at the self-incompatibility locus of *Solanum tuberosum*. *Mol. Gen. Genet.* 226:457-466.

Kerns, G., O.N. Okunev, V.M. Ananin, and E.L. Golovlev. 1987. Enhanced formation of β-glucosidase by *Aspergillus niger* VKMF-2092 in fed batch operation with frequency intermittent glucose addition. *Acta Biotechnol.* 7:535-545.

Kirch, H.H., H. Uhrig, F. Lottspeich, F. Salamini, and R.D. Thompson. 1989. Characterization of proteins associated with self-incompatibility in *Solanum tuberosum*. *Theor. Appl. Genet.* 78:581-588.

Laemmli, U.K. 1970. Cleavage of structural proteins during the assembly of the head of bacteriophage T4. *Nature* 227:680-685.

Lee, H-S, A. Singh, and T-h. Kao. 1992. RNase X2, a pistil-specific ribonuclease from *Petunia inflata*, shares sequence similarity with solanaceous S proteins. *Plant Mol. Biol.* 20:1131-1141.

Li, L.H. and K.W. King. 1963. Fractionation of β-glucosidase and related extracellular enzymes from *Aspergillus niger*. *Appl. Microbiol.* 11:320-325.

- McClure, B.A., V. Haring, P.R. Ebert, M.A. Anderson, R.J. Simpson, F. Sakyama, and A.E. Clarke. 1989. Style self-incompatibility gene products of *Nicotiana glauca* are ribonucleases. *Nature* 342:955-957.
- Newbiggin, E., M.A. Anderson, and A.E. Clarke. 1994. Gametophytic self-incompatibility in *Nicotiana glauca*, p. 5-18. In: E.G. Williams, A.E. Clarke, and R.B. Knox (eds.). *Genetic control of self-incompatibility and reproductive development in flowering plants*. Kluwer Academic Publishers, Dordrecht, Germany.
- Nurnberger, T., S. Abel, W. Jost, and K. Glund. 1990. Induction of extracellular ribonucleases in cultured tomato cells upon phosphate starvation. *Plant Physiol.* 92:970-976.
- Ohgi, K., H. Horiuchi, H. Watanabe, M. Takagi, K. Yano, and M. Irie. 1991. Expression of RNase Rh from *Rhizopus niveus* in yeast and characterization of the secreted proteins. *J. Biochem.* 109:776-785.
- Ohgi, K., H. Watanabe, M. Takizawa, Y. Kimura, K. Matsutani, E. Kakinuma, and M. Irie. 1983. Characterization of two forms of base non-specific and adenylic acid preferential ribonucleases from *Aspergillus saitoi*. *J. Biochem.* 94:767-775.
- Ozeri, U. 1995. Biological thinning of deciduous fruits and decreasing seed number in citrus fruits using fungal RNase. MS thesis, Hebrew Univ. Jerusalem.
- Parry, S., E. Newbiggin, D. Craik, K.T. Nakamura, A. Bacic, and D.Oxley. 1998. Structural analysis and molecular model of a self-incompatibility RNase from wild tomato. *Plant Physiol.* 116:463-469.
- Rademacher, T.W., R.B. Parekh, and R.A. Dwek. 1988. *Glycobiology*. Annu. Rev. Biochem. 57:785-838.
- Roiz, L., R. Goren, and O. Shoseyov. 1995. Stigmatic RNase in calamondin (*Citrus reticulata* var. *Austera* x *Fortunella* sp.). *Physiol. Plant.* 94:585-590.
- Roiz, L. and O. Shoseyov. 1995. Stigmatic RNase in self-compatible peach (*Prunus persica*). *Intl. J. Plant Sci.* 156:37-41.
- Rombout, F.M. and W. Pilnik. 1978. Enzymes in fruit and vegetable juice technology. *Process Biochem.* 89-13.
- Sassa, H., H. Hirano, and H. Ikehashi. 1992. Self-incompatibility-related RNases in styles of Japanese pear (*Pyrus serotina* Rehd). *Plant Cell Physiol.* 33:811-814.
- Shoseyov, O., B.A. Bravdo, R. Ikan, and I. Chet. 1988. Endo β -glucosidase from *Aspergillus niger* grown on a monoterpene glycoside-containing medium. *Phytochemistry* 27:1973-1976.
- Singh, A. and T-H. Kao. 1992. Gametophytic self-incompatibility: Biochemical, molecular, genetic and evolutionary aspects. *Intl. Rev. Cytol.* 140:449-483.
- Watanabe, H., A. Naitoh, Y. Suyama, N. Inokichi, H. Shimada, T. Koyama, K. Ohgi, and M. Irie. 1990. Primary structure of base non-specific and adenylic acid preferential ribonuclease from *Aspergillus saitoi*. *J. Biochem.* 108:303-310.